

LIGHT-CONE BEHAVIOR OF HADRONIC WAVEFUNCTIONS  
IN QCD AND EXPERIMENTAL CONSEQUENCES

Thesis By  
Darrell Richard Jackson

In Partial Fulfillment of the Requirements  
for the Degree of

Doctor of Philosophy

California Institute of Technology  
Pasadena, California

1977

(Submitted April 4, 1977)

## ACKNOWLEDGEMENTS

It is a pleasure to acknowledge the guidance and support of my advisor, Professor Glennys Farrar, who suggested this topic of study. Her great enthusiasm and constant willingness to discuss this problem and physics in general made this investigation both educational and inspirational for me.

One of the most pleasurable aspects of my stay at Caltech was the chance to argue about physics with fellow graduate students. I was greatly influenced by the collective wisdom of the students on the fourth floor of Lauritsen and have to acknowledge the patience of Chris Hill, Dave Crewther, Bert Barrois, and Dan Novoseller in the extended arguments and discussions we had.

This work could not have been done without financial support provided in various forms. I am grateful for the receipt of an Earl C. Anthony Fellowship as well as for the receipt of ARCS Foundation fellowships. The chance to teach Physics 2 under Professors Barish and Sciulli greatly eased the financial burden, but, more importantly, taught me a lot about physics and teaching itself.

I owe a special debt of gratitude to my wife, Barbara, and children for their moral support in spite of the difficulties my returning to graduate school caused them.

Finally, I want to thank Barbara for typing the first draft of this dissertation and Dianne Dodge for doing such a beautiful job on the final typing.

## ABSTRACT

LIGHT-CONE BEHAVIOR OF HADRONIC WAVEFUNCTIONS  
IN QCD AND EXPERIMENTAL CONSEQUENCES

Predictions are made for the high energy behavior of hadronic structure functions and form factors in Quantum Chromodynamics (QCD). These predictions follow from ladder-approximation calculations of the light-cone behavior of pion and nucleon Bethe-Salpeter wavefunctions. For the pion, some justification for the ladder approximation is found in its agreement with the operator-product expansion of the wavefunction. Our model gives logarithmic corrections to the asymptotic form factor expressions obtained by Brodsky and Farrar and also makes predictions for the threshold behavior of structure functions. We find Ezawa's results,  $(1-x)^2$ ,  $(1-x)^3$  for the pion and nucleon transverse structure functions, respectively, with additional powers of  $\ln(1-x)$ . A careful examination of the pion result suggests that an infrared singularity in the wavefunction may produce a slower falloff near threshold. For the longitudinal structure functions of the pion and nucleon, we find  $1/Q^2$  and  $(1-x)^3/Q^2$  threshold behavior, modulo logarithms. In the nucleon structure function calculation, it is noted that photons having momentum near threshold strike only quarks having spin parallel to that of the parent nucleon. This gives  $W_T(\text{neutron})/W_T(\text{proton}) \rightarrow 3/7$  as  $x \rightarrow 1$ . These results are consistent with experiment, although experimental error prevents a convincing test at present. A prediction is made for the magnitude of the asymptotic pion form factor and found to be in reasonable agreement with experiment. We find that the Brodsky-Farrar rules do not automatically give  $1/Q^4$  behavior for the  $N \rightarrow \Delta$  transition form factor.

If the amplitudes for a photon to strike quarks with either spin direction are equal, the model gives  $1/Q^6$  behavior for the  $N \rightarrow \Delta$  transition form factor and the neutron  $F_1$  form factor, consistent with experiment.

## TABLE OF CONTENTS

<u>Chapter</u>		<u>Page</u>
	Acknowledgements - - - - -	ii
	Abstract - - - - -	iii
I	INTRODUCTION AND SUMMARY - - - - -	1
	1.1 Key Assumptions - - - - -	2
	1.2 Outline and Summary of Results - - - - -	7
	References and Footnotes - - - - -	11
II	BORN DIAGRAM APPROACH TO PION ELECTROMAGNETIC FORM FACTOR AND STRUCTURE FUNCTIONS - - - - -	12
	2.1 Spinology - - - - -	14
	2.2 Pion Form Factor - - - - -	17
	2.3 Pion Structure Function - - - - -	18
	2.4 Drell-Yan-West Relation - - - - -	22
	2.5 Bloom-Gilman Duality - - - - -	24
	2.6 Order- $g^6$ Diagrams - - - - -	25
	2.7 Conclusions - - - - -	25
	References and Footnotes - - - - -	28
III	THE PION BETHE-SALPETER WAVEFUNCTION - - - - -	29
	3.1 Definition of the Bethe-Salpeter Wavefunction -	29
	3.2 Feynman Rules for the Bethe-Salpeter Wavefunction - - - - -	31
	3.3 Discrete Symmetries - - - - -	33
	3.4 Spectral Representation of Bethe-Salpeter Wavefunction - - - - -	37
	3.5 Wavefunction on the Light Cone and at Short Distances - - - - -	41

## TABLE OF CONTENTS (Continued)

<u>Chapter</u>		<u>Page</u>
	References and Footnotes - - - - -	46
IV	ASYMPTOTIC BEHAVIOR OF THE PION BETHE-SALPETER WAVEFUNCTION AS DETERMINED BY THE RENORMALIZATION GROUP - - - - -	47
	4.1 Symmetry Constraints on the Operator Product Expansion - - - - -	48
	4.2 Moments of the Wavefunction - - - - -	58
	4.3 The Renormalization Group - - - - -	61
	References and Footnotes - - - - -	67
V	ASYMPTOTIC SOLUTION OF THE BETHE-SALPETER EQUATION - -	68
	5.1 The Asymptotic Equation - - - - -	69
	5.2 $\gamma_5$ -odd Solution - - - - -	76
	5.3 $\gamma_5$ -even Solution - - - - -	83
	5.4 Conclusions - - - - -	87
	References and Footnotes - - - - -	88
VI	EXPERIMENTAL CONSEQUENCES FOR PION - - - - -	89
	6.1 Infrared Singularities - - - - -	89
	6.2 Pion Electromagnetic Form Factor - - - - -	91
	6.3 $\gamma_5$ -Even Contribution to Form Factor - - - - -	98
	6.4 Pion Structure Functions - - - - -	99
	References and Footnotes - - - - -	105

## TABLE OF CONTENTS (Continued)

<u>Chapter</u>		<u>Page</u>
VII	NUCLEON FORM FACTORS - - - - -	106
	7.1 $G_E/G_M$ Scaling - - - - -	107
	7.2 Simple Wavefunction, Approximations - - - - -	109
	7.3 Evaluating Diagrams - - - - -	112
	7.4 SU(6) Results - - - - -	116
	7.6 Asymptotic Freedom - - - - -	120
	References and Footnotes - - - - -	121
VIII	NUCLEON STRUCTURE FUNCTIONS - - - - -	122
	8.1 Born Diagrams - - - - -	122
	8.2 Heuristic Derivation - - - - -	126
	8.3 Consequences of the Spin Selection Rule - - - - -	128
	8.4 Quark Spin Selection for Longitudinal Structure Functions - - - - -	130
	8.5 Comparison with Experiment - - - - -	131
	References and Footnotes - - - - -	137
<u>Appendices</u>		
A	DETAILED EVALUATION OF BORN DIAGRAM FOR PION STRUCTURE FUNCTIONS - - - - -	138
B	DETAILED EVALUATION OF BORN DIAGRAMS FOR NUCLEON STRUCTURE FUNCTIONS - - - - -	148

## LIST OF FIGURES

<u>Figure</u>		<u>Page</u>
1.1	Exact Bethe-Salpeter calculation of the pion form factor - - - - -	3
1.2	Approximate calculation for the asymptotic pion form factor - - - - -	3
1.3	(a) The Bethe-Salpeter equation for the pion and (b) the ladder approximation to the kernel, with momentum-dependent coupling constant - - - - -	5
1.4	Born diagrams contributing to (a) the pion form factor, (b) the nucleon form factors, and (c) the pion structure functions. The incoming bosons are photons and the other bosons are gluons - - - - -	6
2.1	Diagrams contributing to (a) the pion form factor and (b) the nucleon form factors - - - - -	13
2.2	Vertex and propagator factors in the calculation of the asymptotic behavior of the pion form factor. The heavy arrows are spin directions and the light arrows are directions of three-momentum in the Breit frame - - -	19
2.3	Some order $-g^6$ diagrams contributing to the pion structure functions - - - - -	26
6.1	Monopole (solid line) and monopole x logarithm (dashed line) compared to spacelike pion form factor summarized by Bebek et al. - - - - -	97
6.2	Amplitude for $e^+ + e^- \rightarrow \text{pion} + \text{anything}$ - - - - -	101
6.3	Diagram for the pion structure functions - - - - -	101
7.1	Born diagrams contributing to nucleon form factors in the Feynman gauge. $u_N$ is normalized to $2M(\text{nucleon})$ - - - - -	108
8.1	Diagrams making a non-leading contribution to the nucleon transverse structure function in the Feynman gauge - - - - -	125



## LIST OF FIGURES (Continued)

<u>Figure</u>		<u>Page</u>
8.2	Diagrams that do not contribute to the transverse structure function in the scaling limit - - - - -	125
8.3	Data for proton transverse structure function as presented by Atwood compared to Expression (8-24) with $m = 250$ and $350$ MeV - - - - -	134
8.4	Experimental data for proton magnetic form factor presented by Atwood compared to expression (8-21) - -	134
A.1	Born diagram for pion structure functions - - - - -	139
A.2	Additional order $g^4$ diagrams for pion structure functions - - - - -	147
A.3	Some diagrams that do not contribute to the pion structure function in the limit $\omega \rightarrow 1$ - - - - -	147
B.1	The first phase space integration viewed as a calculation of the structure function for nucleon $\rightarrow$ quark + anything - - - - -	149
B.2	Allowed and favored regions for the final phase space integration in the nucleon structure function calculation - - - - -	153

## Chapter I

## INTRODUCTION AND SUMMARY

Quantum chromodynamics (QCD) is a renormalizable strong interaction theory that appears to be consistent with scaling phenomena observed in hadronic processes at high energy. Asymptotic freedom is a key element in deriving scaling laws as approximations in QCD. At high energies, the effective gluon coupling constant should be small, minimizing the intrusion of logarithmic factors that contain the renormalization mass. A small coupling constant makes perturbative calculations possible and offers hope that quantitative comparisons of experiment and theory can be made.

In this dissertation, an attempt is made to obtain quantitative QCD predictions for hadron-electromagnetic processes at high energies. The approach used here is inspired by the success of many of the scaling laws obtained by Brodsky and Farrar from a quark-quark scattering picture [1]. We will consider quasielastic scattering

$$(\text{Spacelike } \gamma) + (\text{Hadron A}) \rightarrow (\text{Hadron B})$$

$$(\text{Timelike } \gamma) \rightarrow (\text{Hadron } \bar{A}) + (\text{Hadron B})$$

and inclusive scattering

$$(\text{Spacelike } \gamma) + (\text{Hadron}) \rightarrow (\text{Anything})$$

$$(\text{Timelike } \gamma) \rightarrow (\text{Hadron}) + (\text{Anything})$$

The form factors contain the essentials of elastic scattering, while the structure functions contain the essentials of inclusive scattering.

### 1.1 Key Assumptions

Hadrons are assumed to be bound states in QCD, which immediately brings the Bethe-Salpeter formalism to the fore [2]. The pion form factor provides a good illustration of the assumptions we make in order to simplify the Bethe-Salpeter approach. These assumptions can be partly justified or at least suggested by renormalization-group methods, and our hope is that we have stripped away low energy detail and retained the essentials needed for a description of asymptotic behavior.

Figure 1.1 shows a schematic diagram for obtaining the pion form factor from a convolution of pion wavefunctions (round blobs) with the quark-photon scattering kernel (square box). Further discussion is given in Chapter III, but, for the present, it is only necessary to know that the scattering kernel contains a profusion of gluons. Our first assumption is that these gluons decouple at high energies (as the effective coupling constant goes to zero), leading to the simpler diagram of Figure 1.2, which shows the photon coupled to a quark with no gluon dressing. The photon momentum will flow primarily into one wavefunction over part of the domain of loop integration and primarily into the other wavefunction over the remainder. One can say that the photon is probing the high momentum "tails" of the wavefunctions, and that knowledge of the asymptotic behavior of form factors can be used to determine the asymptotic behavior of the wavefunction and vice-versa.

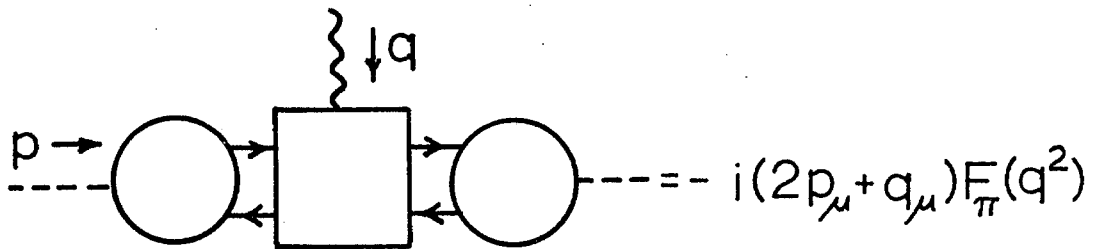


Figure 1.1

Exact Bethe-Salpeter Calculation of the Pion Form Factor

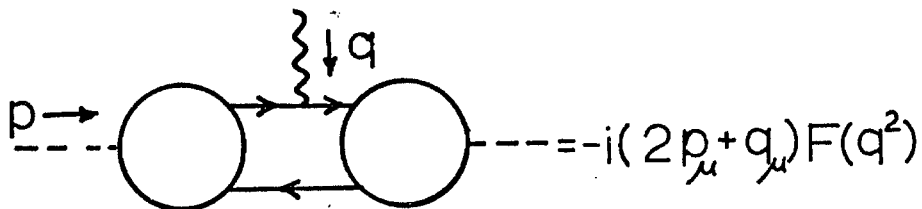


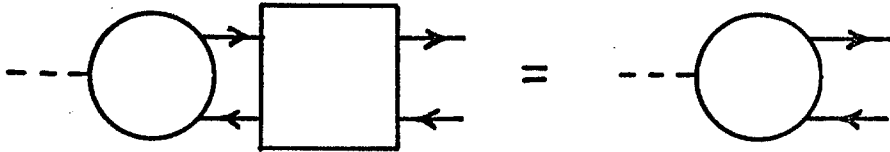
Figure 1.2

Approximate Calculation for the Asymptotic Pion Form Factor

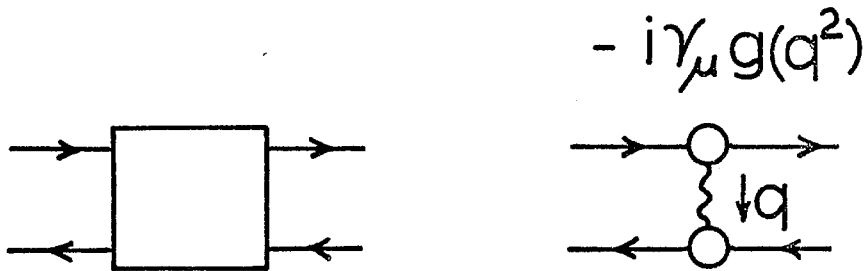
Our second assumption has to do with calculating the tail of the wavefunction. The exact Bethe-Salpeter equation is given diagrammatically in Figure 1.3a. We assume that the gluons in the quark-quark scattering kernel decouple at high energies, leaving a single gluon with momentum-dependent coupling as shown in Figure 1.3b. This is a "ladder" approximation, almost certainly incorrect when quark momentum is low, but hopefully exact when used to calculate the tail of the wavefunction.

We aspire to calculations in the spirit of Figure 1.3, but, in some cases, this proves too difficult and an additional assumption is introduced [3]. This is the assumption of Brodsky and Farrar that the wavefunction constrains the constituent quarks to have comparable shares of the hadron momentum. This constraint is supposed to be strong enough that the tail of the wavefunction can be estimated by the exchange of the minimum number of gluons required to accelerate the quarks to large momenta (one gluon for pions, two gluons for nucleons). This leads to simple Born diagrams of the type shown in Figure 1.4.

Our intent is to go beyond scaling laws, to determine the dependence of cross-sections not only upon energy, but upon dimensionless variables as well, such as angles and the scaling variable,  $x$ . For pion processes, it is possible to go even further. By normalizing the wavefunction to give the correct value for the pion decay constant, one can make predictions for the absolute magnitude of the form factor and structure functions. Further, the two-body bound state problem is simple enough in the ladder approximation to allow calculation of logarithmic violations of power scaling laws.



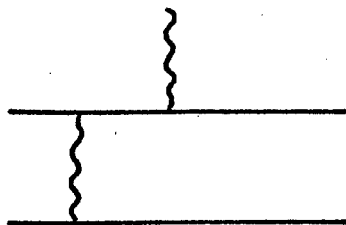
(a)



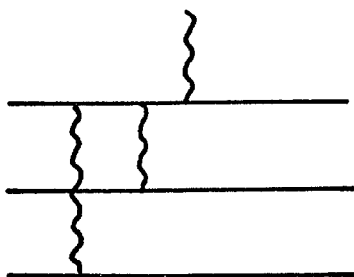
(b)

Figure 1.3

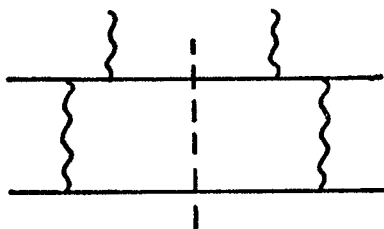
(a) The Bethe-Salpeter Equation for the Pion and (b) the Ladder Approximation to the Kernel, With Momentum-Dependent Coupling Constant



(a)



(b)



(c)

Figure 1.4

Born Diagrams Contributing to (a) the Pion Form Factor, (b) the Nucleon Form Factors, and (c) the Pion Structure Functions. The Incoming Bosons are Photons and the Other Bosons are Gluons.

## 1.2 Outline and Summary of Results

Chapter II develops the Born diagram approach for the pion. Simple spinology rules are discussed, and applied to obtain the results

$$W_T \propto (1-x)^2, \quad x \approx 1$$

$$W_L \propto \frac{1}{q}, \quad x \approx 1$$

for the pion transverse and longitudinal structure functions. The same result for the transverse structure function was obtained by Ezawa [4] in a similar model. Other models give  $W_T \propto 1-x$  [5] and  $W_T = \text{constant}$  [6] in the threshold ( $x \approx 1$ ) region. Experimental errors are too great at present to clearly favor one model over the others [7].

The Born diagram approach oversimplifies the wavefunction. As a first step toward remedying this deficiency, Chapter III collects assorted facts about the two-body wavefunction from the literature. The simplifications resulting from symmetry of the wavefunction under parity, G-parity, and time reversal are derived. The Wick spectral representation for the wavefunction is introduced in preparation for its extensive use in the following three chapters. It is shown that the tail of the wavefunction in momentum space corresponds to the light cone in configuration space.

The first real use of QCD is made in Chapter IV, where the operator product expansion of the wavefunction on the light cone is developed. Appelquist and Poggio [8] have pointed out the analogy between moments of Wick's spectral function and moments of structure functions. Both carry logarithmic factors whose fractional powers are directly related to the anomalous dimensions of local operators. We find that this analogy



fails in two important respects. First, the  $n^{\text{th}}$  moment of the spectral function receives contributions not only from the operator with  $n$  derivatives, but also from operators with  $n-2$ ,  $n-4$ , ... derivatives. Second, operators of twist three turn out to be just as important as operators of twist two. These properties are important to the comparison of the operator product results with definite wavefunctions found in Chapter V.

Using the ladder approximation (Figure 1.3b), asymptotic solutions are obtained in Chapter V for the two-body Bethe-Salpeter equation in QCD. These solutions exhibit all the properties demanded by the operator product expansion, which suggests that the ladder approximation may be valid when computing the wavefunction on the light cone. At this stage, an inconsistency in the simpler Born diagram approach becomes evident. In the ladder approximation, the tail of the wavefunction appears in the left- and right-hand sides of the Bethe-Salpeter equation, so that one can say that the tail begets the tail. In the Born diagrams, the low-momentum part of the wavefunction produces the tail through a single gluon exchange. This gives the correct  $1/k^4$  behavior for the wavefunction tail, but this falloff is too slow to justify the assumption that the ladder approximation loop integral is restricted to small values of momentum. This results in modifications to the Born diagram results, as discussed in Chapter VI.

Chapter VI adopts the simplest Bethe-Salpeter solution for comparison with experiment, even though the wavefunction, in principle, must be a superposition of the entire sequence of solutions. The Born diagram results for the pion form factor and longitudinal structure function are only modified by inverse powers of  $\ln q^2$  and  $\ln(1-x)$ , respectively,

coming from the effective gluon coupling constant. The predicted magnitude for the asymptotic pion form factor is found to be in reasonable agreement with experiment [9], while the predicted magnitude for the longitudinal structure function near threshold is consistent with the upper bound set by experiment [7].

An infrared singularity in the asymptotic wavefunction makes it impossible to perform a consistent calculation of the transverse structure function. This singularity appears as the (momentum)<sup>2</sup> of either quark approaches zero, a region in which the asymptotic solution is not supposed to be valid. If the correct infrared behavior is this singularity regulated by a mass parameter,  $W_T \propto (1-x)^{2/3}$  results. If this singularity can be disregarded (for some unknown reason), we get the Born diagram result  $W_T \propto (1-x)^2$  modified by two inverse powers of  $\ln(1-x)$ .

As a concession to the difficulties of the three-body Bethe-Salpeter formalism, we do not attempt a derivation of the tail of the nucleon wavefunction. Instead, we revert to the method of estimating the tail from the low-momentum part of the wavefunction with minimal gluon exchanges. The results of the pion calculation indicate that form factors and structure functions obtained in this way should be valid up to logarithmic factors, barring infrared problems. A simple, phenomenological low-momentum wavefunction is adopted, with SU(6) symmetry. The gluon exchanges then provide an explicit SU(6) breaking mechanism for the wavefunction tail.

In Chapter VII, we show that  $G_E/G_M$  scaling holds in this model, with  $G_M \propto 1/Q^4$ , the Brodsky-Farrar result [1]. The N- $\Delta$  transition form factor

also goes as  $1/Q^4$ , with a constant of proportionality determined by a free parameter in the model. This free parameter is the ratio of the amplitudes for the photon to strike quarks with spin parallel and antiparallel to that of the nucleon. Setting this ratio equal to unity suppresses the  $N-\Delta$  transition, as experiment suggests is the case [10], and gives the interesting result

$$F_1(\text{neutron}) \propto \frac{1}{Q^6}$$

Applying this model to the nucleon transverse structure function in Chapter VIII, we find that the amplitude for a transverse photon to strike a quark with spin antiparallel to the nucleon is zero near threshold. One of the principal results of this SU(6) violation is that the ratio of neutron to proton structure functions should approach 3/7 as  $x \rightarrow 1$ . Experimental data favor the value 1/4 [10], but systematic errors large enough to give the 3/7 ratio cannot be ruled out. This model gives  $W_T \propto (1-x)^3$ ,  $W_L \propto (1-x)^3/Q^2$ . Based on the pion results, we conjecture that eight powers of the effective coupling constant should appear in the structure function. This produces reasonable agreement with the fourth-power behavior for  $W_T$  suggested by experiment [10].

Chapter I References and Footnotes

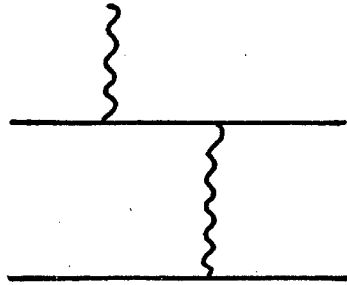
1. S. J. Brodsky and G. R. Farrar, Phys. Rev. Letters 31, 1153 (1973), and Phys. Rev. D 11, 1309 (1975); V. Matveev et al., Lett. Nuovo Cimento 7, 719 (1973).
2. K. Huang and H. A. Weldon, Phys. Rev. D 11, 257 (1975); S. Mandelstam, Proc. Roy. Soc. A 233, 248 (1955); E. E. Salpeter and H. A. Bethe, Phys. Rev. 84, 1232 (1951).
3. G. R. Farrar and D. R. Jackson, Phys. Rev. Letters 35, 1416 (1975).
4. Z. Ezawa, Nuovo Cimento 23A, 271 (1974).
5. G. Schierholz and M. G. Schmidt, CERN Reports Ref. TH.2106-CERN (1975), and Ref. TH.2013-CERN (1975).
6. R. P. Feynman, private communication and seminar at Caltech.
7. R. F. Schwitters, SLAC-PUB-1666 (1975), and R. Hollebeek, Lawrence Berkeley Laboratory Report No. LBL-3874.
8. T. Appelquist and E. Poggio, Phys. Rev. D 10, 3280 (1974).
9. M. Bernardini et al., Phys. Lett. 46B, 261 (1973); L. Paoluzi, Acta Phys. Pol. B5, 839 (1974); C. J. Bebek et al., Phys. Rev. D 13, 25 (1976).
10. W. B. Atwood, SLAC Rept. No. 185 (1975); E. M. Riordan et al., SLAC-PUB-1634 (1975); A. Bodek, MIT Lab. for Nuc. Science Tech. Rept. No. COO-3069-116 (1972).

## Chapter II

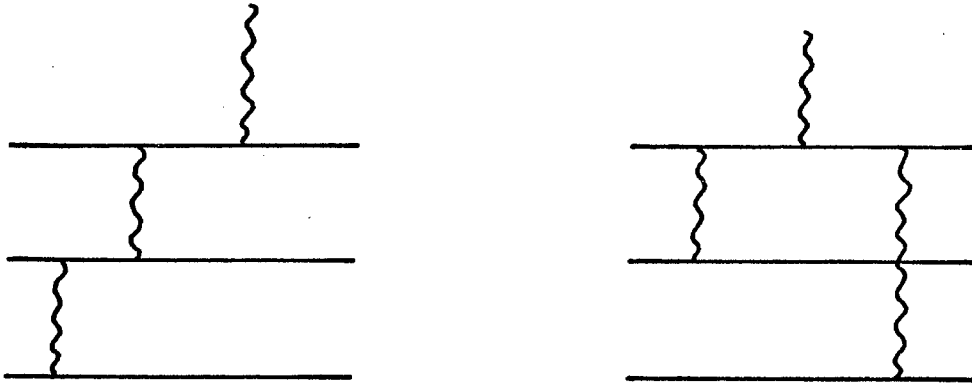
BORN DIAGRAM APPROACH TO PION  
ELECTROMAGNETIC FORM FACTOR AND STRUCTURE FUNCTIONS

Brodsky and Farrar [1] have argued that the asymptotic behavior of form factors is governed by Born diagrams such as those in Figure 2.1. These diagrams contain a minimal number of gluons which serve to "reassemble" the constituent quarks into a hadron after one quark has been struck by a photon. In slightly more elegant terms, the gluon exchanges give a ladder approximation to the Bethe-Salpeter wavefunction at large quark momentum differences. Taking the incoming and outgoing quarks as on-shell is a further approximation amounting to the assumption that the quarks spend most of their time with small relative four-momentum. For convenience, but somewhat loosely, we will refer to the wavefunction region in which the rest-frame components of relative four-momentum have values on the order of  $m_\pi$  as "the normal wavefunction" and the region in which some components are large as "the tail of the wavefunction."

In this chapter, the pion structure functions will be calculated in the Brodsky-Farrar spirit, adding the parton model assumption that the hadronic final state,  $X$ , in  $e^+e^- \rightarrow \pi + X$  can be approximated by quarks with small values of squared four-momentum. It will develop that these calculations can make sense only near threshold (scaling variable  $\omega \rightarrow 1$ ). The main results turn out to be that the transverse structure function goes as  $(\omega-1)^2$  near threshold while the longitudinal structure function goes as  $1/q^2$ . These results are consistent with the data but disagree with some other predictions based on the Drell-Yan-West relation. We will discuss this point, and will delve into the spinology



(a)



(b)

Figure 2.1

Diagrams Contributing to (a) the Pion  
Form Factor and (b) the Nucleon Form Factors

of the present model to better understand the physics of this somewhat unusual result.

## 2.1 Spinology

Evaluation of the Born diagrams is straightforward and is carried out in some detail in the Appendices. In this section, a short-cut method will be developed which will make it possible to "get inside" the Feynman diagrams and keep track of the flow of linear and angular momentum. The result will be some simple rules that permit heuristic discussion of the threshold behavior of structure functions and the asymptotic behavior of form factors. These rules will be derived for vector and scalar gluons and will be applied to  $L = 0$  mesons and baryons.

If transverse momentum is limited, frames can be found in which the 3-momenta in a given Feynman diagram are nearly in the z-direction. If spin is quantized in this direction, spin states become helicity states. It will be crucial in the following to distinguish between helicity and chirality, which are the same only for massless fermions. It will develop that the pion structure function threshold suppression is due to conflicting demands for helicity and chirality conservation.

In the standard Dirac matrix representation with

$$\gamma^0 = \begin{pmatrix} 1 & 0 \\ 0 & -1 \end{pmatrix}, \quad \gamma^i = \begin{pmatrix} 0 & \sigma^i \\ -\sigma^i & 0 \end{pmatrix}, \quad \gamma^5 = \gamma_5 = \begin{pmatrix} 0 & 1 \\ 1 & 0 \end{pmatrix} \quad (2-1)$$

the spinors of positive and negative helicity with momentum  $K$  in z-direction are

$$u_1 = \sqrt{E+m} \begin{pmatrix} 1 \\ 0 \\ K \\ \frac{K}{E+m} \\ 0 \end{pmatrix} \quad u_{-1} = \sqrt{E+m} \begin{pmatrix} 0 \\ 1 \\ 0 \\ -K \\ \frac{K}{E+m} \end{pmatrix} \quad (2-2)$$

with

$$E^2 - K^2 = m^2 \quad (2-3)$$

Spinors of definite chirality are produced by the projection matrices  $\left(1 \pm \gamma_5\right)/2$ , making it possible to break a spinor of definite helicity into pieces that have "correct" and "incorrect" chirality. If  $E \gg m$ ,

$$u_S = \sqrt{2E} \left[ e_{SS} + \frac{m}{2E} e_{S(-S)} \right] \quad (2-4)$$

where  $e_{SC}$  is a unit norm spinor having spin  $S = \pm 1$  and chirality  $C = \pm 1$ .

$$\bar{e}_{S_1 C_1} e_{S_2 C_2} = \delta_{S_1 S_2} \delta_{C_1 (-C_2)} \quad (2-5)$$

From (2-4), one sees that the ratio of "incorrect" to "correct" chirality amplitude is  $m/(2E)$ .

Simple selection rules for the emission of scalar bosons follow from (2-5) while, for vector bosons, we need the following:

$$\begin{aligned} \gamma^0 e_{SC} &= e_{S(-C)} & \gamma^3 e_{SC} &= SC e_{S(-C)} \\ \gamma^1 e_{SC} &= C e_{(-S)(-C)} & \gamma^2 e_{SC} &= i SC e_{(-S)(-C)} \end{aligned} \quad (2-6)$$

Consider the amplitude



$$\bar{u}_2 \Gamma u_1 = \frac{\text{---} \xrightarrow{k_1} \text{---} \xrightarrow{+k_2} \text{---}}{\text{---} \xrightarrow{q} \text{---}} \quad (2-7)$$

where  $\Gamma$  is a Dirac matrix (unit matrix) for vector (scalar) boson emission. The selection rules for chirality are well-known and obvious from relations (2-5) and (2-6): Emission or absorption of a vector (scalar) boson does not (does) change fermion chirality.

Angular momentum conservation demands that the component of spin along the direction of the single outgoing or incoming particle be conserved and, since we consider only colinear frames, scalar bosons and longitudinal vector bosons do not flip the fermion spin, while transverse bosons do flip the spin. Considering the Breit frame where

$$q = (0, 0, 0, -Q) \quad , \quad k_1 = \left( E, 0, 0, \frac{Q}{2} \right) \quad , \quad k_2 = \left( E, 0, 0, -\frac{Q}{2} \right) \quad ,$$

it follows that emission or absorption of a longitudinal vector boson produces an helicity-chirality conflict, since the former is changed while the latter is not. This costs a factor  $\frac{m}{2E}$ .

$$\text{---} \xrightarrow{k_1} \text{---} \xrightarrow{q} \text{---} = \begin{cases} Q & \text{Scalar Boson or} \\ & \text{Transverse Vector Boson} \\ m & \text{Longitudinal Vector Boson} \end{cases} \quad (2-8)$$

We have omitted phase factors and will take these from (2-6) whenever there is more than one diagram to evaluate.

The discussion has so far been restricted to on-shell fermions. We wish to consider diagrams in which the incoming and outgoing fermions

are on-shell but which may contain several virtual fermion lines. One can still assign vertex factors when one or more of the fermions is off-shell by defining off-shell spinors identical to (2-2), but with  $m$  replaced by the square root of squared four-momentum (imaginary if the fermion momentum is spacelike). Fermion propagator numerators can then be expressed in terms of off-shell spinors through the completeness relation

$$k + m = \sum_{S,C} \left[ u_{SC} \bar{u}_{SC} + \frac{m}{\sqrt{k^2}} u_{SC} \bar{u}_{S(-C)} \right] \quad (2-9)$$

This shows that the chirality of an off-shell fermion can flip as it propagates, but this costs an amplitude factor  $m/\sqrt{k^2}$ . The vertex factors (2-8) can be generalized to the case where at least one fermion is off-shell, but our immediate needs are satisfied by the simple observation that longitudinal vector bosons suffer no  $m/Q$  suppression relative to transverse bosons when coupling to off-shell fermions because the off-shell "mass" is  $\sqrt{k^2} = O(Q)$ . When quantitative results are needed, one can work in a special frame, displaying all propagators and vertices as explicit Dirac matrices and using relations (2-5) and (2-6). When evaluating Brodsky-Farrar form factors, this inelegant approach proves to be much faster and simpler than using traces.

## 2.2 Pion Form Factor

The amplitude for a pion of momentum  $p$  to absorb a photon of momentum  $q$  and polarization  $e$  is  $e \cdot (2p+q) F_{\pi} [q^2]$ . In the Breit frame,  $2p + q = \{2E_{\pi}, 0, 0, 0\}$ , and it is clear that the photon polarization must

be longitudinal. One of the two Born diagrams for calculating the asymptotic behavior of  $F_\pi$  is shown in Figure 2.2.

The heavy arrows denote spin direction and the other arrows are momentum reference directions. The incoming photon is longitudinal, denoted L, and the exchanged vector gluon must be transverse, denoted T, to avoid an  $m/Q$  suppression factor at the lower vertex. One sees that the spins undergo a single flip in going through the diagram. Neglecting phases and numerical factors of order unity,  $QF_\pi$  has a power of  $Q$  coming from each of the three boson vertices and a factor  $1/Q^2$  from each of the two propagators. The numerator of the fermion propagator is accounted for by two of the vertex factors just noted and an additional factor unity because no chirality flip is required of the virtual fermion. No chirality flip is required as the upper fermion has the "correct" chirality entering and leaving the diagram (as does the lower fermion). Adding up powers of  $Q$ , one obtains the Brodsky-Farrar result,

$$F_\pi \propto \frac{1}{Q^2} \tag{2-10}$$

### 2.3 Pion Structure Function

A detailed calculation of the Born diagram for the pion structure function is given in Appendix A. Equivalent results will be developed here using the spinology rules. The pion structure functions are measured in electron-positron annihilation experiments, which means that  $q$  is time-like. In the Born diagram approach, there is no essen-

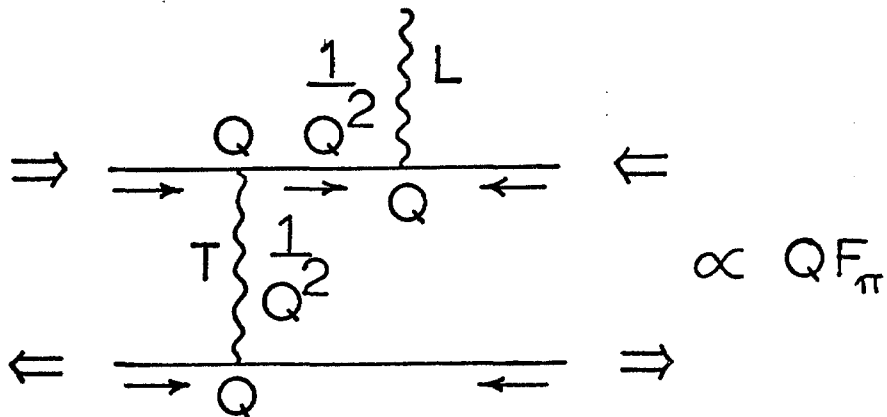


Figure 2.2

Vertex and Propagator Factors in the Calculation of the Asymptotic Behavior of the Pion Form Factor. The Heavy Arrows are Spin Directions and the Light Arrows are Directions of Three-momentum in the Breit Frame.

tial difference between the timelike and spacelike cases, so the somewhat more familiar spacelike case will be discussed here.

The diagram of Figure 2.2 will serve for the structure function calculation if the outgoing quarks have unconstrained momenta. The longitudinal structure function is the square of this amplitude,  $|M|^2$ , integrated over the phase space of the outgoing quarks.

$$W_L \propto \int d^4 k_1 |M|^2 \delta(k_1^2 - m^2) \delta(k_2^2 - m^2) \quad (2-11)$$

The momentum of the outgoing quark is  $k_1$ , and the momentum of the outgoing antiquark is  $k_2$ . The transverse structure function,  $W_T$ , is found in the same fashion with  $M$  computed for a transverse photon. The structure functions depend upon only  $q^2$  and the scaling variable

$$\omega = \frac{-2p \cdot q}{q^2} \quad (2-12)$$

The invariant mass of the outgoing quarks is

$$W^2 = (p+q)^2 = q^2(1-\omega) + m_\pi^2 \quad (2-13)$$

We wish to examine the Bjorken limit

$$q^2 \rightarrow \infty, \quad \omega = \text{finite}$$

It will prove necessary to specialize further to the threshold region

$$\omega \rightarrow 1, \quad W^2 \gg m_\pi^2$$

For present purposes, a crude evaluation of the phase space integral (2-11) is sufficient. The quark and gluon propagators restrict (trans-

verse momentum)<sup>2</sup> to a region of order  $m^2$ , giving a phase space factor  $m^2/W$ . The virtual quark and gluon have

$$(\text{momentum})^2 = O\left(\frac{m^2}{\omega-1}\right)$$

This can be seen very simply by noting that, near threshold, the gluon must transfer a fraction  $\frac{2}{\omega} - 1$  of the momentum of the unstruck quark to the struck quark. This would leave the unstruck quark off-shell, so the gluon must dribble a small fraction,  $y$ , of the photon momentum down to the unstruck quark.

$$\left[\left(1-\frac{1}{\omega}\right)\frac{p}{2} + yq\right]^2 = m^2$$

$$y = O\left(\frac{-m^2}{p \cdot q \left(1-\frac{1}{\omega}\right)}\right)$$

It follows that the virtual quark and gluon have  $(\text{momentum})^2 = O\left(\frac{m^2}{\omega-1}\right)$ . If  $m$  is large enough, and  $\omega$  is close enough to unity, the virtual particle will be far off-shell. In an asymptotically free theory, this lends credence to the perturbation approach used here. One can readily verify that scalar gluons give the same power behavior as vector gluons, although the lack of asymptotic freedom in scalar gluon theories makes this case less interesting.

The  $\omega$ - and  $q^2$ -dependence of  $|M|^2$  is gotten by taking a factor  $m^2/(\omega-1)$  for the photon vertex (the "(mass)<sup>2</sup>" of the virtual quark),  $m^2/(\omega-1)$  for each gluon vertex, and  $(\omega-1)^2/m^4$  for each propagator.

Appending the phase space factor gives

$$W_L \propto 1/Q^2$$

Unlike  $W_L$ ,  $W_T$  is suppressed by an helicity-chirality conflict. With a transverse photon and a transverse gluon, the outgoing struck quark has reversed helicity. To make the chirality agree, a suppression factor  $\omega-1$  must be used for the quark propagator. The photon vertex factor is  $Q^2$  in this case, giving

$$W_T \propto (\omega-1)^2$$

With a longitudinal gluon, no suppression arises in the quark propagator, but the lower gluon vertex factor becomes  $m^2$  rather than  $\frac{m^2}{\omega-1}$ , giving  $W_T \propto (\omega-1)^2$  again.

#### 2.4 Drell-Yan-West Relation

The scaling part of the transverse structure function goes as  $(\omega-1)^2$  near threshold. It is often asserted that the Drell-Yan-West relation [2] gives  $W_T \propto \omega-1$  if the pion form factor,  $F_\pi$ , falls off as  $1/q^2$ . Feynman [3] has pointed out that, because the elastic process  $e^+e^- \rightarrow \pi^+\pi^-$  is mediated by longitudinal photons, the Drell-Yan-West argument actually gives a relation between  $W_L$  and  $F_\pi$ .

$$W_L(Q^2, \omega) \Big|_{\substack{\omega \approx 1 \\ \text{Fixed } W^2}} \propto q^2 \Big| F_\pi \Big|^2$$

If we assume  $W_L$  falls off as  $1/q^2$  for fixed  $\omega$ , then  $W_L$  must be independent of  $\omega$  near threshold. Further, if  $W_L/W_T \propto 1/q^2$ , Feynman's argument gives a transverse structure function that is also independent of  $\omega$  near threshold.

We see that our model agrees with the Drell-Yan-West relation in giving

$$W_L \propto \frac{1}{q}$$

apart from a mild logarithmic dependence on  $W^2$  as shown in Appendix A. It differs from Feynman in giving an  $\omega$ -dependent  $W_L/W_T$  ratio.

$$\frac{W_L}{W_T} = \frac{\mu^2}{q^2 (\omega-1)^2} \quad (2-14)$$

The calculation of Appendix A shows that  $\mu$  depends upon the quark mass in the following way

$$\mu^2 = \frac{4}{13} m^2 \ln \frac{W^2}{m^2} - 1 \quad (2-15)$$

In the present, somewhat naive, approach, quark mass parameters cannot be differentiated from dimensional parameters originating in the wavefunction. The dependence of  $\mu$  on wavefunction parameters is derived in Chapter VI.

Experimentally [4],  $W_L/W_T \ll 1$  for  $1.1 < \omega < 2$ ,  $q^2 = (7.4 \text{ GeV})^2$ . The predicted fall-off of  $W_T$  as  $\omega \rightarrow 1$  is so rapid that  $W_L > W_T$  for  $\omega - 1 < \mu^2/W^2$  [5]. Whether this unusual prediction is experimentally testable depends on the size of  $\mu$ . We can only consider  $W > 2\text{GeV}$ , and the arguments of Chapter VI suggest that  $\mu$  is of the order of  $m_\pi$ . This places the test of our  $W_L/W_T$  prediction somewhat beyond the capabilities of present experiments.



## 2.5 Bloom-Gilman Duality

Bloom and Gilman view the structure function in the scaling region as a summation of contributions from individual resonances [6]. If the resonance form factors have the same large  $-q^2$  behavior as the elastic form factor, the Drell-Yan-West relation results. If our model is to exhibit Bloom-Gilman duality, the zero-helicity transition form factors must fall off as  $1/q^2$  (a fraction of the resonances could fall off faster without upsetting things) and the  $\pm 1$  helicity form factors must fall off as  $(1/q^2)^2$ .

The simplest transition form factor to treat in this model is that for  $\gamma \rightarrow \pi + \rho$  where  $\gamma$  is a time-like photon. We cannot use the  $\pi$ - $\rho$  transition to comment on Bloom-Gilman duality for the longitudinal structure function, as  $\gamma \neq \pi + \rho$  for longitudinal photons. One way to see this is to consider the decay of a time-like longitudinal photon at rest into  $\pi + \rho$  moving in opposite directions along the z-axis. The  $\pi + \rho$  orbital momentum must be  $L = 1$  in order that the overall parity be the same as the photon, and the component of orbital momentum along the decay axis is necessarily zero. A longitudinal photon at rest has no angular momentum in the z-direction, so the only possible decay is into a  $\rho$  with  $s_z = 0$ . The Clebsch-Gordon coefficient connecting the photon spin state  $|1,0\rangle$  to the final spin orbital state  $|1,0\rangle \times |1,0\rangle$  vanishes, so the decay is forbidden. Similarly, the production process  $\gamma + \pi \rightarrow \rho$  is forbidden if  $\gamma$  is longitudinal.

Using the spinology rules with a transverse photon, it is a simple matter to show that the  $\pi$ - $\rho$  transition suffers from an helicity-chirality suppression of the  $\pi$ - $\rho$  amplitude by a factor  $m/Q$  relative to the  $\pi$ - $\pi$  ampli-

tude. If the  $\pi$ - $\rho$  transition form factor is proportional to the  $\pi$ - $\rho$  amplitude with a Lorentz factor  $p^\mu q^\nu$  removed, the form factor will go as  $(1/q^2)^2$ , consistent with Bloom-Gilman duality.

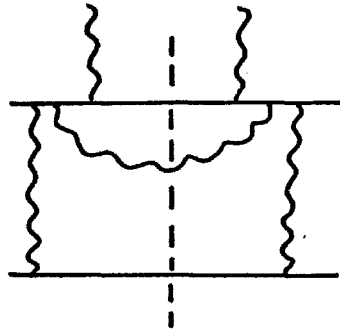
Having shown that our model is consistent with Bloom-Gilman duality up to the simplest resonance, one should next worry about resonances having orbital excitation. We have not done this, but note that  $L = 0$ ,  $S = 0$  resonances can contribute only to  $W_L$  and must have transition form factors going as  $1/q^2$  according to Bloom-Gilman duality. Brodsky and Farrar [1] point out that  $L \neq 0$  form factors should vanish more rapidly than  $L = 0$  form factors as  $q^2 \rightarrow \infty$ , but the rate of falloff has not been determined for general  $L$  in the present model.

## 2.6 Order- $g^6$ Diagrams

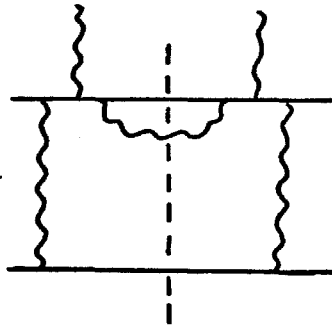
We have examined a very limited set of order- $g^6$  diagrams and find evidence that our main results do not change as one increases the order of the perturbation. Diagrams with additional virtual gluons will not be discussed as these lead into important but unresolved, infrared issues. We have looked only at diagrams with real gluons in the final state (see Figure 2.3), and find that these give  $W_T \propto (\omega-1)^2$ .

## 2.7 Conclusions

The present model of the pion wavefunction "tail" as given by free quarks exchanging one gluon gives results which seem reasonable, if a bit unexpected. The behavior  $W_L \propto m^2/q^2$  is expected from the Drell-Yan-West relation, but the result  $W_T \propto (\omega-1)^2$ , together with Bloom-Gilman duality, demands an unexpectedly rapid falloff of resonance transition



(a)



(b)

Figure 2.3

Some Order  $-g^6$  Diagrams Contributing  
To The Pion Structure Functions

form factors, namely  $(1/q^2)^2$ . This behavior is predicted for the  $\pi$ - $\rho$  transition, suggesting that our model is consistent with Bloom-Gilman duality. A comparison of our results with experiment will be found in Chapter VI, in which a more realistic, properly normalized wavefunction is used.

Chapter II References and Footnotes

1. S. J. Brodsky and G. R. Farrar, Phys. Rev. Letters 31, 1153 (1973), and Phys. Rev. D 11, 1309 (1975); V. Matveev et al., Lett. Nuovo Cimento 7, 719 (1973).
2. S. D. Drell and T. M. Yan, Phys. Rev. Letters 24, 181 (1970); G. B. West, Phys. Rev. Letters 24, 1206 (1970).
3. R. P. Feynman, private communication and seminar at Caltech.
4. R. F. Schwitters, SLAC-PUB-1666 (1975), and R. Hollebeek, Lawrence Berkeley Laboratory Report No. LBL-3874.
5. It is shown in Appendix A that  $W_T$  does not contain an  $\omega$ -independent,  $1/Q^2$  piece and that, therefore,  $W_L/W_T$  grows as  $\omega \rightarrow 1$  with  $Q^2$  finite.
6. E. D. Bloom and F. J. Gilman, Phys. Rev. Letters 25, 1140 (1970).

## Chapter III

## THE PION BETHE-SALPETER WAVEFUNCTION

This chapter is a short introduction to properties of the pion wavefunction that can be discussed without reference to the Bethe-Salpeter equation or the renormalization group. Much of this material can be found in the literature, but we have elaborated areas that are important in the following chapters.

After a brief introduction to the use of the Bethe-Salpeter wavefunction in perturbation theory, its P, G and T symmetry properties are discussed. The final topic is Wick's spectral representation, which is shown to have a close connection with parton model and light-cone ideas.

### 3.1 Definition of the Bethe-Salpeter Wavefunction

The pion wavefunction in configuration space is defined as

$$\chi_{ab}(p, x) = \langle 0 | T u_a \left( \frac{x}{2} \right) \bar{d}_b \left( -\frac{x}{2} \right) | \pi^+ \rangle \quad (3-1)$$

To avoid a proliferation of sub- and superscripts, an explicit choice of quark and hadron flavors has been made, and color indices on the quark fields have been suppressed, but not summed over. The quark Dirac indices are given explicitly as a and b here, but will be suppressed in some later formulae for the sake of brevity.

The wavefunction in momentum space is

$$\phi_{ab}(p, k) = \int d^4x e^{ik \cdot x} \chi_{ab}(p, x) \quad (3-2)$$

Both  $\chi$  and  $\Phi$  depend upon the pion momentum in a way that is most clearly seen by Lorentz-decomposing into scalar wavefunctions. Taking into account the parity of the pion, the general decomposition of the configuration space wavefunction is

$$\begin{aligned} \chi_{ab}(p, x) = & \gamma_5 \{ \chi_1(x^2, p \cdot x) \not{x} + \frac{1}{2} \chi_2(x^2, p \cdot x) [\not{x}, \not{p}] \\ & + \chi_3(x^2, p \cdot x) + \chi_4(x^2, p \cdot x) \not{x} \} \otimes I \end{aligned} \quad (3-3)$$

The pion momentum is  $p$  and  $I$  is a unit color matrix. The scalar wavefunctions  $\chi_i$  depend only upon the invariants  $x^2$  and  $p \cdot x$ .

Considering rotations of the coordinate system, Leutwyler [1] shows that  $\chi_1$  and  $\chi_2$  are, respectively,  $L = 0$  and  $L = 1$  portions of the wavefunction. The same comment applies to  $\chi_3$  and  $\chi_4$ . The corresponding decomposition of the momentum space wavefunction is

$$\begin{aligned} \Phi(p, k) = & \gamma_5 \{ \Phi_1(k^2, p \cdot k) \not{k} + \frac{1}{2} \Phi_2(k^2, p \cdot k) [\not{k}, \not{p}] \\ & + \Phi_3(k^2, p \cdot k) + \Phi_4(k^2, p \cdot k) \not{k} \} \otimes I \end{aligned} \quad (3-4)$$

Because of the  $x$ -dependent Lorentz factors appearing in expression (3-3), the  $\Phi_i$  are not simply the Fourier transforms of  $\chi_i$ .

$$\Phi_1(k^2, p \cdot k) = \chi_1(k^2, p \cdot k) - i \frac{\partial}{\partial p \cdot k} \chi_4(k^2, p \cdot k) \quad (3-5a)$$

$$\Phi_2(k^2, p \cdot k) = -2i \frac{\partial}{\partial k^2} \chi_2(k^2, p \cdot k) \quad (3-5b)$$

$$\Phi_3(k^2, p \cdot k) = \chi_3(k^2, p \cdot k) \quad (3-5c)$$

$$\Phi_4(k^2, p \cdot k) = -2i \frac{\partial}{\partial k^2} \chi_4(k^2, p \cdot k) \quad (3-5d)$$

The Fourier transforms of  $\chi_i(x^2, p \cdot x)$  are denoted  $\chi_i(k^2, p \cdot k)$  above.

### 3.2 Feynman Rules for the Bethe-Salpeter Wavefunction

Huang and Weldon [2] give a very clear exposition of the application of the Bethe-Salpeter formalism to the calculation of physical amplitudes for bound-state scattering. The graphical rules amount to a convolution of Bethe-Salpeter wavefunctions and an irreducible quark kernel. The rules will be illustrated here by means of two examples of particular interest.

The simplest example is the calculation of the pion decay constant, defined by


$$\langle 0 | A_\mu^{\pi^+} | \pi^+ \rangle = i f_\pi p_\mu \quad (3-6)$$

where  $A_\mu^{\pi^+}$  is one member of the isotriplet of axial vector currents, and states are normalized according to

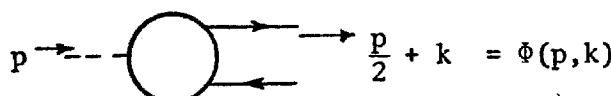
$$\langle m | n \rangle = 2E_n \delta_{mn} (2\pi)^3 \delta^3(\vec{p}_n - \vec{p}_m) \quad (3-7)$$

$$\langle 0 | 0 \rangle = 1 \quad (3-8)$$

Graphically, the calculation for  $f_\pi$  is

$$p_\mu \rightarrow \text{---} \bigcirc \text{---} = i f_\pi p_\mu \quad (3-9)$$


where the momentum space wavefunction is

$$p \rightarrow \text{---} \bigcirc \text{---} = \Phi(p, k) \quad (3-10)$$


What (3-9) really means is



$$\int \frac{d^4 k}{(2\pi)^4} \text{Tr } \phi(k) \left[ -i\gamma_5 \gamma_\mu \right] = i f_\pi p_\mu \quad (3-11)$$

The axial current vertex is bare because the rules prescribe that the quark-antiquark axial-vector current kernel be two-particle irreducible in the pion channel. One may regard the dressing of this vertex as already contained in the wavefunction. The wavefunction also contains, by definition, propagators for the quark and antiquark. The trace in (3-11) is over spin and color indices. In terms of the scalar wavefunctions,

$$f_\pi = 12 \int \left( \phi_1 + \frac{p \cdot k}{m^2} \phi_4 \right) \frac{d^4 k}{(2\pi)^4} \quad (3-12)$$

Expression (3-12) is a sum rule equivalent to one of Leutwyler's light cone sum rules (1).

Another example of interest is the calculation of the pion electromagnetic form factor

$$-i F_\pi(q^2) \left[ q_\mu + 2p_\mu \right] = \begin{array}{c} \text{---} \circlearrowleft \text{---} \\ \text{---} \circlearrowright \text{---} \\ \text{---} \square \text{---} \\ \text{---} \circlearrowright \text{---} \\ \text{---} \circlearrowleft \text{---} \\ \text{---} \text{out} \text{---} \end{array} \quad (3-13)$$

(A curly brace labeled 'q' is above the square vertex in the diagram.)

The photon-quark kernel has no quark legs and is two-particle irreducible in the pion channels. It can be broken down into connected and disconnected parts.

$$\begin{array}{c} \text{---} \square \text{---} \\ \text{---} \square \text{---} \end{array} = \begin{array}{c} \text{---} \circlearrowleft \text{---} \\ \text{---} \circlearrowright \text{---} \end{array}^{-1} + \begin{array}{c} \text{---} \square \text{---} \\ \text{---} \square \text{---} \end{array} \quad (3-14)$$

(The second square vertex in the diagram has an 'X' inside it.)

$$\text{Diagram} = \text{Diagram}_1 + \text{Diagram}_2 + \text{Diagram}_3 + \dots \quad (3-15)$$

$$\text{Diagram} = \text{Diagram}_1 + \text{Diagram}_2 + \dots \quad (3-16)$$

The disconnected part is the proper electromagnetic vertex with gluon interactions, but with no flavor interactions. The outgoing wavefunction in (3-13) is the Fourier transform of

$$\chi_{ab}^{\text{out}}(p, x) = \langle \pi^+ | \text{Td}_a \left( \frac{x}{2} \right) \bar{u}_b \left( -\frac{x}{2} \right) | 0 \rangle \quad (3-17)$$

In the next section, we will find that discrete symmetries enable one to express the outgoing wavefunction in terms of the incoming wavefunction.

### 3.3 Discrete Symmetries

Under the parity operator, fermion fields transform in the standard Dirac matrix representation according to

$$P\psi(\vec{x})P^{-1} = \gamma_0\psi(-\vec{x}) \quad (3-18)$$

Having odd parity, a single pion state of three-momentum  $\vec{p}$  transforms as

$$P|\pi, \vec{p}\rangle = -|\pi, -\vec{p}\rangle \quad (3-19)$$

Taking the vacuum to have even parity, the wavefunction (3-1) must satisfy

$$\chi(\vec{x}, \vec{p}) = -\gamma_0 \chi(-\vec{x}, -\vec{p})\gamma_0 \quad (3-20)$$

This condition dictates the  $\gamma_5$  factor employed in the Lorentz decomposition, expression (3-3).

Under charge conjugation,

$$C \psi C^{-1} = i \gamma^2 \psi^* \quad (3-21)$$

where \* denotes operator conjugate. Applying this to the wavefunction gives a relationship between the  $\pi^+$  and  $\pi^-$  wavefunctions that is not especially useful to us. If G-parity is assumed to be a good symmetry, much of our later work will be simplified. Displaying the fermion isospin indices,

$$G \psi_i G^{-1} = \exp\left[i\pi I_{yij}\right] C \psi_j C^{-1} \quad (3-22)$$

$$G|\pi\rangle = -|\pi\rangle \quad (3-23)$$

This gives

$$\chi(x) = -\gamma^2 \gamma^0 \chi^T(-x)\gamma^0 \gamma^2 \quad (3-24)$$

where T denotes a matrix transposition.

Under time reversal,

$$T \psi(x_0) T^{-1} = i \gamma^1 \gamma^3 \psi(-x_0) \quad (3-25a)$$

$$T \psi^*(x_0) T^{-1} = -i \gamma^1 \gamma^3 \psi^*(-x_0) \quad (3-25b)$$

$$T|\pi, \vec{p}\rangle = |\pi, -\vec{p}\rangle \quad (3-26)$$

Time reversal changes in-states to out-states, but this is immaterial for one-particle states. Splitting the antiunitary time reversal operator into the product of the charge conjugation operator and a unitary operator exposes one pitfall in its use.

$$T = U K \quad (3-27)$$

The Bethe-Salpeter wavefunction is a special case of the inner product  $\langle 0|B\rangle$ .

$$\langle 0|B\rangle = \langle 0|KB\rangle^* = \langle 0|U^{-1}UKB\rangle^* = \langle 0|TB\rangle^* \quad (3-28)$$

One misses the complex conjugation by wrongly acting to the left with  $T^{-1}$  as if  $T$  were unitary.

In order to apply time reversal, it is wise to exhibit the time-ordering of the fields explicitly by means of step functions. TP symmetry gives, as noted by Goldberger, Soper and Guth [3]:

$$\chi^{\text{out}}(x) = -\gamma^1 \gamma^3 \chi^T(-x) \gamma^3 \gamma^1 \quad (3-29)$$

The constraints on the invariant wavefunctions due to GP symmetry are:

$$\chi_1, \chi_2, \chi_3 = \text{even in } p \cdot x \quad (3-30a)$$

$$\chi_4 = \text{odd in } p \cdot x \quad (3-30b)$$

$$\Phi_1, \Phi_2, \Phi_3 = \text{even in } p \cdot k \quad (3-30c)$$

$$\Phi_4 = \text{odd in } p \cdot k \quad (3-30d)$$

Defining

$$\Phi^{\text{out}}(p, k) = \int d^4 x e^{-ik \cdot x} \chi^{\text{out}}(p, x) \quad (3-31)$$

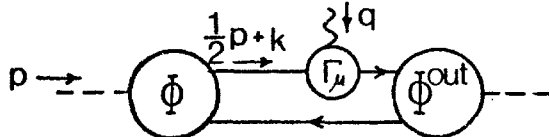
$$\begin{aligned} \Phi^{\text{out}}(p, k) = & \gamma_5 \left[ \Phi_1^{\text{out}}(k^2, p \cdot k) \not{p} \right. \\ & + \frac{1}{2} \Phi_2^{\text{out}}(k^2, p \cdot k) [K, \not{p}] + \Phi_3^{\text{out}}(k^2, p \cdot k) \\ & \left. + \Phi_4^{\text{out}}(k^2, p \cdot k) K \right] \otimes I \end{aligned} \quad (3-32)$$

the TP condition gives

$$\Phi_i^{\text{out}}(k^2, p \cdot k) = \Phi_i(k^2, p \cdot k), \quad i = 1, 2, 4 \quad (3-33a)$$

$$\Phi_3^{\text{out}}(k^2, p \cdot k) = -\Phi_3(k^2, p \cdot k) \quad (3-33b)$$

In order to illustrate the momentum and Dirac index conventions for outgoing wavefunctions, we will write out the loop integral for the disconnected part of the pion form factor.



$$(3-34)$$

$$= \int \frac{d^4 k}{(2\pi)^4} \text{Tr} \Phi^{\text{out}}\left(p+q, k+\frac{q}{2}\right) \Gamma^\mu \Phi(p, k) S_F^{-1}\left(k - \frac{p}{2}\right)$$

Note that an inverse fermion propagator is needed to lop off the lower leg of one of the wavefunctions. The trace is over Dirac and color indices. The color trace simply introduces a factor 3, as the four factors in the integrand of (3-34) are unit color matrices.

### 3.4 Spectral Representation of Bethe-Salpeter Wavefunction

We find it convenient to use Wick's spectral representation [4] for a number of reasons. First, one of the variables in the spectral functions turns out to be a scaling variable closely related to Feynman's  $x$ . Second, the spectral functions are simply related to Leutwyler's light cone spectral functions. Finally, the asymptotic spectral function will be found to factorize in its two variables, facilitating solution of the Bethe-Salpeter equation.

The invariant wavefunctions defined by expression (3-4) depend on two variables, so a two-dimensional spectral representation will be used. Wick introduced the representation

$$\phi_i(k^2, k \cdot p) = \int_0^\infty \int_{-\frac{1}{2}}^{\frac{1}{2}} \frac{g_i(\xi, t) d\xi dt}{\left[ k_1^2 \left( \frac{1}{2} - \xi \right) + k_2^2 \left( \frac{1}{2} + \xi \right) - t + i\epsilon \right]^3} \quad (3-35)$$

where

$$k_1 = \frac{p}{2} + k \quad (3-36)$$

$$k_2 = \frac{p}{2} - k \quad (3-37)$$

The momenta  $k_1$  and  $k_2$  are, respectively, the outgoing momenta of the upper and lower fermion legs. We will use this form for  $i = 1, 3, 4$  and represent  $\phi_2(k^2, p \cdot k)$  by

$$\phi_2(k^2, p \cdot k) = \int_0^\infty \int_{-\frac{1}{2}}^{\frac{1}{2}} \frac{g_2(\xi, t) d\xi dt}{k^2 - 2\xi p \cdot k - t + i\epsilon^4} \quad (3-38)$$

Choice of denominator power is a matter of taste. The choices above make all  $g_i$  dimensionless. The denominator power can always be reduced by integrating by parts on  $t$ , given that  $g_i(\xi, t)$  and a suitable number of derivatives vanish at  $t = 0$ . This is probably true, for it appears that  $g_i(\xi, t)$  must vanish for  $t$  smaller than a value set by the binding energy. The issue is clouded by the apparent nonexistence of the quark mass (in the ordinary sense) in QCD, but if quark states of mass  $m_q$  exist,

$$g_i(\xi, t) = 0 \quad \text{for } t < t_{\min} = m_q^2 - \frac{m_\pi^2}{4} \quad (3-39)$$

This follows from Wick's arguments about the analytic structure of the Bethe-Salpeter wavefunction. Inserting a complete set of states in (3-1)

$$\begin{aligned} \chi_{ab}(p, x) = & \sum_n \langle 0 | u_a \left( \frac{x}{2} \right) | n \rangle \langle n | \bar{d}_b \left( -\frac{x}{2} \right) | \pi^+ \rangle \theta(x_0) \\ & - \sum_m \langle 0 | \bar{d}_b \left( -\frac{x}{2} \right) | m \rangle \langle m | u_a \left( \frac{x}{2} \right) | \pi^+ \rangle \theta(-x_0) \end{aligned} \quad (3-40)$$

Translating the field operators to  $x = 0$  by means of

$$\psi(x) = e^{iP \cdot x} \psi(0) e^{-iP \cdot x} \quad (3-41)$$

$$\begin{aligned} \chi_{ab}(p, x) = & \sum_n e^{i\left(\frac{p}{2} - k_n\right) \cdot x} \langle 0 | u_a(0) | n \rangle \langle n | \bar{d}_b(0) | \pi^+ \rangle \theta(x_0) \\ & - \sum_m e^{-i\left(\frac{p}{2} - k_m\right) \cdot x} \langle 0 | \bar{d}_b(0) | m \rangle \langle m | u_a(0) | \pi^+ \rangle \theta(-x_0) \end{aligned} \quad (3-42)$$

Without worrying about the problem that the intermediate states  $|m\rangle$  and  $|n\rangle$  have quark quantum numbers, (3-42) shows that, for  $t > 0$ , the wavefunction contains only positive frequencies while, for  $t < 0$ , only negative frequencies are present. Taking the Fourier transforms of  $\chi_{ab}(p, x)$  these "Feynman boundary conditions" require  $\Phi(p, k)$  to be analytic everywhere in the  $k_0$  plane except on two cuts. The right-hand cut begins at the minimum frequency appearing in (3-42) for  $t > 0$ , which is

$$\omega_{\min} = k_N^0 - \frac{m_\pi}{2} \quad (3-43)$$

in the pion rest frame.  $|N\rangle$  is the lowest mass intermediate state contributing to the first sum in (3-42) and, if this is a single up-quark state of mass  $m_q$ ,

$$\omega_{\min} = \left( |\vec{k}|^2 + m_q^2 \right)^{\frac{1}{2}} - \frac{m_\pi}{2} \quad (3-44)$$

Taking the down-quark mass equal to the up-quark mass for simplicity, the left-hand cut extends to the least negative frequency in the second sum of (3-42), which turns out to be  $-\omega_{\min}$ .



Returning to the double spectral functions, it can be readily shown that the  $\Phi_i$  are analytic except at the point

$$k_0 = m_\pi \xi \pm \left( m_\pi^2 \xi^2 + |\vec{k}|^2 + t - i\epsilon \right)^{\frac{1}{2}} \quad (3-45)$$

Considering that  $t$  ranges from zero to infinity, this gives two cuts with branch points  $\pm \omega_{\min}$  where

$$\omega_{\min} = \left( \frac{m_\pi^2}{4} + |\vec{k}|^2 + t_{\min} - i\epsilon \right)^{\frac{1}{2}} - \frac{m_\pi}{2} \quad (3-46)$$

At the right-hand branch point, only the  $\xi = -\frac{1}{2}$  part of the spectral function contributes while only the  $\xi = \frac{1}{2}$  part contributes at the left-hand branch point. We have assumed that the spectral functions vanish for  $t < t_{\min}$ , and a comparison of (3-44) and (3-46) shows that  $t_{\min}$  must have the value  $m_q^2 - \frac{m_\pi^2}{4}$ , as given in (3-39). This quantity will be positive if the binding energy is positive, and a positive  $t_{\min}$  (or  $\omega_{\min}$ , which is nearly the same thing) is to be desired, for it allows one to set  $g_i(\xi, t)$  and its derivatives equal to zero at  $t = 0$  and also permits a Wick rotation in the relative energy variable,  $k_0$ .

If quark confinement means that there are no finite-energy states having quark quantum numbers, the above discussion breaks down at its starting point, expression (3-40). Perhaps  $t_{\min}$  and the binding energy are infinite, and the wavefunction is analytic for all values of the relative energy except for an essential singularity at infinity. This would be a problem for us, as the wavefunctions considered here are almost power-behaved and certainly not analytic for all finite values of the relative energy.

To proceed with the present approach, then, the existence of finite-energy states having quark quantum numbers must be admitted. These need not be single-particle states, and could conceivably be coherent states of some sort. The quantity  $m_q$  is the minimum invariant mass for these states, and the branch point at  $k_0 = \omega_{min}$  corresponds to  $k_1^2 = m_q^2$ , where  $k_1 = \frac{p}{2} + k$  is the momentum leaving one leg of the wave function in momentum space. The other branch point corresponds to  $k_2^2 = m_q^2$ , where  $k_2 = \frac{p}{2} - k$ .

### 3.5 Wavefunction on the Light Cone and at Short Distances

The double spectral functions are helpful in discussing properties of the wavefunction on the light cone

$$x^2 \rightarrow 0 \quad (3-47)$$

and at short distances

$$x^\mu \rightarrow 0 \quad (3-48)$$

Considering the wavefunction in momentum space, the primary contribution to the light cone region comes from the momentum space region

$$k^2 \rightarrow \infty, \quad \frac{2p \cdot k}{k^2} = \text{finite} \quad (3-49)$$

while the primary contribution to the short distance region comes from

$$k^2 \rightarrow \infty, \quad \frac{2p \cdot k}{k^2} \rightarrow 0 \quad (3-50)$$

We will refer to (3-49) and (3-50) as the light cone and short distance limits, while remembering that these limits are actually defined by (3-47) and (3-48). For example, at  $x^\mu = 0$ , the configuration space

wavefunction is equal to the integral of the momentum space wavefunction over all momenta. In this sense, large and small momenta enter at short distances.

To gain some insight into the spectral representation, a connection will be established between the variables  $\xi$ ,  $t$ , and the parton model variables  $x$  and  $\vec{k}_T^2$ , where  $x$  is the longitudinal momentum fraction of a quark, and  $\vec{k}_T^2$  is the square of its transverse momentum.

$$k_1 = k_0, \vec{k}_T, x p_3 \quad (3-51)$$

$$p = p_0, \vec{0}, p_3 \quad (3-52)$$

A more convenient momentum to use is  $k = k_1 - \frac{p}{2}$ , in terms of which a typical invariant wavefunction can be written

$$\phi_3 = \frac{1}{2} \int_0^\infty \int_{-\frac{1}{2}}^{\frac{1}{2}} \frac{\partial^2 g_3(\xi, t) / \partial t^2}{k^2 - 2p \cdot k \xi - t + i\epsilon} d\xi dt \quad (3-53)$$

In the infinite-momentum limit,  $p_0, p_3 \rightarrow \infty$ , and on the light cone, a little algebra shows that

$$\frac{k^2}{2p \cdot k} = x - \frac{1}{2} - \frac{\vec{k}_T^2}{2p \cdot k} \quad (3-54)$$

Then

$$\phi_3 \approx \frac{1}{4p \cdot k} \int_0^\infty \int_{-\frac{1}{2}}^{\frac{1}{2}} \frac{\partial^2 g_3(\xi, t) / \partial t^2}{x' - \xi + ip \cdot k \epsilon} d\xi dt \quad (3-55)$$

where

$$x' = x - \frac{1}{2} - \frac{k_T^2 + t}{2p \cdot k} \quad (3-56)$$

For simplicity, assume that  $g_3(\xi, t)$  factorizes into separate functions of  $\xi$  and  $t$ , as will be the case for the wavefunctions that will be encountered in Chapter V. In this case, the  $x$ -dependence of the imaginary part of the wavefunction is approximately the same as the  $\xi$ -dependence of the spectral function. The  $x$ -dependence of the real part of the wavefunction is nearly the same as the  $\xi$ -dependence of the Hilbert transform of the spectral function. Transverse momentum dependence cannot be factored from the  $x$ -dependence, and the scale of transverse momentum is set by the values of  $t$  occurring in the spectral function.

The double spectral functions are intimately related to the single spectral functions used by Leutwyler for the wavefunction on the light cone [1]. The simplest invariant wavefunction to discuss in this connection is  $\chi_3(x^2, p \cdot x)$ , which is the Fourier transform of  $\phi_3(k^2, p \cdot k)$ . Inserting the spectral representation for the latter function into the Fourier integral for  $\chi_3(x^2, p \cdot x)$ ,

$$\chi_3(x^2, p \cdot x) = \int_0^\infty \int_{-\frac{1}{2}}^{\frac{1}{2}} g_3(\xi, t) e^{-i\xi p \cdot x} K(x^2, \mu^2) d\xi dt \quad (3-57)$$

where

$$K(x^2, \mu^2) = \int \frac{d^4 k}{(2\pi)^4} \frac{e^{ik \cdot x}}{[k^2 - \mu^2 + i\epsilon]^3} \quad (3-58)$$

$$\mu^2 = t - \left(\frac{1}{4} - \xi^2\right) m_\pi^2 \quad (3-59)$$

The function  $K(x^2, \mu^2)$  can be recognized as the second derivative of a Feynman propagator.

$$K(x^2, \mu^2) = \frac{1}{2} \frac{\partial^2}{\partial(\mu^2)^2} \Delta_F(x^2, \mu^2) \quad (3-60)$$

$$\Delta_F(x^2, \mu^2) = \int \frac{d^4 k}{(2\pi)^4} \frac{1}{k^2 - \mu^2 + i\epsilon} \quad (3-61)$$

Expression (3-57) is useful in that it approximately separates the  $x^2$  and  $p \cdot x$  dependence of the wavefunction, the former being a convolution of the  $t$ -distribution with the kernel,  $K$ , and the latter being the Fourier transform of the  $\xi$ -distribution.

To examine the light cone limit,  $\Delta_F$  for small  $x^2$  can be used [5].

$$\begin{aligned} \Delta_F(x^2, \mu^2) &\cong \frac{1}{4\pi} \delta(x^2) + \frac{1}{4\pi^2} \frac{1}{i x^2} - \frac{\mu^2}{16\pi} \theta(x^2) \\ &+ \frac{i\mu^2}{16\pi^2} \ln \frac{\mu^2 |x^2|}{4} + \theta\left[|x^2|^{\frac{1}{2}} \ln|x^2|\right] \end{aligned} \quad (3-62)$$

The logarithmic singularity gives the leading contribution to  $K$  from which the following result can be obtained:

$$\chi_3(0, p \cdot x) = \int_{-\frac{1}{2}}^{\frac{1}{2}} b_3(\xi) e^{-i\xi p \cdot x} d\xi \quad (3-63)$$

$$b_i(\xi) = \frac{i}{32\pi^2} \int_0^{\infty} \frac{g_i(\xi, t) dt}{t - \left(\frac{1}{4} - \xi^2\right) \frac{m^2}{\pi} - i\epsilon} \quad (3-64)$$

Expression (3-63) is Leutwyler's definition of the light-cone spectral function,  $b_3(\xi)$ . Expression (3-64) provides us with a connection between Wick's and Leutwyler's spectral functions.

The other invariant wave functions are not so conveniently expressed in configuration space in terms of the spectral functions. One frequently-occurring linear combination that is expressible in simple form is

$$\chi_1(x^2, p \cdot x) + \frac{p \cdot x}{2} \chi_4(x^2, p \cdot x) = \int_0^{\infty} \int_{-\frac{1}{2}}^{\frac{1}{2}} (g_1 + \xi g_4) e^{-i\xi p \cdot x} K(x^2, \mu^2) d\xi dt \quad (3-65)$$

Chapter III References and Footnotes

1. H. Leutwyler, Nuc. Physics B76, 413 (1974).
2. K. Huang and H. A. Weldon, Phys. Rev. D 11, 257 (1975); S. Mandelstam, Proc. Roy. Soc. A 233, 248 (1955); E. E. Salpeter and H. A. Bethe, Phys. Rev. 84, 1232 (1951).
3. A. H. Guth and D. E. Soper, Phys. Rev. D 12, 1143 (1975); M. L. Goldberger et al., Phys. Rev. D 14, 117 (1976) and Phys. Rev. D 14, 2633 (1976).
4. G. C. Wick, Phys. Rev. 96, 1124 (1954).
5. N. N. Bogoliubov and D. V. Shirkov, Introduction to the Theory of Quantized Fields, p. 152, Wiley-Interscience, New York, 1959.

## Chapter IV

ASYMPTOTIC BEHAVIOR OF THE PION BETHE-SALPETER  
WAVEFUNCTION AS DETERMINED BY THE RENORMALIZATION GROUP

The renormalization group, coupled with the operator product expansion, provides useful information about the asymptotic behavior of the Bethe-Salpeter wavefunction. Appelquist and Poggio apply these methods to the two-body wavefunction in a simple asymptotically-free theory,  $\phi^3$  in six dimensions [1]. Callan and Gross [2] and Goldberger, Soper and Guth [3] discuss the two-fermion wavefunction in finite fixed-point theories. Some of the results of the above papers carry over into QCD, but we will find that a detailed examination of the problem produces several interesting new results.

Appelquist and Poggio have shown that moments of Wick's spectral functions enter into a discussion of the asymptotic wavefunction in much the same way as moments of structure functions enter in treatments of scaling in electroproduction. The operator product expansion does not constrain the pion wavefunction as much as it constrains the electroproduction structure functions. The pion wavefunction is a non-forward matrix element, which brings in a host of operators not found in electroproduction. As a result, the  $m^{\text{th}}$  moment is "contaminated" by the operators from the levels below  $m$  in the spin tower and does not carry a single power of logarithm. In a gauge theory, the wavefunction is not gauge-invariant because it describes the "insides" of the hadron, which are definitely not colorless. To this extent, the wavefunction is non-physical, and predictions about its asymptotic behavior do not translate effortlessly into statements about cross-sections.



Even with these complications, it will be possible to make predictions about the asymptotic behavior of the pion form factor, which we will do in Chapter VI. On the formal side, the renormalization group results will allow us to comment on the existence of some of Leutwyler's light-cone sum rules [4] and will provide a check on asymptotic solutions of the Bethe-Salpeter equation.

#### 4.1 Symmetry Constraints on the Operator Product Expansion

The bilocal operator to be expanded is

$$O(x) = T u_a \left( \frac{x}{2} \right) \bar{d}_b \left( -\frac{x}{2} \right) \quad (4-1)$$

and the matrix element  $\langle 0 | O(x) | \pi \rangle$  is the Bethe-Salpeter wavefunction. The usefulness of the expansion increases if we can argue that certain classes of local operators do not appear because they have the wrong quantum numbers or transformation properties. Further simplification will result by omitting terms that do not contribute to the desired matrix element.

It is helpful to make a list of the properties that the local operators of interest must possess.

1. Proper behavior under local gauge transformations.
2. Singlets under global gauge transformations.
3. Flavor quantum numbers of pion.
4. Odd Parity.
5. Odd G-Parity
6. Leading light cone behavior.

If any of the operators that pass through this sieve turn out to have directly measurable  $\langle 0 | | \pi \rangle$  matrix elements, that is an added bonus, giving sum rules in addition to the asymptotic logarithmic behavior.

In electroproduction, one is interested in an expansion of a bilocal product of color-gauge-invariant currents. Condition (1) is met in that case by admitting only gauge-invariant operators. The operator we wish to expand is obviously gauge-variant, and one expects a mixture of local operators that employ ordinary derivatives and gluon fields, not necessarily in the covariant derivative ( $\mathcal{D}_\mu$ ) combination. We will present an argument that only ordinary derivatives should appear in the expansion, so that operators such as

$$\bar{\psi} \gamma_5 \psi, \bar{\psi} \gamma_5 \partial_\mu \psi, \bar{\psi} \gamma_5 \gamma_\mu \psi$$

are to be included, while operators such as

$$\bar{\psi} \gamma_5 \mathcal{D}_\mu \psi, \bar{\psi} \gamma_5 \gamma_\mu A_\nu \psi$$

are to be excluded.

For simplicity, consider an abelian gauge theory and write a few terms in the expansion of  $\bar{\psi}(0) \psi(x)$ .

$$\begin{aligned} \bar{\psi}(0) \psi(x) = & \bar{\psi} \psi c_0(x^2) + \bar{\psi} \partial_\mu \psi x^\mu c_1(x^2) \\ & + \alpha \bar{\psi} A_\mu \psi x^\mu c_2(x^2) \end{aligned} \tag{4-2}$$

The  $c_i(x^2)$  are dimensionless functions of  $x^2 M^2$ , where  $M^2$  is the renormalization mass. Under a gauge transformation, the right- and left-hand

sides of the expansion should behave in the same way. The fields transform as follows:

$$\psi(x) = e^{ig\theta(x)} \psi'(x), \quad A_\mu(x) = A'_\mu(x) + \partial_\mu \theta(x) \quad (4-3)$$

Taking  $\theta(0) = 0$  for convenience, the left-hand side of (4-2) becomes

$$\begin{aligned} \bar{\psi}(0) \psi(x) &= e^{ig\theta(x)} \bar{\psi}'(0) \psi'(x) \\ &= (1 + ig\partial_\mu \theta x^\mu + \dots) \bar{\psi}'(0) \psi'(x) \end{aligned} \quad (4-4)$$

To see what the right-hand side does, consider the gauge transformation properties of the local operators. First, according to Brandt and Preparata [5], coefficient functions can be generated by taking short distance limits of bilocal operators.

$$\bar{\psi}(0) \psi(0) c_0(x^2) = \lim_{x \rightarrow 0} \bar{\psi}(0) \psi(x) \quad (4-5a)$$

$$\bar{\psi}(0) \partial_\mu \psi(0) c_1(x^2) = \lim_{x \rightarrow 0} \bar{\psi}(0) \partial_\mu \psi(x) - \bar{\psi}(0) \psi(0) \partial_\mu c_0(x^2) \quad (4-5b)$$

$$\bar{\psi}(0) A_\mu(0) \psi(0) c_2(x^2) = \lim_{x \rightarrow 0} \bar{\psi}(0) A_\mu(x) \psi(x) \quad (4-5c)$$

Substituting (4-3) into the right-hand side of (4-5), and allowing the coefficient functions to be gauge-dependent,

$$\bar{\psi} \psi c_0(x^2) = \bar{\psi}' \psi' c'_0(x^2) \quad (4-6a)$$

$$\bar{\psi} \partial_{\mu} \psi c_1(x^2) = \bar{\psi}' \partial_{\mu} \psi' c_1'(x^2) + ig \partial_{\mu} \theta \bar{\psi}' \psi' c_0'(x^2) \quad (4-6b)$$

$$\bar{\psi} A_{\mu} \psi c_2(x^2) = \bar{\psi}' A'_{\mu} \psi' c_2'(x^2) + \partial_{\mu} \theta \bar{\psi}' \psi' c_0'(x^2) \quad (4-6c)$$

After an infinitesimal gauge transformation, expression (4-2) in the short distance limit is

$$\begin{aligned} \left(1 + ig \partial_{\mu} \theta x^{\mu}\right) \bar{\psi}' \psi' c_0'(x^2) &= \left(1 + ig \partial_{\mu} \theta x^{\mu} \right. \\ &\left. + \alpha \partial_{\mu} \theta x^{\mu}\right) \bar{\psi}' \psi' c_0'(x^2) \end{aligned} \quad (4-7)$$

This result shows that the  $\bar{\psi} A_{\mu} \psi$  operator has no place in the expansion, as it upsets the gauge transformation properties.

This argument can be readily extended to exclude all  $A_{\mu}$  terms from the operator product expansion. Of course, the validity of this argument is entirely dependent upon assumption (4-5). To lend plausibility to the above result, consider the gauge-invariant operator

$$\bar{\psi}(0) e^{-ig \int_0^x A^{\mu} dx_{\mu}} \psi(x)$$

The expansion of this operator would contain covariant derivatives and no ordinary derivatives. The gauge-invariant wavefunction formed by taking the  $\langle 0 | |\pi\rangle$  matrix element of the above operator gives the amplitude to find a quark at  $x$ , an antiquark at the origin, and an infinity of gluons at points between. In the operator product expansion, these gluons stem from the vector potential terms. The Bethe-Salpeter wavefunction, on the other hand, gives the amplitude to find a quark and an

antiquark with no gluons. Since this is the case, it would be embarrassing to find gluon fields in the operator product expansion of  $\bar{\psi}(0) \psi(x)$ . The expansion of this operator is similar to an ordinary Taylor series with ordinary derivatives, but no covariant derivatives. The expansion of a current-current product is more complicated because the fields in the expansion are not the currents themselves.

It appears that the same argument that excludes gluon fields from the expansion also excludes ghost fields, since their presence would change the gauge transformation properties of the right-hand side of the expansion.

Conditions (2) and (3) above lead to the admission of color singlet local operators and the exclusion of flavor singlet operators. This means that we escape the complication that arises in electroproduction due to the existence of two classes of flavor singlet operators.

Condition (4) will be partially met if attention is restricted to the bilocal operators

$$O(x) = T \bar{d}_a \left[ -\frac{x}{2} \right] \gamma_5 u_a \left( \frac{x}{2} \right) \quad (4-8)$$

$$O^\mu(x) = T \bar{d}_a \left[ -\frac{x}{2} \right] \gamma^\mu \gamma_5 u_a \left( \frac{x}{2} \right) \quad (4-9)$$

$$O^{\mu\nu}(x) = T \bar{d}_a \left[ -\frac{x}{2} \right] [\gamma^\mu, \gamma^\nu] \gamma_5 u_a \left( \frac{x}{2} \right) \quad (4-10)$$

The common subscript "a" denotes a sum on color indices. Dirac indices are suppressed, but summed over in the usual way.

It remains to list the local operators of odd parity. Following common practice, these will be organized according to spin and twist = (dimension-spin). To produce an operator of definite spin from something like  $\bar{\psi} \gamma^\mu \partial^\nu \psi$  requires a symmetrization and trace subtraction that will not be made explicit. The list of local operators is given in Table 4.1

		<u>Twist 3</u>		
G-Parity	Spin	↙ 0	↙ 1	↙ 2
-		$\bar{d} \gamma_5 u, \partial_\alpha \bar{d} \gamma_5 u, \partial_\alpha \partial_\beta \bar{d} \gamma_5 u, \dots$		
+		$\bar{d} \gamma_5 \overleftrightarrow{\partial}_\mu u, \partial_\alpha \bar{d} \gamma_5 \overleftrightarrow{\partial}_\mu u, \partial_\alpha \partial_\beta \bar{d} \gamma_5 \overleftrightarrow{\partial}_\mu u, \dots$		
-		$\bar{d} \gamma_5 \overleftrightarrow{\partial}_\mu \overleftrightarrow{\partial}_\nu u, \dots$		
		<u>Twist 2</u>		
		↙ 0	↙ 1	
-		$\bar{d} \gamma^\mu \gamma_5 u, \partial_\alpha \bar{d} \gamma^\mu \gamma_5 u, \partial_\alpha \partial_\beta \bar{d} \gamma^\mu \gamma_5 u, \dots$		
+		$\bar{d} \gamma^\mu \gamma_5 \overleftrightarrow{\partial}_\nu u, \dots$		
		...		

Table 4.1. Local Operators of Odd Parity

Operators not on this list, but satisfying conditions 1-4, have been excluded either by reducing them to one of the above by means of Dirac algebra, or by noting that they are antisymmetric with respect to Lorentz indices. In the notation above,

$$\bar{d} \gamma_5 \partial_\mu u = \left\{ \bar{d}(x) \gamma_5 \partial_\mu u(x) - \left[ \partial_\mu d(x) \right] \gamma_5 u(x) \right\} \quad x = 0$$

$$\partial_\mu \bar{d} \gamma_5 u = \left\{ \partial_\mu \left[ \bar{d}(x) \gamma_5 u(x) \right] \right\} \quad x = 0$$

Goldberger, Guth, and Soper make the same distinction between anti-symmetric and symmetric derivatives [3]. This is especially important for us, because the two types of derivative have opposite G-parity, as will be seen. To understand why it is necessary to worry about two types of operator derivative, we shall examine a general matrix element of a local operator formed by taking a derivative of another local operator, denoted  $O_L(x)$ . Let A and B be states having definite four-momentum  $p_A$  and  $p_B$ . Then

$$\begin{aligned} \langle A | \partial_\mu O_L(0) | B \rangle &\equiv \left\{ \partial_\mu \langle A | O_L(x) | B \rangle \right\} \quad x = 0 \\ &= \left\{ \partial_\mu \langle A | e^{i p \cdot x} O_L(0) e^{-i p \cdot x} | B \rangle \right\} \quad x = 0 \\ &= i(p_A - p_B)_\mu \langle A | O_L(0) | B \rangle \end{aligned}$$

In electroproduction, one is interested in a forward matrix element where  $p_A = p_B$ , so the symmetrical derivatives do not enter. It is clear that the symmetrical derivative operators are trivially related to the operator from which they are derived, and that any renormalization procedure that makes matrix elements of  $O(0)$  finite will do the same for  $\partial_\mu O(0)$ . It follows that a symmetrically-derived operator has the same anomalous dimensions as its "parent."

There are three operator product expansions to be performed, and in order to apply condition 5 above, it is necessary to study the behavior

under G-parity of the 3 bilocals given by expressions (4-8, -9, -10).

With the G-parity operator as defined in expression (3-22),

$$G0(x)G^{-1} = -0(-x) \quad (4-11a)$$

$$G0^\mu(x)G^{-1} = -0^\mu(-x) \quad (4-11b)$$

$$G0^{\mu\nu}(x)G^{-1} = 0^{\mu\nu}(-x) \quad (4-11c)$$

The local operators have definite G-parity. They are normal-ordered rather than time-ordered, but the treatment of G-parity proceeds in the same way as for the time-ordered bilocals. The essential point is that the G-parity transformation changes  $u$  to  $\bar{d}$  and vice-versa, and that the transposition needed to place  $u$  and  $\bar{d}$  in their original order introduces a minus sign. Setting  $x = 0$  in (4-11), it follows that  $\bar{d} \gamma_5 u$  and  $\bar{d} \gamma^\mu \gamma_5 u$  have odd G-parity. With  $N$  antisymmetric derivatives, transposition introduces an additional factor  $(-1)^N$ . Symmetrical derivatives do not affect transposition, so any number can be applied without changing G-parity. Given the odd G-parity of the pion, only operators having an even number of antisymmetric derivatives will have non-vanishing  $\langle 0|0|\pi\rangle$  matrix elements.

In determining the degree of singularity of the coefficient functions near the light cone, dimensional analysis leads to the conclusion that the twist-two operators will be dominant if the coefficient functions contain no powers of mass. At least one such power of mass must be present in the twist-two coefficient functions of  $T \bar{d} \left(\frac{x}{2}\right) \gamma_5 u \left(-\frac{x}{2}\right)$  and  $T \bar{d} \left(\frac{x}{2}\right) [\gamma^\mu, \gamma^\nu] \gamma_5 u \left(-\frac{x}{2}\right)$ , because these operators have odd  $\gamma_5$ -symmetry.



In the next chapter, fermion mass is set equal to zero in order to simplify the solution of the Bethe-Salpeter equation, so we will omit twist-two operators in the expansions of the  $\gamma_5$ -odd bilocals.

For our purposes, the relevant terms in the operator product expansions are

$$\begin{aligned}
T \bar{d}\left(\frac{x}{2}\right) \gamma_5 u\left(-\frac{x}{2}\right) &= \bar{d} \gamma_5 u a_0(x^2) + \left\{ c_{02} [\partial_{\mu_1} \partial_{\mu_2} \bar{d} \gamma_5 u] a_0(x^2) \right. \\
&+ \left. \bar{d} \gamma_5 \overleftrightarrow{\partial}_{\mu_1} \overleftrightarrow{\partial}_{\mu_2} u a_2(x^2) \right\} x^{\mu_1} x^{\mu_2} \\
&+ \left\{ c_{04} [\partial_{\mu_1} \partial_{\mu_2} \partial_{\mu_3} \partial_{\mu_4} \bar{d} \gamma_5 u] a_0(x^2) \right. \\
&+ c_{24} [\partial_{\mu_1} \partial_{\mu_2} \bar{d} \gamma_5 \overleftrightarrow{\partial}_{\mu_3} \overleftrightarrow{\partial}_{\mu_4} u] a_2(x^2) \\
&+ \left. \bar{d} \gamma_5 \overleftrightarrow{\partial}_{\mu_1} \overleftrightarrow{\partial}_{\mu_2} \overleftrightarrow{\partial}_{\mu_3} \overleftrightarrow{\partial}_{\mu_4} u a_4(x^2) \right\} x^{\mu_1} x^{\mu_2} x^{\mu_3} x^{\mu_4}
\end{aligned} \tag{4-12a}$$

$$\begin{aligned}
T \bar{d}\left(\frac{x}{2}\right) \gamma^\mu \gamma_5 u\left(-\frac{x}{2}\right) &= \bar{d} \gamma^\mu \gamma_5 u b_1(x^2) \\
&+ \left\{ a_{02} [\partial_{\mu_1} \partial_{\mu_2} \bar{d} \gamma^\mu \gamma_5 u] b_1(x^2) \right. \\
&+ \left. \bar{d} \gamma^\mu \gamma_5 \overleftrightarrow{\partial}_{\mu_1} \overleftrightarrow{\partial}_{\mu_2} u b_3(x^2) \right\} x^{\mu_1} x^{\mu_2} + \dots \\
&+ x^\mu d_{01} \bar{d} \gamma_{\mu_1} \gamma_5 u x^{\mu_1} b_1(x^2) \\
&+ x^\mu \left\{ d_{03} [\partial_{\mu_1} \partial_{\mu_2} \bar{d} \gamma_{\mu_3} \gamma_5 u] b_1(x^2) \right. \\
&+ \left. d_{23} \bar{d} \gamma_{\mu_1} \gamma_5 \overleftrightarrow{\partial}_{\mu_2} \overleftrightarrow{\partial}_{\mu_3} u b_3(x^2) \right\} x^{\mu_1} x^{\mu_2} x^{\mu_3} + \dots
\end{aligned} \tag{4-12b}$$

$$\begin{aligned}
\tau \bar{d}\left(\frac{x}{2}\right) \left[ \gamma^\mu, \gamma^\nu \right] \gamma_5 u \left( -\frac{x}{2} \right) &= \left[ \left( x^\mu \partial^\nu - x^\nu \partial^\mu \right) \bar{d} \gamma_5 u \right]_{b_{00}} a_0(x^2) \\
&+ \left\{ \left[ \left( x^\mu \partial^\nu - x^\nu \partial^\mu \right) \partial_{\mu_1} \partial_{\mu_2} \bar{d} \gamma_5 u \right]_{b_{02}} a_0(x^2) \right. \\
&+ \left. \left[ \left( x^\mu \partial^\nu - x^\nu \partial^\mu \right) \bar{d} \gamma_5 \overset{\leftarrow}{\partial}_{\mu_1} \overset{\leftarrow}{\partial}_{\mu_2} u \right]_{b_{22}} a_2(x^2) \right\} x^{\mu_1} x^{\mu_2} \\
&+ \dots
\end{aligned} \tag{4-12c}$$

Conditions (4-11a, -11b, -11c) have been used in the above to eliminate terms having an odd number of powers of  $x$  from the first two expansions and an even number of powers of  $x$  from the third expansion.

The features that are important to us are somewhat obscured by the overabundant subscripts in (4-12) and are best described in words. First note that there are really only a few different operators appearing. For example,  $\bar{d} \gamma_5 u$ , with its coefficient function  $a_0(x^2)$  is responsible for three of the terms exhibited in (4-12a). Owing to the symmetric derivative terms, this operator appears in the coefficient of every power of  $x$ . The operator  $\bar{d} \gamma_5 \overset{\leftarrow}{\partial}_{\mu_1} \overset{\leftarrow}{\partial}_{\mu_2} u$  does not appear in the zero-power term, but appears in all higher terms, and so on for higher derivative operators. The same sort of comment applies to the other two expansions.

The  $\bar{d}\left(\frac{x}{2}\right) \gamma^\mu \gamma_5 u \left( -\frac{x}{2} \right)$  expansion shows another feature of interest. The terms in this expansion divide into two classes: those in which  $\mu$  attaches to a derivative and those in which  $\mu$  simply appears in a factor  $x^\mu$ . The first class will contribute to  $\chi_1(x^2, p \cdot x)$ , the second to  $\chi_4(x^2, p \cdot x)$ .

## 4.2 Moments of the Wavefunction

To make a connection between the invariant wavefunctions and the bilocal operator expansions, traces should be taken of the wavefunction, (3-1), after multiplication by  $\gamma_5$ ,  $\gamma_5 \gamma^\mu$ , and  $\gamma_5 [\gamma^\mu, \gamma^\nu]$ .

$$\chi_3(x^2, p \cdot x) = -\frac{1}{12} \langle 0 | T \bar{d} \left[ -\frac{x}{2} \right] \gamma_5 u \left( \frac{x}{2} \right) | \pi \rangle \quad (4-13a)$$

$$\begin{aligned} p^\mu \chi_1(x^2, p \cdot x) + x^\mu \chi_4(x^2, p \cdot x) = \\ -\frac{1}{12} \langle 0 | T \bar{d} \left[ -\frac{x}{2} \right] \gamma^\mu \gamma_5 u \left( \frac{x}{2} \right) | \pi \rangle \end{aligned} \quad (4-13b)$$

$$\begin{aligned} [p^\mu, x^\nu] \chi_2(x^2, p \cdot x) = \\ -\frac{1}{48} \langle 0 | T \bar{d} \left[ -\frac{x}{2} \right] [\gamma^\mu, \gamma^\nu] \gamma_5 u \left( \frac{x}{2} \right) | \pi \rangle \end{aligned} \quad (4-13c)$$

Since proper normalization is one of our interests, it is worth stressing that  $\bar{d} u$  implies a sum over color indices while  $u \bar{d}$  (as in (3-1) ) does not.

The next step is to insert the operator product expansions into (4-13). Without explicitly showing the index symmetrization and trace subtractions, the matrix elements of interest are

$$\langle 0 | \bar{d} \gamma_5 \overleftrightarrow{\partial}_{\mu_1} \overleftrightarrow{\partial}_{\mu_2} \dots \overleftrightarrow{\partial}_{\mu_n} u | \pi \rangle \equiv (-i)^n p_{\mu_1} \dots p_{\mu_n} A_n \quad (4-14)$$

$$\langle 0 | \bar{d} \gamma_{\mu_1} \gamma_5 \overleftrightarrow{\partial}_{\mu_2} \dots \overleftrightarrow{\partial}_{\mu_n} u | \pi \rangle \equiv (-i)^n p_{\mu_1} \dots p_{\mu_n} B_n \quad (4-15)$$

The matrix element  $B_1$  is directly measurable, being the pion decay constant,  $f_\pi$ . If  $x^2$  is small, the invariant wavefunctions can now be expressed in the form

$$\chi_1(x^2, p \cdot x) = \frac{i}{12} \sum_{\substack{n=0 \\ \text{(even)}}}^{\infty} (-ip \cdot x)^n \sum_{\substack{m=0 \\ \text{(even)}}}^n a_{mn} B_{m+1} b_{m+1}(x^2) \quad (4-16a)$$

$$\chi_2(x^2, p \cdot x) = \frac{i}{48} \sum_{\substack{n=0 \\ \text{(even)}}}^{\infty} (ip \cdot x)^n \sum_{\substack{m=0 \\ \text{(even)}}}^n b_{mn} A_m a_m(x^2) \quad (4-16b)$$

$$\chi_3(x^2, p \cdot x) = -\frac{1}{12} \sum_{\substack{n=0 \\ \text{(even)}}}^{\infty} (-ip \cdot x)^n \sum_{\substack{m=0 \\ \text{(even)}}}^n c_{mn} A_m a_m(x^2) \quad (4-16c)$$

$$\chi_4(x^2, p \cdot x) = -\frac{1}{12} \sum_{\substack{n=1 \\ \text{(odd)}}}^{\infty} (-ip \cdot x)^n \sum_{\substack{m=0 \\ \text{(even)}}}^{n-1} d_{mn} B_{m+1} b_{m+1}(x^2) \quad (4-16d)$$

The renormalization group will give the asymptotic behavior of the coefficient functions  $a_m(x^2)$  and  $b_m(x^2)$ . The relative size of terms involving the same operator is unknown, and the constants  $a_{nm}$ , etc., have been included to reflect this fact. Without losing generality, we can set

$$a_{n0} = c_{n0} = 1 \quad (4-17)$$

It is now possible to determine the asymptotic  $t$ -dependence of the spectral function moments. To take the simplest case first, expand  $\chi_3(x^2, p \cdot x)$  in powers of  $-ip \cdot x$ , using the representation given in expression (3-57). Comparing with the coefficients of  $(-ip \cdot x)^n$  in (4-16c) gives

$$\begin{aligned}
& - \frac{1}{12} \sum_{m=0}^{\infty} c_{mn} A_m a_m(x^2) \\
& \quad \text{(even)} \\
& = \frac{1}{n!} \int_0^{\infty} \int_{-1/2}^{1/2} \xi^n g_3(\xi, t) K(x^2, \mu^2) d\xi dt \quad (4-18)
\end{aligned}$$

The kernel  $K$  is the Fourier transform of  $[k^2 - \mu^2 + i\epsilon]^{-3}$  with  $\mu^2$  given by expression (3-59). Taking a Fourier transform of (4-18) and doing the  $t$ -integration.

$$\begin{aligned}
\frac{1}{12} \sum_{m=0}^{\infty} c_{mn} A_m a_m(k^2) & = \frac{g_3^{(n)}(-k^2)}{n! 2(k^2)^2} \\
& \quad \text{(even)} \quad (4-19)
\end{aligned}$$

The spectral moments appearing above are defined by

$$g_i^{(n)}(t) = \int_{-1/2}^{1/2} \xi^n g_i(\xi, t) d\xi \quad (4-20)$$

In doing the  $t$ -integration, the leading  $k^2$ -behavior was found by assuming that  $k$  is spacelike and that  $g_3(\xi, t)$  depends logarithmically on  $t$ . This is in anticipation of the renormalization group results, which will show that  $a_m(k^2)$  and  $b_m(k^2)$  behave for spacelike  $k$  as  $(k^2)^{-2} (\ln|k^2|)^{\gamma(m)}$  with  $\gamma(m)$  a number of order unity. A similar situation is encountered in electroproduction, but here there is less predictive power because the  $m^{\text{th}}$  moment receives contributions from the  $m^{\text{th}}$  level on the operator "tower" as well as from all lower levels. As mentioned earlier, this happens because we are dealing with a non-forward matrix element.

Results similar to (4-19) can be obtained for the other spectral functions, but there are minor complications due to the x-dependent Lorentz factors. The simplest and most important case is the combination  $g_1(\xi, t) + \xi g_4(\xi, t)$ , for which we find

$$-\frac{1}{12} \sum_{\substack{n \\ m=0 \\ \text{(even)}}} \left( a_{mn} + \frac{d_{m(n-1)}}{m^2} \right) B_{m+1} b_{m+1} (k^2) = \frac{g_1^{(n)}(-k^2) + g_4^{(n+1)}(-k^2)}{n! 2(k^2)^2} \quad (4-21)$$

Because of the assumption that G-parity is a perfect symmetry,  $g_{1,2,3}$  have only even moments, with the  $n^{\text{th}}$  moment being a linear combination of  $a_m(k^2)$  or  $b_m(k^2)$  containing all even  $m \leq n$ . The remaining spectral function,  $g_4$ , has only odd moments, with the  $(n+1)^{\text{th}}$  moment being a linear combination of  $b_m(k^2)$  containing all even  $m \leq n$ .

### 4.3 The Renormalization Group

The fractional power of  $\ln(-k^2)$  found in each coefficient function is related to the anomalous dimension of the corresponding local operator. In order to establish the notation to be used in connection with the renormalization group, we will summarize the well-known procedure for finding fractional powers of logarithms [6].

If a Green's function can be renormalized by absorbing the unrenormalized coupling constant and regulation parameter into a renormalized coupling constant and field renormalization factors in the following fashion:

$$G(k_1, \dots, k_N, g, M) = \sqrt{Z} G_{\text{un}}(k_1, \dots, k_N, g_{\text{un}}) \quad (4-22)$$

then

$$\gamma = \frac{M}{2Z} \frac{\partial Z}{\partial M} \quad (4-23)$$

is the anomalous dimension of  $G$ . The mass parameter  $M$  sets the scale at which all Green's functions of the theory are to be renormalized. The scaling behavior of  $G$  for large non-time-like momenta is determined by solving the renormalization group equation

$$\mathcal{D}G = \gamma G \quad (4-24)$$

where

$$\mathcal{D} = M \frac{\partial}{\partial M} + \beta \frac{\partial}{\partial g} \quad (4-25)$$

$$\beta = M \frac{\partial g}{\partial M} \quad (4-26)$$

In QCD,

$$\beta \approx -bg^3 \quad (4-27)$$

$$b = \frac{1}{16\pi^2} \left[ 11 - \frac{2}{3} N_F \right] \quad (4-28)$$

$N_F$  = number of flavors

If

$$\gamma \approx dg^2 \quad (4-29)$$

as in the cases that concern us, then

$$G(\lambda k_1 \dots \lambda k_N, g, M) = \frac{G(\lambda k_1, \dots, \lambda k_N, g(\lambda), M) \lambda^D}{[1 + bg^2 \ln \lambda^2]^{d/(2b)}} \quad (4-30)$$

The effective coupling constant is

$$g^2(\lambda) = \frac{g^2}{1 + bg^2 \ln \lambda^2}$$

and  $D$  is the naive, integer, dimension of  $G$ .

We are dealing with operator product expansions of the form

$$O(x) = \sum_{n,m} O_{mn}^{\mu_1 \dots \mu_n} x_{\mu_1} \dots x_{\mu_n} c_{mn}(x^2) \quad (4-31)$$

Sandwiching (4-31) between the states  $u(y)|0\rangle$  and  $d(z)|0\rangle$  and Fourier transforming

$$G^{(4)}(k, p, q, g, M) = \sum_{n,m} G_{mn}^{(2)\mu_1 \dots \mu_n}(p, q, g, M) (i)^n \frac{\partial}{\partial k^{\mu_1}} \dots \frac{\partial}{\partial k^{\mu_n}} c_{mn}(k^2) \quad (4-32)$$

The momenta  $k$ ,  $p$ , and  $q$  are conjugate, respectively, to  $x$ ,  $y$ , and  $z$ .

Acting on (4-32) with the renormalization group operator,  $\mathcal{D}$ , the left-hand side is a four-quark Green's function (unamputated) for which

$$\mathcal{D}G^{(4)} = -4 \gamma_F G^{(4)} \quad (4-33)$$

The two-point functions on the right-hand side with operator insertions obey

$$\mathcal{D}G_{nm}^{(2)} = -\left(2 \gamma_F + \gamma_{nm}\right) G_{nm}^{(2)} \quad (4-34)$$

When calculated to lowest non-trivial order,

$$\gamma_F = d_F g^2 \quad (4-35)$$

$$\gamma_{mn} = d_{mn} g^2 \quad (4-36)$$



so the logarithmic dependence of  $G^{(4)}$  and  $G^{(2)}$  is of the form (4-30).

$$G^{(4)}(\lambda k, \lambda p, \lambda q, g, M) \approx \frac{G^{(4)}(k, p, q, g, M) \lambda^{-6}}{[1 + b g^2 \ln \lambda^2]^{1-2d_F/b}} \quad (4-37)$$

$$G_{mn}^{(2)}(\lambda k, g, M) \approx \frac{G_{mn}^{(2)}(k, 0, M) \lambda^{n-2}}{[1 + b g^2 \ln \lambda^2]^{-(d_{mn}-2d_F)/(2b)}} \quad (4-38)$$

Interpreting expression (4-37), it is significant that this Green's function is proportional to  $g^2$  in lowest order, giving an extra inverse power of  $\ln \lambda^2$ . The two-point functions are non-vanishing with  $g^2 = 0$ , which permits the approximation  $G^{(2)}(g(\lambda)) = G^{(2)}(0)$ .

The left-hand and right-hand sides of (4-32) must scale in the same way, giving the asymptotic behavior

$$c_{mn}(k^2) \approx \frac{1}{[k^2]^2 [\ln k^2]^{1+(d_{mn}+2d_F)/(2b)}} \quad (4-39)$$

In (4-39),  $n$  is the number of derivatives, and  $m$  is the spin of the parent operator. The anomalous dimensions are therefore independent of  $n$ . Calculating the anomalous dimensions in a gauge with gluon propagator

$$D_{\mu\nu} = -i \frac{g_{\mu\nu} - (1-\alpha) k_\mu k_\nu / k^2}{k^2} \quad (4-40)$$

one finds

$$d_m^{(2)} = \frac{1}{6\pi^2} \left[ 1 - \frac{2}{m(m+1)} \right] \quad (4-41)$$

for the twist-two operators [6] and

$$d_m^{(3)} = \frac{1}{6\pi^2} \left[ \alpha - \frac{3+\alpha}{m+1} \right] \quad (4-42)$$

for the twist-three operators. For the fermions,

$$d_F = \frac{\alpha}{12\pi^2} \quad (4-43)$$

Finally,

$$a_m(k^2) \approx \frac{1}{(k^2)^2 [\ln k^2]^{1 + \left( d_m^{(3)} + 2d_F \right) / (2b)}} \quad (4-44)$$

$$b_m(k^2) \approx \frac{1}{(k^2)^2 [\ln k^2]^{1 + \left( d_m^{(2)} + 2d_F \right) / (2b)}} \quad (4-45)$$

which, together with expressions (4-19) and (4-21), give the asymptotic behavior of the spectral function moments. Although we have not written an expression for  $g_2^{(n)}(-k^2)$ , it contains the same powers of  $\ln k^2$  as  $g_3^{(n)}(-k^2)$ . The moments of all four spectral functions have logarithmic, but no power dependence on  $k^2$ .

The "Fermi" gauge defined by (4-40) does have ghosts, but the problem of ghost mixing [6] does not arise for fermion-antifermion operators. Note that, even though the twist-two operators are gauge-variant, their anomalous dimensions (4-41) do not depend upon the Fermi gauge parameter,  $\alpha$ . We do not know whether this invariance extends to all gauges and all powers of  $g$ . The anomalous dimensions of the twist-three operators, on the other hand, are explicitly gauge-variant.

The Landau gauge ( $\alpha = 0$ ) is especially convenient for us, since the fermion anomalous dimension is zero in that gauge, and  $\alpha$  need not be

treated as a running parameter. The Landau gauge will be used in the following chapter in order to simplify the solution of the Bethe-Salpeter equation.

Chapter IV References and Footnotes

1. T. Appelquist and E. Poggio, Phys. Rev. D 10, 3280 (1974).
2. C. G. Callan, Jr. and D. J. Gross, Phys. Rev. D 11, 2905 (1974).
3. A. H. Guth and D. E. Soper, Phys. Rev. D 12, 1143 (1975); M. L. Goldberger et al., Phys. Rev. D 14, 117 (1976) and Phys. Rev. D 14, 2633 (1976).
4. H. Leutwyler, Nuc. Physics B 76, 413 (1974).
5. R. A. Brandt and G. Preparata, Nuc. Phys. B 27, 545 (1971).
6. D. J. Gross and F. Wilczek, Phys. Rev. D 8 3633 (1973) and Phys. Rev. D 9, 980 (1974); H. D. Politzer, Phys. Repts. 14, 129 (1974).

## Chapter V

## ASYMPTOTIC SOLUTION OF THE BETHE-SALPETER EQUATION

Although the operator product expansion gives information about the asymptotic behavior of the wavefunction moments, it does not predict the relative size of the moments. Furthermore, each moment is a mixture of logarithmic terms having different anomalous dimensions, and the relative size of these terms is also unknown. In order to determine the wavefunction on the light cone, one must appeal ultimately to the Bethe-Salpeter equation. Appelquist and Poggio do this for  $\phi^3$  in six dimensions [1], but only succeed in obtaining the short-distance behavior. Nevertheless, their solution is quite interesting, as it shows how the Bethe-Salpeter equation can be used to calculate anomalous dimensions.

In this chapter, we will obtain a solution of the asymptotic Bethe-Salpeter equation, valid over the entire light cone. More accurately, we will obtain a family of solutions, in which the anomalous dimensions appear as eigenvalues. We show that the boundary condition

$$g_i \left( \xi = \pm \frac{1}{2}, t \right) = 0 \quad (5-1)$$

produces solutions having all the properties dictated by the operator product expansion. If the first solution in the family is associated with the pion, only two anomalous dimensions enter and a definite wavefunction emerges. If the pion is a superposition of solutions, we have only slightly more information than the operator product expansion gives. In the following chapter, the simplest solution is used to predict the absolute magnitude of the pion electromagnetic form factor and structure functions.

A careful reading of the title of this chapter exposes a certain faintheartedness. One would like to see a discussion of the "Asymptotic Behavior of Solutions of the Bethe-Salpeter Equation." It must be stressed that we deal with an asymptotic form for the Bethe-Salpeter kernel and do not prove that solutions of the resulting equation share the asymptotic behavior of solutions of the exact equation. The consistency of the solutions found here with the operator product expansion encourages the hope that infrared effects will not destroy our results.

### 5.1 The Asymptotic Equation

In graphical form, the Bethe-Salpeter equation is

$$\begin{array}{c} \text{---} \\ \circlearrowleft \\ \Gamma \end{array} \begin{array}{l} \xrightarrow{*} \\ \xleftarrow{*} \end{array} = \begin{array}{c} \text{---} \\ \circlearrowleft \\ \Phi \end{array} \begin{array}{l} \xrightarrow{*} \\ \xleftarrow{*} \end{array} \begin{array}{c} \square \\ K \end{array} \begin{array}{l} \xrightarrow{*} \\ \xleftarrow{*} \end{array} \quad (5-2)$$

The amputated wavefunction is

$$\begin{array}{c} p \rightarrow \text{---} \\ \circlearrowleft \\ \Gamma \end{array} \begin{array}{l} \xrightarrow{*} \\ \xleftarrow{*} \end{array} \begin{array}{c} \rightarrow p/2 + k \\ \rightarrow p/2 + k \end{array} = \Gamma(p, k) \quad (5-3)$$

$$\Phi(p, k) = S_F \left[ \frac{p}{2} + k \right] \Gamma(p, k) S_F \left[ k - \frac{p}{2} \right] \quad (5-4)$$

and the Bethe-Salpeter kernel is the two-particle-irreducible four-point function

$$\begin{array}{c} \rightarrow * \\ \square \\ K \\ \leftarrow * \end{array} \begin{array}{l} \xrightarrow{*} \\ \xleftarrow{*} \end{array} = \begin{array}{c} \text{---} \\ \text{---} \\ \text{---} \\ \text{---} \end{array} + \begin{array}{c} \text{---} \\ \text{---} \\ \text{---} \\ \text{---} \end{array} + \begin{array}{c} \text{---} \\ \text{---} \\ \text{---} \\ \text{---} \end{array} + \begin{array}{c} \text{---} \\ \text{---} \\ \text{---} \\ \text{---} \end{array} + \dots \quad (5-5)$$

The crosses are used as a reminder that  $K$  is an amputated Green's function.

If all incoming momenta are large, non-exceptional, and non-timelike, the renormalization group tells us that the Bethe-Salpeter kernel behaves as

$$\begin{array}{c}
 \lambda \left( \frac{p}{2} + k \right) \\
 \rightarrow \text{---} \times \\
 \lambda \left( \frac{p}{2} - k \right) \\
 \rightarrow \text{---} \times
 \end{array}
 \begin{array}{c}
 \text{---} \times \\
 \text{---} \times \\
 \text{---} \times \\
 \text{---} \times
 \end{array}
 \begin{array}{c}
 \text{---} \times \\
 \text{---} \times \\
 \text{---} \times \\
 \text{---} \times
 \end{array}
 \begin{array}{c}
 \lambda \left( \frac{p}{2} + q \right) \\
 \rightarrow \\
 \lambda \left( \frac{p}{2} - q \right) \\
 \rightarrow
 \end{array}
 \approx \frac{i g^2 \gamma^\alpha \otimes \gamma^\beta \left( g_{\alpha\beta} - \frac{1}{l^2} \right)}{[1 + b g^2 \ln \lambda^2] l^2 \lambda^2} \quad (5-6)$$

$$l = q - k \quad (5-7)$$

This is in the Landau gauge, where the fermion anomalous dimension vanishes. In our application, the s-channel momentum,  $p$ , is exceptional. Because the Bethe-Salpeter kernel has no singularities corresponding to bound states in this channel, it is plausible that (5-6) should represent the asymptotic behavior of the Bethe-Salpeter kernel even when  $p^2$  is small, provided all quark lines carry large (momentum)<sup>2</sup>.

Our principal assumption, then, is that the asymptotic Bethe-Salpeter kernel is

$$\begin{array}{c}
 \frac{p}{2} + k \\
 \rightarrow \text{---} \times \\
 \frac{p}{2} - k \\
 \rightarrow \text{---} \times
 \end{array}
 \begin{array}{c}
 \text{---} \times \\
 \text{---} \times \\
 \text{---} \times \\
 \text{---} \times
 \end{array}
 \begin{array}{c}
 \frac{p}{2} + q \\
 \rightarrow \text{---} \times \\
 \frac{p}{2} - q \\
 \rightarrow \text{---} \times
 \end{array}
 \approx \frac{i \gamma^\alpha \otimes \gamma^\beta \left( g_{\alpha\beta} - \frac{1}{l^2} \right)}{b l^2 \ln \left( l^2 / M^2 \right)} \quad (5-8)$$

For large spacelike momentum, the asymptotic fermion propagator in the Landau gauge is

$$S_F(k) \approx \frac{i \not{k}}{k^2} \quad (5-9)$$

Because the fermion propagator is simple, the relationship between the amputated and unamputated wavefunctions is simple. Defining the invariant amputated wavefunctions,

$$\Gamma(p, k) = \gamma_5 \left[ \Gamma_1 \not{p} + \frac{1}{2} \Gamma_2 [\not{k}, \not{p}] + \Gamma_3 + \Gamma_4 \not{k} \right] \quad (5-10)$$

in which the  $\Gamma_i$  depend only upon  $k^2$  and  $p \cdot k$ , one finds the relations

$$\Gamma_1 = -k^2 \phi_1 - \frac{1}{2} p \cdot k \phi_4 \quad (5-11a)$$

$$\Gamma_2 = -k^2 \phi_2 - \phi_3 \quad (5-11b)$$

$$\Gamma_3 = (p \cdot k)^2 \phi_2 + k^2 \phi_3 \quad (5-11c)$$

$$\Gamma_4 = 2 p \cdot k \phi_1 + k^2 \phi_4 \quad (5-11d)$$

The asymptotic Bethe-Salpeter equation is

$$\Gamma(p, q) = \frac{4i}{3b \ln[q^2/M^2]} \int \frac{d^4 k}{(2\pi)^4} \frac{\gamma^\mu \Phi(p, k) \gamma^\nu [g_{\mu\nu} - 1_\mu 1_\nu / 1^2]}{1^2 + i\epsilon} \quad (5-12)$$

Expressions (5-6) and (5-8) should have been written with color matrix factors for the gluon-fermion vertices. These were omitted for the sake of brevity, but the appropriate color factor,  $4/3$ , has been included in the asymptotic equation, (5-12). The logarithmic factor in the kernel is slowly-varying compared to the other power-behaved factors in the integrand. Treating the logarithmic factor as a constant will give an approximation valid to within a factor  $1 + O\left(\frac{1}{\ln q^2/M^2}\right)$ . This



same order of approximation is found in the operator product expansion and will be adequate here.

Over part of the range of integration, the momenta of the virtual quarks will not be large and spacelike, even if the external momenta  $\frac{p}{2} + q$  and  $\frac{p}{2} - q$  are large and spacelike. Finiteness of the spectral functions at  $\xi = \pm \frac{1}{2}$  is a sufficient condition for non-dominance of this infrared contribution, as will be seen.

The loop integration is readily performed if the spectral representation is used. For example, one term in the integration is

$$\int \frac{d^4 k \phi_3}{1^2 + i\epsilon} = \int_0^\infty dt \int_{-1/2}^{1/2} d\xi g_3(\xi, t) L(\xi, t, q, p) \quad (5-13)$$

where L is

$$L(\xi, t, q, p) = \int \frac{d^4 k}{(1^2 + i\epsilon) [k^2 - 2\xi p \cdot k - t + i\epsilon]^3}$$

After a Feynman parameterization and a shift in k,

$$L(\xi, t, q, p) = 3 \int_0^1 b^2 db \int \frac{d^4 k}{[k^2 + b(1-b)(q^2 - 2\xi p \cdot q) - bt + i\epsilon]^4}$$

If the external momentum is spacelike and satisfies

$$\left| \frac{q^2}{2 p \cdot q} \right| > 1, \quad (5-14)$$

a Wick rotation can be performed, leaving

$$L(\xi, t, q, p) = \frac{i\pi^2}{2} \int_0^1 \frac{db}{[(1-b)(q^2 - 2\xi p \cdot q) - t]^2} \quad (5-15)$$

Recognizing that the  $t$ -integrand is  $L(\xi, t, q, p)$  multiplied by a logarithmic function,  $g_3(\xi, t)$ , the leading-log approximation will be obtained if we treat (5-15) as if  $t \ll |q^2 - 2\xi p \cdot q|$ , giving

$$L(\xi, t, q, p) \approx \frac{-i\pi^2}{2[q^2 - 2\xi p \cdot q]t} \quad (5-16)$$

As  $t$  approaches  $|p \cdot q|$ ,  $L(\xi, t, q, p)$  drops off sharply from the value given by (5-16), so that in the leading-log approximation,

$$\int \frac{d^4 k \phi_3}{l^2 + i\epsilon} = -\frac{i\pi^2}{2} \int_{-1/2}^{1/2} \frac{b_3(\xi, p \cdot q)}{q^2 - 2p \cdot q \xi} d\xi \quad (5-17)$$

where  $b_3(\xi, t)$  is a regulated version of Leutwyler's light-cone spectral function,

$$b_i(\xi, t) = \int_0^t \frac{g_i(\xi, t) dt}{t} \quad (5-18)$$

The renormalization group forewarns us that

$$g_i(\xi, t) \sim (\ln t)^{-\gamma}$$

This is a good point at which to pause and examine the legality of our calculation so far. The Wick rotation was more than just a formal device. In fact, a Wick rotation in only one momentum is not always possible, rather, all external momenta must in general be rotated. We certainly do not wish to rotate the pion momentum,  $p$ , and would rather

not rotate the external momentum,  $q$ . Taking  $q$  to be spacelike and imposing (5-14) was essential to the rotation, and the rotation places the internal quark momenta in the Euclidean region. The quark momenta are of order

$$k^2 \sim b(1-b) \left( q^2 - 2\xi p \cdot q \right) - bt \sim t \sim p \cdot q$$

This puts us safely in the deep Euclidean region and strengthens the hope that the asymptotic kernel can be used. There remain worries about infrared singularities in the kernel and the wavefunction itself. Singularities such as  $k^{-4}$  or stronger would undoubtedly upset our results. Once specific wavefunctions have been obtained, it will at least be possible to check their infrared behavior for consistency.

The other loop integrations can be done in a manner similar to the above. After gathering coefficients of  $\gamma_5 \not{p}, \gamma_5 [k, \not{p}], \gamma_5$  and  $\gamma_5 k$ , the asymptotic equation can be written in the following form:

$$\Gamma_1(k^2, p \cdot k) = B(p \cdot k) \int_{-1/2}^{1/2} \frac{x' - 2\xi}{[x' - \xi]^2} (b_1 + \xi b_4) d\xi \quad (5-19a)$$

$$\Gamma_2(k^2, p \cdot k) = \frac{B(p \cdot k)}{6p \cdot k} \int_{-1/2}^{1/2} \frac{b_2}{[x' - \xi]^2} d\xi \quad (5-19b)$$

$$\Gamma_3(k^2, p \cdot k) = -3B(p \cdot k) \int_{-1/2}^{1/2} \frac{b_3}{x' - \xi} d\xi \quad (5-19c)$$

$$\Gamma_4(k^2, p \cdot k) = B(p \cdot k) \int_{-1/2}^{1/2} \frac{b_1 + \xi b_4}{[x' - \xi]^2} d\xi \quad (5-19d)$$

In the above expressions, the  $b_i$  are given by (5-18) with arguments  $\xi$  and  $p \cdot k$ . Because of the logarithmic behavior of the  $b_i$ , it is immaterial which of  $p \cdot k$ ,  $k^2$ ,  $\xi p \cdot k$ , etc., is used. For convenience, the variable

$$x' = \frac{k^2}{2p \cdot k} \quad (5-20)$$

has been employed. Also, we have defined

$$B(p \cdot k) = \frac{1}{48\pi^2 b(p \cdot k) \ln(p \cdot k/M^2)} \quad (5-21)$$

which exhibits the gross behavior of the amputated wavefunction. The anomalous powers of log and the  $x'$  dependence are contained in the integral factors

The asymptotic Bethe-Salpeter equation has separated into two uncoupled sets of equations. Equations (5-19a, -19d) are to be solved for the  $\gamma_5$ -odd part of the wavefunction, while (5-19b, -19c) give the  $\gamma_5$ -even part. The odd part contributes to  $f_\pi$ ,  $F_\pi$ ,  $W_L$ , and  $W_T$ , while the even part contributes only to  $W_T$ .

As discussed in Chapter III, the branch points (as seen in relative energy) that arise when one of the quarks is on-shell correspond to  $\xi = \pm \frac{1}{2}$ . If the spectral functions are finite at these points, and  $|x'| > \frac{1}{2}$ , this infrared portion of the wavefunction will not contribute to the Bethe-Salpeter loop integral, as (5-19) shows. However, (5-19) also shows a singularity as  $|x'| \rightarrow \frac{1}{2}$ , and this is precisely the condition under which one of the quarks approaches its mass shell. To avoid

infrared singularities in the amputated wavefunctions, the spectral functions must vanish at the end points more rapidly than  $\left(\frac{1}{4} - \xi^2\right)^2$ . We will find that all solutions have infrared singularities, but that these singularities are sufficiently tame as not to invalidate the Bethe-Salpeter solution technique.

## 5.2 $\gamma_5$ -Odd Solution

From the equations for  $\Gamma_1$  and  $\Gamma_4$  one can obtain

$$\begin{aligned} \phi_1(k^2, p \cdot k) + x' \phi_4(k^2, p \cdot k) \\ = \frac{B(p \cdot k)}{2p \cdot k} \int_{-1/2}^{1/2} \int_0^{-k^2} \frac{g_1(\xi, t) + \xi g_4(\xi, t)}{(x' - \xi)^2 t} \end{aligned} \quad (5-22)$$

$$2p \cdot k \left[ 4 k^2, p \cdot k \right] = \frac{2B(p \cdot k)}{(x')^2 - \frac{1}{4}} \int_{-1/2}^{1/2} \int_0^{-k^2} \frac{g_1(\xi, t) + \xi g_4(\xi, t)}{(x' - \xi)^2 t} dt d\xi \quad (5-23)$$

Before proceeding with the general light cone solution, it is wise to consider the short-distance limit  $|x'| \rightarrow \infty$ . In this limit, the squared momenta of the two quarks are equal. The two integrations become identical, giving the relation

$$\phi_4 \rightarrow -\frac{4p \cdot k}{k^2} \phi_1, \quad x' \rightarrow \infty \quad (5-24)$$

$$f_\pi = 12 \int \frac{d^4 k}{(2\pi)^4} \left( \phi_1 + \frac{p \cdot k}{m_\pi} \phi_4 \right) \quad (5-25)$$

will be finite, because

$$\frac{1}{4} - \frac{(p \cdot k)^2}{p^2 k^2} \quad (5-26)$$

integrates to zero over the hypersphere in four dimensions. Without recourse to the Bethe-Salpeter equation, there is every reason to worry about the existence of the integral for  $f_\pi$ . In terms of the spectral functions,

$$f_\pi = \frac{-3i}{8\pi^2} \int_0^\infty \frac{g^{(0)}(t) + g^{(1)}(t)}{t} dt \quad (5-27)$$

The renormalization group tells us that

$$g_1^{(0)}(t) + g_4^{(1)}(t) \sim \frac{1}{\ln t} \quad (5-28)$$

which would cause  $f_\pi$  to be infinite were it not for the cancellation enforced by the Bethe-Salpeter equation. Phrasing this point differently, the invariant wavefunctions  $\chi_i \left[ x^\mu \right]$  may be infinite at the origin, but the linear combination that determines the rate of quark annihilation is finite at the origin.

Returning to the full light cone, solutions will be sought that factorize in the form

$$g_i(\xi, t) = \frac{f_i(\xi)}{\left( \ln \frac{t}{M^2} \right)^{1-\epsilon}} \quad (5-29)$$

It will turn out that an infinity of such solutions exists, each solution having a power,  $\epsilon$ , corresponding to one of the twist-two operators.

Consistency with the operator product expansion demands more than this, and we shall find that the  $f_i(\xi)$  have all the required properties.

The  $t$ -integrals on the right-hand side of the Bethe-Salpeter equation have the form

$$\int \frac{-k^2 dt}{t \left( \ln \frac{t}{M^2} \right)^{1-\epsilon}} = \frac{\left( \ln \frac{-k^2}{M^2} \right)^\epsilon}{\epsilon} + \text{constant}$$

while, on the left-hand side,

$$\int_0^\infty \frac{dt}{\left( k^2 - 2p \cdot k \xi - t \right)^3 \left( \ln t/M^2 \right)^{1-\epsilon}} = \frac{-1}{8(p \cdot k)^2 (x' - \xi)^2 \left( \ln -k^2/M^2 \right)^{1-\epsilon}}$$

As pointed out by Appelquist and Poggio [1], the cut-off on the right-hand integral occurs when the loop momentum through the kernel approaches the external momentum. This cut-off eliminates one power of logarithm, but this power is replaced by the logarithm from the kernel. One finds, then, the same power of log on both sides of the Bethe-Salpeter equation. Appelquist and Poggio assert that  $\epsilon > 0$  is a necessary condition for consistency. This would certainly be true if we were seeking an exact solution, for otherwise the constant term in the right-hand  $t$ -integral would dominate the fractional power of log at large  $k^2$ . We expect non-leading powers of log in the  $g_i(\xi, t)$ , however, and these generate constant terms of the same type. Consistency simply demands a connection between the magnitude of leading and non-leading logarithmic pieces of  $g_i(\xi, t)$ , but finding this connection is not possible with the present approach. It is important that we be

able to handle the case  $\epsilon < 0$ , because the renormalization group shows that  $g_1(\xi, t)$  and  $g_4(\xi, t)$  will have this behavior.

Cancellation of the common fractional power of log on the right- and left-hand sides of the Bethe-Salpeter equation leaves the following:

$$\int_{-1/2}^{1/2} \frac{f_1(\xi) + x' f_4(\xi)}{(x' - \xi)^2} d\xi = -\frac{2\beta}{\epsilon} \int_{-1/2}^{1/2} \frac{f_1(\xi) + \xi f_4(\xi)}{(x' - \xi)^2} d\xi \quad (5-30)$$

$$\int_{-1/2}^{1/2} \frac{f_4(\xi)}{(x' - \xi)^2} d\xi = \frac{-4\beta/\epsilon}{(x')^{2-\frac{1}{4}}} \int_{-1/2}^{1/2} \frac{f_1(\xi) + \xi f_4(\xi)}{x' - \xi} d\xi \quad (5-31)$$

$$\beta = \frac{2}{3 \left[ 11 - \frac{2}{3} N_F \right]} \quad (5-32)$$

It is possible to obtain a single equation in the unknown

$$f(\xi) = f_1(\xi) + \xi f_4(\xi) \quad (5-33)$$

This is accomplished by noting that

$$\frac{f_1(\xi) + x' f_4(\xi)}{(x' - \xi)^2} = \frac{f(\xi)}{(x' - \xi)^2} + \frac{f_4(\xi)}{x' - \xi}$$

$$\int_{-1/2}^{1/2} \frac{f_4(\xi)}{(x' - \xi)^2} d\xi = -\frac{d}{dx'} \int_{-1/2}^{1/2} \frac{f_4(\xi)}{x' - \xi} d\xi$$

The equation thus obtained is



$$\left(\xi^2 - \frac{1}{4}\right) \frac{d^2}{d\xi^2} F(\xi) = \frac{4}{2 + \frac{\epsilon}{\beta}} F(\xi) \quad (5-34)$$

where  $F(\xi)$  is the Hilbert transform of  $f(\xi)$  .

$$F(\xi) = \int_{-1/2}^{1/2} \frac{f(\xi') d\xi'}{\xi - \xi'} \quad (5-35)$$

Equation (5-34) has only been established for  $|\xi| > \frac{1}{2}$ , but we will assume its validity over the entire range of  $\xi$ . Hilbert transforming (5-34), one finds that  $f(\xi)$  obeys the same equation. Equation (5-34) is a special case of the ultraspherical equation [2].

$$(1-x^2) C_m^{(\alpha)''} (x) - (2\alpha+1)x C_m^{(\alpha)'} (x) + m(m+2\alpha) C_m^{(\alpha)} (x) = 0$$

Our interest is in the case  $\alpha = -\frac{1}{2}$  .

$$f_{(m)}(\xi) = C_{m+1}^{(-1/2)}(2\xi), \quad m = 1, 3, 5, \dots \quad (5-36)$$

The first few solutions are

$$\begin{aligned} f_{(1)}(\xi) &= 1 - (2\xi)^2 \\ f_{(3)}(\xi) &= 1 - 6(2\xi)^2 + 5(2\xi)^4 \\ f_{(5)}(\xi) &= 1 - 15(2\xi)^2 + 35(2\xi)^4 - 21(2\xi)^6 \\ f_{(7)}(\xi) &= 1 - 28(2\xi)^2 + 126(2\xi)^4 - \frac{924}{5}(2\xi)^6 + \frac{429}{5}(2\xi)^8 \end{aligned} \quad (5-37)$$

with corresponding anomalous powers for the logarithm

$$\epsilon_m = -\frac{4}{3} \frac{1 - \frac{2}{m(m+1)}}{11 - \frac{2}{3} N_F}, \quad m = 1, 3, 5, \dots \quad (5-38)$$

These are precisely the powers obtained (with much greater ease) from the operator product expansion. This is a gratifying result, but consistency demands further that these powers appear only in certain moments. The general solution is a superposition

$$g_1(\xi, t) + \xi g_4(\xi, t) = \sum_{\substack{m=1 \\ (\text{odd})}}^{\infty} a_m \frac{C_{m+1}^{(-1/2)}(2\xi)}{\left[ \ln t / M^2 \right]^{1-\epsilon_m}} \quad (5-39)$$

According to (4-21), the  $n^{\text{th}}$  moment of this expression should contain only the powers

$$\epsilon_{n+1}, \epsilon_{n-1}, \dots, \epsilon_1$$

This requires that some of the moments of the  $C_m^{(-1/2)}$  vanish, specifically,

$$\mu_m^{(n)} = \int_{-1}^1 x^n C_m^{(-1/2)}(x) dx = 0, \quad n < m-2 \quad (5-40)$$

This condition is met, as can be verified by evaluating moments of (5-37). A better method is to multiply the ultraspherical differential equation by  $x^n$  and integrate from  $-1$  to  $+1$ . The result is a recursion relation for the moments.

$$n(n-1)\mu_m^{(n-2)} + (m^2 + 2\alpha m - n^2 + 2\alpha n - 2n + 2\alpha - 1)\mu_m^{(n)} - 2(2\alpha - 1)C_m^{(\alpha)}(1) = 0 \quad (5-41)$$

The inhomogeneous term vanishes for  $|\alpha| = \frac{1}{2}$  (For  $\alpha = \frac{1}{2}$ , the ultraspherical polynomials are Legendre polynomials while, for  $\alpha = -\frac{1}{2}$ ,  $C_m^{(\alpha)}(\pm 1) = 0$ ). Setting  $n = m-2$  in (5-41) shows that the  $(m-4)^{\text{th}}$  and lower moments vanish if  $\alpha = -\frac{1}{2}$ , just as desired.

The simplest solution has  $f(\xi) = 1 - (2\xi)^2$  and vanishing anomalous dimensions. Using (5-22) and (5-23), the momentum-space wavefunction can be constructed.

$$\begin{aligned} \Phi_1(k^2, p \cdot k) &= \frac{4f_\pi}{12b(p \cdot k)^2 \ln(p \cdot k/M^2)} \left[ \frac{x'^2}{\frac{1}{4} - x'^2} \right. \\ &\quad \left. - 1 - 2x' \ln \left| \frac{\frac{1}{2} - x'}{\frac{1}{2} + x'} \right| \right] \end{aligned} \quad (5-42)$$

$$\begin{aligned} \Phi_4(k^2, p \cdot k) &= \frac{-4f_\pi}{12b(p \cdot k)^2 \ln(p \cdot k/M^2)} \left[ \frac{x'^2}{\frac{1}{4} - x'^2} \right. \\ &\quad \left. - \ln \left| \frac{\frac{1}{2} - x'}{\frac{1}{2} + x'} \right| \right] \end{aligned} \quad (5-43)$$

The normalization of  $\Phi_1$  and  $\Phi_4$  has been adjusted to agree with the sum rule (5-27). If the pion contains a substantial admixture of the

higher-order terms, the lowest term will still be normalized according to (5-42) and (5-43), as the other terms have vanishing zeroth moments and do not contribute to  $f_\pi$ .

Because the spectral functions vanish at the end points, there is no consistency problem arising from wavefunction infrared infinities (finiteness at the end points would have been sufficient). This is not to say that the wavefunctions remain finite as the quarks approach their mass shell. Expressions (5-42) and (5-43) have first-power singularities as  $|x'| \rightarrow \frac{1}{2}$ . This singularity is due to the fermion propagators, and, when these are removed via expression (5-11), only a logarithmic singularity remains in the amputated wavefunction.

### 5.3 $\gamma_5$ -Even Solution

Using the techniques employed in the  $\gamma_5$ -odd case, a differential equation can be obtained for

$$g_2(\xi, t) = \frac{f(\xi)}{\left(\ln \frac{t}{M^2}\right)^{1-\varepsilon}} \quad (5-44)$$

$$\left(\frac{1}{4} - \xi^2\right)f''(\xi) - \frac{8\beta}{\varepsilon} \xi f'(\xi) - \frac{6\beta}{\varepsilon} \left(\frac{2\beta}{\varepsilon} - 1\right)f(\xi) = 0 \quad (5-45)$$

Polynomial solutions of this equation do not vanish at the end points. This gives an infrared singularity in the wavefunction as the squared four-momentum of either quark approaches zero. We will discuss such singularities in the next chapter, but will tentatively enforce the boundary condition

$$f(\xi) = 0, \quad \xi = \pm \frac{1}{2} \quad (5-46)$$

This condition was automatically satisfied by regular solutions for the antiparallel wavefunction. Further justification for (5-46) can be obtained by looking at the recursion relation for the moments of  $f(\xi)$ . Putting condition (5-46) and the anomalous dimensions of the operator product expansion into (5-41), one finds vanishing moments precisely where demanded by the operator product expansion.

Near  $\xi = \frac{1}{2}$ , the solution must approach

$$f(\xi) \sim \left(\frac{1}{2} - \xi\right)^\delta$$

with

$$\delta = 1 - \frac{4\beta}{\epsilon} \quad (5-47)$$

Taking  $f(\xi)$  to have the form

$$f(\xi) = \left(\frac{1}{4} - \xi^2\right)^\delta h(\xi) \quad (5-48)$$

we must now solve

$$\left(\frac{1}{4} - \xi^2\right) h''(\xi) - 2\left(2 - \frac{4\beta}{\epsilon}\right) h'(\xi) - \left(\frac{12\beta^2}{\epsilon^2} - \frac{14\beta}{\epsilon} + 2\right) h(\xi) \quad (5-49)$$

This equation has two sets of  $n^{\text{th}}$ -order polynomial solutions, one with

$$\frac{\epsilon}{\beta} = \frac{6}{n+1} \quad (5-50)$$

and the other with

$$\frac{\epsilon}{\beta} = \frac{2}{n+2} \quad (5-51)$$

The fractional powers given by (5-50) agree with the operator product expansion, while those given by (5-51) do not. Only one solution meets our tentative boundary condition. It is

$$f(\xi) = \left(\frac{1}{4} - \xi^2\right)^{1/3} \quad (5-52)$$

with

$$\frac{\varepsilon}{\beta} = 6 \quad (5-53)$$

It may be significant that the surviving anomalous dimension, corresponding to the local operator  $\bar{\psi} \gamma_5 \psi$ , is the only gauge-invariant twist-three anomalous dimension (see expression 4-42). All of the twist-two anomalous dimensions were (apparently) gauge invariant, and all of them appeared in the Bethe-Salpeter solution.

We will content ourselves with the solution

$$g_2(\xi, t) = \frac{\left(\frac{1}{4} - \xi^2\right)^{1/3}}{\left(\ln t/M^2\right)^{1-4/\left(11 - \frac{2}{3}N_F\right)}} \quad (5-54)$$

Conformal invariance gives [3]

$$g_2(\xi, t) = \left(\frac{1}{4} - \xi^2\right)\theta(t) \quad (5-55)$$

One might have expected an asymptotically-free theory with zero fermion mass to come closer than this to the conformal solution.

In the previous section, it was found that Leutwyler's sum rule for the pion decay constant was convergent in QCD. The corresponding

sum rule for the  $\gamma_5$ -even part of the wavefunction is obtained by postulating a bilocal divergence relation [4], which connects the value of  $\chi_2(x^2, p \cdot x)$  at the origin with the quark mass,  $m$ .

$$24m \chi_2(0,0) = \left( m_\pi^2 - 4m^2 \right) f_\pi \quad (5-56)$$

In terms of the spectral function, the wavefunction at the origin is

$$\chi_2(0,0) = - \frac{1}{192\pi^2} \int_{-1/2}^{1/2} \int_0^\infty \frac{g_2(\xi, t) dt d\xi}{t} \quad (5-57)$$

According to the operator product expansion and the Bethe-Salpeter equation, the zeroth moment of  $g_2(\xi, t)$  falls off more slowly than  $(\ln t)^{-1}$ , showing that  $\chi_2(x^2, p \cdot x)$  must be infinite at the origin. We conjecture that sum rule (5-56) can be resurrected in QCD with quark mass evaluated at  $(\text{momentum})^2 = t$  and the wavefunction evaluated at a distance  $(t)^{-1/2}$  from the origin. In terms of the regulated single spectral function, one expects the relation

$$- \frac{m(t)}{8\pi^2} \int_0^t \frac{g_2^{(0)}(t) dt}{t} = \left[ m_\pi^2 - 4m^2(t) \right] f_\pi \quad (5-58)$$

This agrees with the operator product expansion result of relation (5-58) if one sets

$$m(t) \approx \frac{1}{\left[ \ln t \right]^{4/3} \left[ 11 - \frac{2}{3} N_F \right]}$$

in agreement with the asymptotic behavior of quark mass in QCD [5].

#### 5.4 Conclusions

Lacking real physical insight into these asymptotic solutions, it is hard to judge their relevance to the bound-state problem in QCD. The  $\gamma_5$ -odd solutions inspire more confidence than the  $\gamma_5$ -even solutions, because of the close correspondence with operator product expansion results. Recalling that, in the operator product expansion, we banished twist-two operators from the  $\gamma_5$ -even wavefunction by setting the quark mass equal to zero, it is natural to wonder whether this assumption is the cause of the present infrared difficulty. In the Born diagram calculation of Appendix A, the masses appearing in the fermion propagators are certainly important, as they make a leading contribution to  $W_T$  (but not to  $W_L$ ).

The  $\gamma_5$ -odd solution appears to be quite useful, especially in providing absolute normalization for  $F_\pi$  and  $W_L$ . In the next chapter we will look at the phenomenological consequences of the asymptotic solutions, with particular emphasis on the expected modifications of the naive scaling laws due to anomalous dimensions and infrared singularities.



Chapter V References and Footnotes

1. T. Appelquist and E. Poggio, Phys. Rev. D 10, 3280 (1974).
2. M. Abramowitz and I. A. Stegun, Handbook of Mathematical Functions, Dover, New York, 1965.
3. C. G. Callan, Jr. and D. J. Gross, Phys. Rev. D 11, 2905 (1974).
4. H. Leutwyler, Nuc. Physics B 76, 413 (1974).
5. H. Georgi and H. D. Politzer, Phys. Rev. D 14, 1829 (1976).

## Chapter VI

## EXPERIMENTAL CONSEQUENCES FOR PION

Predictions for the pion electromagnetic form factor and structure functions will be made using the asymptotic wavefunctions found in the previous chapter. The  $\gamma_5$ -odd wavefunction gives expressions for  $F_\pi$  and  $W_T$  differing only by logarithms from the Born diagram results. The infrared singularity of the  $\gamma_5$ -even solution upsets the Born diagram result for  $W_T$ , giving a  $(\omega-1)^{2/3}$  threshold dependence (presumably with additional logarithmic fall-off).

The  $f_\pi$  sum rule provides absolute normalization for  $F_\pi$  and  $W_L$ , if derivative operator terms in the wavefunction can be neglected. The result for  $F_\pi$  is in reasonable agreement with experiment, while the data for  $W_L$  are too coarse to allow a comparison between theory and experiment.

### 6.1 Infrared Singularities

Although the asymptotic wavefunctions were derived under the assumption that both quarks carried large (momentum)<sup>2</sup>, infrared singularities are evident in both the  $\gamma_5$ -odd and  $\gamma_5$ -even wavefunctions. These may or may not be representative of the true infrared behavior of the exact wavefunctions, but it is necessary to verify that these singularities do not make infinite contributions to the form factor and structure functions. In the following, attention is restricted to the lowest-order solutions, corresponding to operators with no antisymmetric derivatives.

It is expected that the unamputated wavefunction will have singularities due to the fermion propagators. The interesting singularities are those left over when the legs are removed. For example, the  $\gamma_5$ -odd

wavefunction given by expressions (5-42) and (5-43) has a first-power singularity as

$$|x'| \rightarrow \frac{1}{2}$$

This is equivalent to  $k_1^2 \rightarrow 0$  or  $k_2^2 \rightarrow 0$  where  $k_1$  and  $k_2$  are the momenta of quark and antiquark. This singularity is absent in the amputated wavefunction

$$\Gamma_1(p, k, x') = \frac{4f_\pi}{3b p \cdot k \ln \frac{p \cdot k}{M^2}} \left[ x' + \left( x'^2 - \frac{1}{8} \right) \ln \left| \frac{\frac{1}{2} - x'}{\frac{1}{2} + x'} \right| \right] \quad (6-1)$$

$$\Gamma_4(p, k, x') = \frac{-2f_\pi}{3b p \cdot k \ln \frac{p \cdot k}{M^2}} \left[ 1 + x' \ln \left| \frac{\frac{1}{2} - x'}{\frac{1}{2} + x'} \right| \right] \quad (6-2)$$

The amputated wavefunction does have a logarithmic infrared singularity, but we shall find that  $F_\pi$  and  $W_L$  depend upon only the following linear combination.

$$\Gamma_1 + \frac{1}{2} \Gamma_4 = \frac{4f_\pi}{3b p \cdot k \ln \frac{p \cdot k}{M^2}} \left[ x' - \frac{1}{4} + \left( x' - \frac{1}{2} \right) \left( x' + \frac{1}{4} \right) \cdot \right.$$

$$\left. \ln \left| \frac{\frac{1}{2} - x'}{\frac{1}{2} + x'} \right| \right] \quad (6-3)$$

This combination has no singularity as the (momentum)<sup>2</sup> of the unstruck quark approaches zero ( $x' \rightarrow \frac{1}{2}$ ).

Things do not work out so favorably in the case of the  $\gamma_5$ -even solution. Its only contribution is to  $W_T$  through the amputated wavefunction.

$$k^2 \Gamma_2 + \Gamma_3 = (2p \cdot k)^2 \left( \frac{1}{4} - x'^2 \right) \Phi_2 \quad (6-4)$$

Up to a logarithmic factor,

$$\Phi_2 \propto \frac{1}{(2p \cdot k)^3} \int_{-1/2}^{1/2} \frac{\left( \frac{1}{4} - \xi^2 \right)^\gamma}{\left( x' - \xi \right)^3} d\xi \quad (6-5)$$

where

$$\gamma = \frac{1}{3} \quad (6-6)$$

This gives a singularity

$$\Phi_2 \propto \frac{1}{(2p \cdot k)^3 \left( \frac{1}{2} - x' \right)^{2-\gamma}} \quad (6-7)$$

as  $x' \rightarrow \frac{1}{2}$

This singularity is virulent enough to upset the calculation for  $W_T$ , but causes no trouble in the calculations for  $F_\pi$  and  $W_L$ . If the spectral function had vanished more rapidly at the end points, with  $\gamma > 1$ , there would have been no infrared singularity to worry about.

## 6.2 Pion Electromagnetic Form Factor

We will consider the case in which  $q^2$  is large and negative. If all quarks carry large, spacelike momenta, and the momentum in every channel

is non-exceptional (large, negative invariant mass in every channel), the renormalization group says that the asymptotic form of the photon-quark kernel of expression (3-14) is simply the bare photon-quark vertex plus an inverse propagator for the unstruck quark. This is because all gluon dressing disappears as the effective coupling constant goes to zero. Of course, the momenta in the pion channels are exceptional, but we will assume, as in Chapter V, that the two-particle irreducibility of the kernel allows a smooth continuation from non-exceptional to exceptional momenta.

If integration regions where any of the quark momenta are timelike can be ignored, the pion form factor calculation is

$$-i \left\{ 2p_\mu + q_\mu \right\} F_\pi(q^2) = \text{---} \xrightarrow{p} \text{---} \left( \Phi \right) \xrightarrow{\frac{1}{2}p+k} \left( \Phi^{\text{out}} \right) \text{---} \quad (6-8)$$

As Menotti has shown [1], the  $\gamma_5$ -odd part of the wavefunction makes the leading contribution, giving

$$F_\pi \propto \frac{1}{q^2}$$

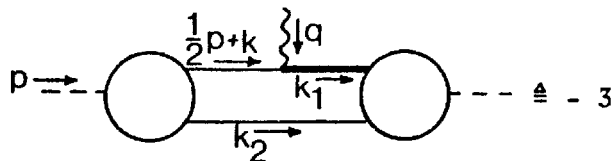
while the  $\gamma_5$ -even part contributes a  $1/(q^2)^2$  term, barring infrared problems.

Following Brodsky and Farrar [2], the loop integration will be divided into two regions, one in which the left upper line carries greater (momentum)<sup>2</sup> than the right-upper line and one in which the opposite situation holds. We are not to assume that one line carries (momentum)<sup>2</sup> of order  $m^2$ , because the wavefunction falls off as  $1/k^4$  at large momenta.

We shall find leading log terms generated by the same mechanism as appeared in the Bethe-Salpeter solution. One log is generated from the region in which the photon momentum flows mainly through the right-hand line. A logarithm is generated at the boundary in  $k$ -space where the integrand changes from  $1/k^4$  due to the left-hand wavefunction (the right-hand wavefunction being "saturated" by the photon momentum and effectively independent of the loop momentum) to  $1/k^7$  due to both wavefunctions and the inverse propagator. This leading log term is proportional  $p^\mu$ . A second leading log term proportional to  $p^\mu + q^\mu$  is generated at the boundary where the left-hand wavefunction goes from the "saturated" to "unsaturated" condition.

We will perform the loop integration using the spectral functions. This makes the calculation easy, but makes it difficult to identify particular regions of loop momentum as important or unimportant. We have not been able to prove the dichotomy of  $k$ -space described above, but believe that this is the true situation, based upon experience with the simpler case of the Bethe-Salpeter equation and the discussion of leading-log generation given by Appelquist and Poggio [3].

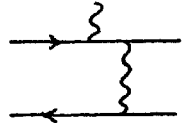
One of the two leading-log terms is



$$\text{---} \cong -3 \int \frac{d^4 k}{(2\pi)^4} \frac{M_\mu}{k_1^2} \quad (6-9)$$

$$M_\mu = \text{Tr} \left[ \left( \not{p} + \not{q} \right) \Gamma_1 + \left( \not{k} + \frac{1}{2} \not{q} \right) \Gamma_4 \right] \left[ \frac{1}{2} \not{p} + \not{q} + \not{k} \right] \gamma_\mu \left[ \phi_1 \not{p} + \phi_4 \not{k} \right] \quad (6-10)$$

The heavy quark line and the symbol  $\Delta$  indicate that we are calculating the leading log term emanating from desaturation of the right-hand wavefunction. The right-hand wavefunction is used in its amputated form while the left-hand wavefunction is unamputated. This mode of expression is mostly a matter of convenience, and is suggestive of the corresponding Born diagram



$$\propto F_{\pi} p_{\mu} \quad (6-11)$$

The wavefunction arguments are not shown in expression (6-10) but it should be noted that  $\Phi$  depends upon the invariants  $k^2$  and  $p \cdot k$ , while the corresponding invariants for  $\Gamma$  are  $\left(k + \frac{1}{2}q\right)^2$  and  $(p+q) \cdot \left(k + \frac{1}{2}q\right)$ .

Doing the spin trace (the color trace produced the factor 3 in (6-9)), one obtains

$$\begin{aligned} M_{\mu} = & 4 \left( \Gamma_1 + \frac{1}{2} \Gamma_4 \right) \left[ \Phi_1 p_{\mu} (q \cdot k - q \cdot p) + \Phi_4 k_{\mu} \left( 2q \cdot k - \frac{3}{2} p \cdot q \right) \right. \\ & + \Phi_1 k_{\mu} p \cdot q + \frac{1}{2} \Phi_4 p_{\mu} k \cdot q \left. \right] + 4 \left[ \left[ p \cdot q k_{\mu} - \right. \right. \\ & \left. \left. - k \cdot q p_{\mu} \right] \left( \Gamma_1 \Phi_4 - \Gamma_4 \Phi_1 \right) \right] \end{aligned} \quad (6-12)$$

Upon integrating, the  $q_{\mu}$  term is found to be non-leading, while the  $p_{\mu}$  term is proportional to  $\Gamma_1 + \frac{1}{2} \Gamma_4$ , which has no infrared singularity. We will approximate this slowly-varying function of  $k_2^2$  (where  $k_2 = \frac{1}{2}(p-k)$  is the momentum of the unstruck quark) by its  $k_2^2 = 0$  value.

$$\Gamma_1 + \frac{1}{2} \Gamma_4 \approx \frac{f_\pi}{3b \left[ \ln \frac{k_1^2}{M^2} \right] k_1^2} + 0 \frac{k_2^2}{\left( k_1^2 \right)^2} \quad (6-13)$$

Using the spectral form for  $\phi$ , we encounter integrals of the form

$$\left( I, I^\mu, I^{\mu\nu} \right) = \frac{d^4 k \left[ 1, k^\mu, k^\mu k^\nu \right]}{\left[ q \cdot \left( k - \frac{1}{2} p \right) \right]^2 \left[ k^2 - 2k \cdot p \xi - t \right]^3} \quad (6-14)$$

With the approximations used in the previous chapter,

$$\left( I, I^\mu, I^{\mu\nu} \right) = - \frac{i\pi^2 \left[ 1, \xi p^\mu, \xi^2 p^\mu p^\nu \right]}{2(p \cdot q)^2 \left( \xi - \frac{1}{2} \right)^2 t} \quad (6-15)$$

The leading log will be generated, as in the Bethe-Salpeter solution, by the  $t$ -integration. Because the leading-log expression contains no  $q^\mu$  factors, the terms we have neglected in expression (6-13) make no contribution. After doing the  $t$ -integration, the final result is

$$F_\pi = \frac{4f_\pi^2}{|q^2| b \ln \left| \frac{q^2}{M^2} \right|} \int_{-1/2}^{1/2} \frac{f_1(\xi) + \xi f_4(\xi)}{\frac{1}{2} - \xi} d\xi \quad (6-16)$$

The functions  $f_i(\xi)$  are defined in the preceding chapter. The normalization used here is such that, for the lowest-order solution,

$$f_1(\xi) + \xi f_4(\xi) = \frac{1}{4} - \xi^2 \quad (6-17)$$

This gives



$$F_{\pi} = \frac{2f_{\pi}^2}{|q^2|b \ln \left| \frac{q^2}{M^2} \right|} \quad (6-18)$$

where

$$b = \frac{11 - \frac{2}{3} N_F}{16\pi^2} \quad (6-19)$$

Data on  $F_{\pi}$  extend to  $q^2 = -4(\text{GeV})^2$  and are consistent with [4]

$$F_{\pi} = \frac{1}{1 - 2.1 q^2} \quad (6-20)$$

The pion decay constant contains the cosine of the Cabbibo angle. Removing this factor gives  $f_{\pi} = 132 \text{ MeV}$ . Our asymptotic expression is supposed to be valid for

$$b g^2 \ln \left| \frac{q^2}{M^2} \right| \gg 1 \quad (6-21)$$

Since this condition is not met by the present data, we attempt to continue the asymptotic expression to smaller  $q^2$  by adopting the monopole form of (6-20) in place of the  $1/q^2$  factor of (6-18) and noting that  $b \ln \left| \frac{q^2}{M^2} \right|$  is just the asymptotic value of the effective coupling constant.

$$F_{\pi} = \frac{4.2 f_{\pi}^2 g^2(q^2)}{(1 - 2.1 q^2)} \quad (6-22)$$

Matching the two expressions for  $F_{\pi}$  at  $q^2 = -2(\text{GeV})^2$  as shown in Figure 6.1 gives  $g^2/4\pi \sim .8$  at  $M = 2 \text{ GeV}$ . Given the ambiguities in determining

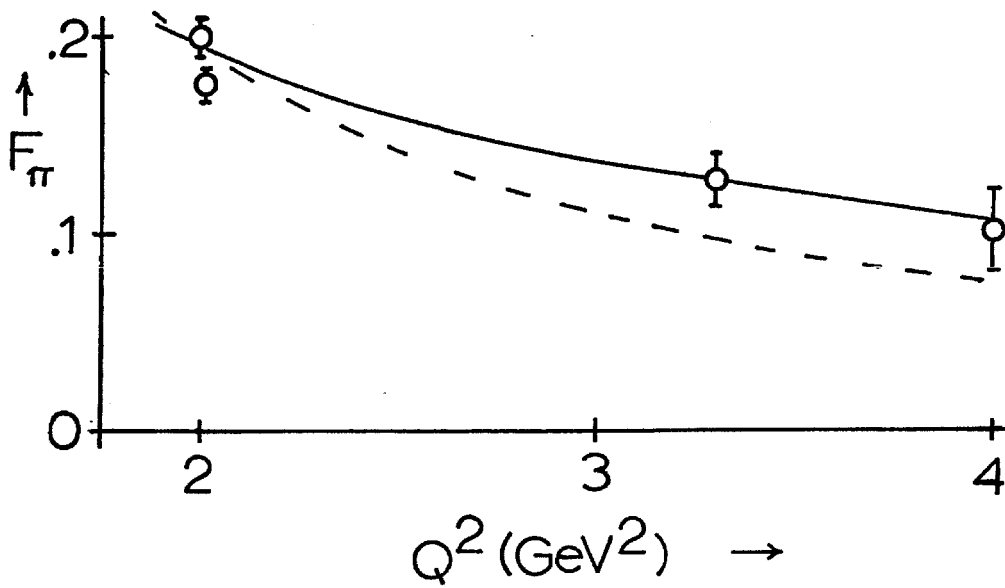


Figure 6.1

Monopole (solid line) and monopole x logarithm (dashed line) compared to spacelike pion form factor data summarized by Bebek et al. The logarithmic curve has  $g^2/4\pi = 0.8$  and  $N_F = 6$  flavors.

the form factor with hydrogen and deuterium targets [4] and the ambiguities of our extrapolation, this result seems reasonable.

Larger  $|q^2|$  values are available in colliding beam experiments, which provide information on the time-like form factor. The errors in these data are too large at present to permit a comparison of theory and experiment [5]. We have not looked into the difficulties the present model might have for time-like  $q$ .

### 6.3 $\gamma_5$ -even Contribution to Form Factor

It is easy to see why the  $\gamma_5$ -even part of the wavefunction makes a non-leading contribution to the pion form factor. First, to the extent that quark masses can be neglected, the odd and even parts of the wavefunction do not interfere in the  $F_\pi$  calculation. The  $\Gamma_3$  part of the amputated wavefunction has no  $\not{q}$  factor, as do  $\Gamma_1$  and  $\Gamma_4$ . With  $\Gamma_1$  and  $\Gamma_4$ , this  $\not{q}$  factor gives rise to a  $p \cdot q$  factor, which is lacking in the  $\Gamma_3$  contribution to  $F_\pi$ . The  $\Gamma_2$  term has a factor  $\not{q}$ , but this is compensated by the  $1/(q^2)^2$  falloff of  $\Gamma_2$ .

All of this amounts to dimensional analysis, assuming that no quark masses enter. If the  $\gamma_5$ -even wavefunction contains no infrared singularities, direct calculation bears out the result of dimensional analysis. Our solution is infrared singular with power behavior

$$\left[ \frac{1}{k^2} \right]^{3-2\gamma}, \quad \gamma = \frac{1}{3}$$

for the integrand in the  $F_\pi$  calculation. A factor

$$\frac{1}{\left(k_2^2\right)^{1-\gamma}}$$

comes from each amputated wavefunction with an additional power of  $1/k_2^2$  coming from two quark propagators. The loop integration is infinite, but we can assume that this infinity would be replaced by a factor

$$\frac{d^4k}{\left(k_2^2\right)^{3-2\gamma}} \rightarrow \left(\frac{1}{m^2}\right)^{1-2\gamma}$$

if masses were taken into account. Using dimensional analysis again, the contribution of the  $\gamma_5$ -even part of the wavefunction to  $F_\pi$  should go as

$$\left(q^2\right)^{-2} \left(q^2\right)^{1-2\gamma} = \left(q^2\right)^{-1-2\gamma}$$

With  $\gamma > 0$ , this is non-leading. Note that  $\gamma > 0$  is also the condition for vanishing of the spectral function  $g_2(\xi, t)$  at the end points,  $\xi = \pm \frac{1}{2}$ .

#### 6.4 Pion Structure Functions

The structure function calculation is beset by two difficulties not encountered in the form factor calculation. First, we have no asymptotic form for the imaginary part of the 4-quark, 2-photon Green's function. As in the Born diagram approach, we shall simply assume that on-shell quarks can be used to approximate the final state. The second problem is that experimental data only exist for time-like photon momen-

tum. The spectral functions provide a means of continuing the wavefunction to timelike momentum, but one may be suspicious of using a bare vertex for timelike photons.

Ignoring these difficulties, the

$$e^+ e^- \rightarrow \pi + \text{Anything}$$

cross-section will be computed from the diagram of Figure 6.2. With

$$x = \frac{2p \cdot q}{q^2} \quad (6-23)$$

and, in the photon rest frame

$$\vec{p} \cdot \vec{k} = |\vec{p}| |\vec{k}| \cos \theta \quad (6-24)$$

the  $\pi^+$  cross-section for unpolarized beams is

$$\frac{d\sigma}{dx d \cos \theta} = \sigma_T (1 + \cos^2 \theta) + \sigma_L \sin^2 \theta \quad (6-25)$$

The transverse and longitudinal cross-sections are given by

$$\sigma_L = \frac{\alpha^2}{4q^2} \frac{p^\mu p^\nu}{p \cdot q} W_{\mu\nu} \quad (6-26)$$

$$\sigma_T + \frac{1}{2} \sigma_L = - \frac{\alpha^2}{8(q^2)^2} \frac{p \cdot q}{2} W_\alpha^\alpha \quad (6-27)$$

where  $\alpha$  is the fine-structure constant and  $W_{\mu\nu}$  is given by the diagram of Figure 6.3.

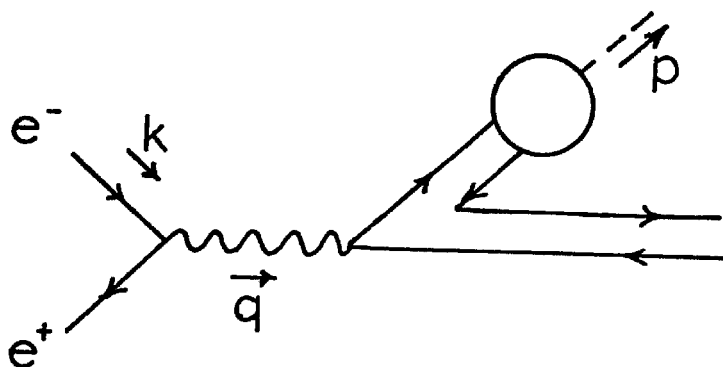


Figure 6.2

Amplitude for  $e^+ + e^- \rightarrow \text{pion} + \text{anything}$

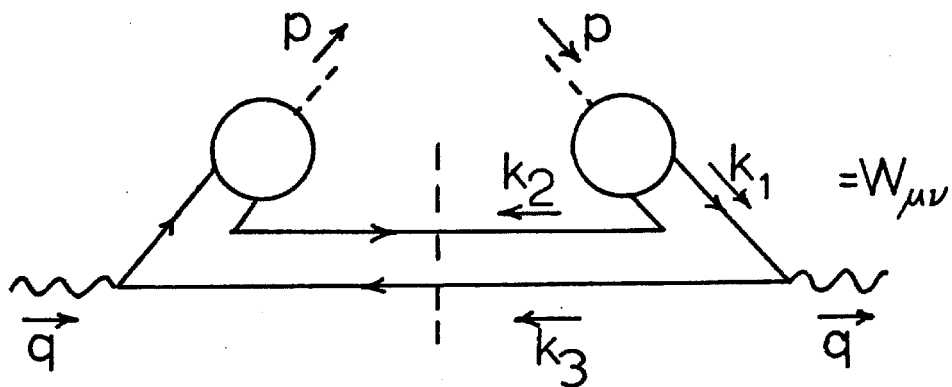


Figure 6.3

Diagram for the pion structure functions

$$W_{\mu\nu} = \int \frac{d^4 k_1}{(2\pi)^2} \frac{T_{\mu\nu}}{[k_1^2]^2} \delta(k_2^2 - m^2) \delta(k_3^2 - m^2) \quad (6-28)$$

$$T_{\mu\nu} = \text{Tr} \left[ (k_3 + m) \gamma_\mu (k_1 + m) \Gamma (k_2 + m) \bar{\Gamma} (k_1 + m) \right] \quad (6-29)$$

The unstruck quark has  $k_2^2 = m^2$ . If the amputated wavefunction has no singularities as  $k_2^2 \rightarrow 0$ , it can be written in the form

$$\Gamma(k_2^2 = 0) = \gamma_5 \left\{ \frac{A}{p \cdot k} \not{p} + \frac{1}{2} \frac{B}{(p \cdot k)^2} [k, \not{p}] + \frac{C}{p \cdot k} + \frac{D}{p \cdot k} \not{k} \right\} \otimes I \quad (6-30)$$

$$k_1 = \frac{1}{2} k + k \quad (6-31)$$

where  $I$  is a unit color matrix. The trace in  $T_{\mu\nu}$  is to be taken over color and spin. Doing the phase space integral (see Appendix A), one obtains the following results:

$$W_{\alpha}^{\alpha} = \frac{-3(1-x)^2}{\pi m^2} \left[ \left( A + \frac{1}{2} D \right)^2 + \frac{(B+C)^2}{m^2} \right] \cdot \frac{5}{9} \quad (6-32)$$

$$p^\mu p^\nu W_{\mu\nu} = \frac{3 \left( A + \frac{1}{2} D \right)^2}{\pi} \left( \ln \frac{W^2}{m^2} - 1 \right) \cdot \frac{5}{9} \quad (6-33)$$

The factor  $5/9$  is the sum of the squares of the two quark charges, and the factor  $3$  comes from the color trace. The normalization of  $p^\mu p^\nu W_{\mu\nu}$  is determined by the sum rule for  $f_\pi$ . The "constants"  $A$  and  $D$  actually have a logarithmic dependence on the (momentum)<sup>2</sup> of the struck quark. Replacing this logarithm by the effective coupling constant,

$$A + \frac{1}{2} D = \frac{1}{3} f_{\pi} g^2 \left( \frac{m^2}{(1-x)M^2} \right) \quad (6-34)$$

This gives

$$q^2 \sigma_L = \frac{5f_{\pi}^2 \alpha^2}{54\pi q^2} g^4 \left( \frac{m^2}{(1-x)M^2} \right) \left( \ln \frac{W^2}{m^2} - 1 \right) \quad (6-35)$$

The data on  $\sigma_L$  in the region  $x \sim 0.8$ ,  $q^2 = 7.4$  set an upper limit  $q^2 \sigma_L < (25 \text{ MeV})^2/q^2$  [6]. This limit is much too high to permit a test of (6-35).

The prediction for  $\sigma_T$  is more uncertain, owing to the infrared singularity of the  $\gamma_5$ -even wavefunction. Following the line of reasoning used for  $F_{\pi}$ ,  $q^2 \sigma_T$  should scale with  $(1-x)^{2/3}$  threshold dependence, rather than the  $(1-x)^2$  dependence indicated by (6-27) and (6-32).

If we simply ignore the  $\gamma_5$ -even wavefunction,

$$q^2 \sigma_T = \frac{5\alpha^2 f_{\pi}^2 (1-x)^2}{432\pi m^2} g^4 \left( \frac{m^2}{(1-x)M^2} \right) \quad (6-36)$$

The quark mass,  $m$ , comes from the mass-shell delta function for the unstruck quark, and appears in (6-36) because it determines an important phase space boundary: the minimum invariant mass of the hadrons produced by the unstruck quark. It seems reasonable to take  $m \sim m_{\pi}$ , which gives values for  $q^2 \sigma_T$  that are two orders of magnitude smaller than the measured values. A quark mass of several MeV would give a more reasonable magnitude for  $q^2 \sigma_T$ , but the effective coupling constant would be substantially greater than unity, invalidating the entire calculation.



We are led to the conclusion that the  $\gamma_5$ -even part of the wavefunction is the dominant contributor to  $\sigma_T$ .

Chapter VI References and Footnotes

1. P. Menotti, Phys. Rev. D 14, 3560 (1976).
2. S. J. Brodsky and G. R. Farrar, Phys. Rev. Letters 31, 1153 (1973), and Phys. Rev. D 11, 1309 (1975); V. Matveev et al., Lett. Nuovo Cimento 7, 719 (1973).
3. T. Appelquist and E. Poggio, Phys. Rev. D 10, 3280 (1974).
4. C. J. Bebek et al., Phys. Rev. D 13, 25 (1976).
5. M. Bernardini et al., Phys. Lett. 46B, 261 (1973); L. Paoluzi, Acta Phys. Pol. B5, 839 (1974).
6. R. F. Schwitters, SLAC-PUB-1666 (1975), and R. Hollebeek, Lawrence Berkeley Laboratory Report No. LBL-3874.

## Chapter VII

## NUCLEON FORM FACTORS

Our treatment of nucleon form factors and structure functions will be less ambitious than the preceding discussion of the pion problem. We revert to the Born diagram approach, but use a more realistic wavefunction than the free quark model of Chapter II and Appendix A. Employing a phenomenological wavefunction with parameters adjusted to give SU(6) symmetry for the "normal" part, we are left with a free parameter that can be adjusted to suppress the  $N \rightarrow \Delta$  electromagnetic transition, in conformity with experiment. This leads to the interesting prediction

$$F_1^{(\text{neutron})} \sim \frac{1}{(q^2)^3}$$

Suppression of the  $N \rightarrow \Delta$  transition is found to be impossible with scalar glue. The spinology rules show that both vector and scalar glue give  $G_E/G_M$  scaling.

The previous chapters indicate that the Born diagram approach gives the correct leading behavior for the pion form factor, provided the infrared singularities of the wavefunction are as tame as those found in the asymptotic solution of the Bethe-Salpeter equation. In applying the Born diagram approach to the nucleon, we are assuming a similar degree of tameness for the nucleon wavefunction, but do not attempt an explicit statement of the required infrared behavior.

## 7.1 $G_E/G_M$ Scaling

In this section, the spinology rules will be applied to a representative diagram to obtain the Brodsky-Farrar predictions for  $G_E$  and  $G_M$ . Three different classes of Born diagrams can be identified in the lowest-order form factor calculation, as illustrated in Figure 7.1. For the sake of brevity, we will only apply the spinology rules to "Class b" diagrams, in which the struck quark emits a single gluon.

Each gluon in the diagrams of Figure 7.1 must carry a sizeable fraction of the photon momentum  $q$ , giving a denominator factor  $1/Q^8$  due to the quark and gluon propagators. The lower gluon in the Class b diagrams must be transverse to avoid an  $m/Q$  suppression factor. The middle quark suffers no change in chirality due to the gluon exchange and must flip its spin in order to avoid an helicity-chirality conflict. This forces the upper gluon to be longitudinal, but carries no penalty because this gluon couples to off-shell quarks. Considering the struck quark, there is no conflict with a transverse photon and an  $m/Q$  suppression factor for the longitudinal photon. The form factors are proportional to the amplitudes of Figure 7.1 divided by the amplitude for a single point fermion to absorb a photon. Including vertex factors, we get

$$G_M \propto G_E \propto 1/Q^4 \quad (7-1)$$

This is the Brodsky-Farrar prediction for nucleon form factors [1], in good agreement with experiment [2]. In the following sections we will consider all Born diagrams and will see that each gives a  $1/Q^4$  contribution. Scalar gluons also give  $G_M \propto G_E \propto 1/Q^4$ , although Class b diagrams have an helicity-chirality conflict and only contribute a  $1/Q^6$  term to  $G_M$ .

$$= \frac{-2\bar{u}'_N \gamma_\mu u_N}{Q^4 (1-z_2)(1-z'_1) z_2 z'_2 z_3 z'_3} = a_1(123)$$

$$= \frac{-2\bar{u}'_N \gamma_\mu u_N}{Q^4 (1-z'_2)(1-z_1) z_2 z'_2 z_3 z'_3} = a_2(123)$$

$$= \frac{2\bar{u}'_N \gamma_\mu u_N}{Q^4 (1-z_1)^2 (1-z'_1)^2 z_3 z'_3} = b(123)$$

$$= 0$$

$$= \frac{2\bar{u}'_N \gamma_\mu u_N}{Q^4 (1-z_3)(1-z'_2) z_2 z'_2 z_3 z'_3} = c(123)$$

Figure 7.1

Born diagrams contributing to nucleon form factors in the Feynman gauge.  $u_N$  is normalized to  $2M(\text{nucleon})$ .

## 7.2 Simple Wavefunction, Approximations

The  $N$ - $N$  and  $N$ - $\Delta$  form factors can be obtained in the ladder approximations by a convolution of the diagrams of Figure 7.1 with appropriate wavefunctions. These diagrams are divided into three classes, according to the type of spin selection rule they obey with vector glue. We will concentrate on vector glue and merely note the places in which scalar glue gives significantly different results.

Diagrams of Class a select the spin of the struck quark to be the same as that of the nucleon. The two gluons are transverse, so the lowest incoming quark line must have spin antiparallel to the nucleon spin. Two and only two quarks must have spin parallel to the nucleon if  $L = 0$ , so Class a diagrams select all 3 quark spins.

Diagrams of Class b also select parallel spin for the struck quark and nucleon, but place a less stringent selection rule on the unstruck quarks, because the gluon connecting to the struck quark is longitudinal, "insulating" that quark from the spin flips of the lower two. These are connected by a transverse gluon and must, in consequence, have antiparallel spins.

Class c diagrams contain two transverse gluons and select all 3 quark spins. Unlike Class a diagrams, the spin of the struck quark is antiparallel to the spin of the nucleon.

With scalar glue, there are no such spin selection rules, and Class b diagrams are non-leading.

In order to gain a degree of generality, we will not assume that the incoming and outgoing quarks are on-shell but will assume that, in the "normal" wavefunction, quark spins can be described by free spinors of mass  $m_N/3$ .

$$\not{p}u = m_N u, \quad \bar{u}u = \frac{2}{3} M_N, \quad p^2 = m_N^2$$

where  $p$  is the four-momentum of the nucleon. This type of wavefunction is used in the relativistic quark model of Feynman, Kislinger, and Ravndal [3]. It is important to recognize that the quarks are not assumed to be free. Rather, the wavefunction has been assumed to factorize into spin and spatial pieces. In a non-relativistic model, one would say that we are neglecting spin-orbit coupling. We shall assume that the spatial part of the wavefunction makes no orbital contribution to hadron spin. While this type of wavefunction may not be a good approximation to reality, it does have the virtues of simplicity and Lorentz covariance. For present purposes, the greatest virtue of this wavefunction is that it can be made SU(6)-symmetric. The gluon exchanges of the Born diagrams provide an explicit SU(6)-breaking mechanism for the "tail" of the wavefunction. It is these breaking effects that we wish to compute and compare with experiment.

As a further approximation, it will be assumed that the wavefunction restricts the squared four-momenta to small values. We neglect the dependence of the Born diagrams of Figure 7.1 upon quark transverse momentum and assume that the only significant wavefunction invariants are the two that measure the fraction of the nucleon momentum carried by each quark in the infinite momentum frame. These fractions will be denoted  $z_1, z_2, z_3$  at the input of the diagram and  $z'_1, z'_2, z'_3$  at the output. Of course,

$$z_1 + z_2 + z_3 = z'_1 + z'_2 + z'_3 = 1 \quad (7-2)$$

The index 1 corresponds to the top (struck) quark in each diagram, and the indices run from top to bottom.

Although no candidate spatial wavefunction is proposed here, it is at least possible to be explicit about its definition. The Bethe-Salpeter wavefunction in configuration space for a nucleon of momentum  $p$  is

$$\chi(p, x_1, x_2) \equiv \langle 0 | T q(x_1) q(x_2) q(0) | p \rangle \quad (7-3)$$

We have suppressed the color and flavor indices of the quark fields,  $q(x)$ . The Fourier transform of  $\chi$  is the unamputated momentum space wavefunction for which we assume the form

$$\Phi(p, k_1, k_2) = \varphi(p, k_1, k_2) \sum_{\alpha, \beta, \gamma} a_{\alpha\beta\gamma} u_{\alpha}(p) \times u_{\beta}(p) \times u_{\gamma}(p) \quad (7-4)$$

The Greek letters are SU(6) indices and  $\varphi(p, k_1, k_2)$  is a scalar function of the five invariants  $k_1^2$ ,  $k_2^2$ ,  $k_1 \cdot k_2$ ,  $p \cdot k_1$ , and  $p \cdot k_2$ . "Convolution" of the Born diagrams with the wavefunction means integrating over  $k_1$  and  $k_2$  at the input and  $k_1'$  and  $k_2'$  at the output. The  $z$ 's introduced earlier are Sudakov variables, defined for a dummy momentum,  $l$ .

$$k_1 = z_1 p + y_1 l + r, \quad r_1 \cdot p = r_1 \cdot l = 0 \quad (7-5)$$

$$k_2 = z_2 p + y_2 l + r, \quad r_2 \cdot p = r_2 \cdot l = 0 \quad (7-6)$$

We assume that the wavefunction falls off rapidly with respect to the  $y_i$  and  $r_i$  in comparison to the Born diagrams, so the convolution involves the two-dimensional wavefunction

$$f(z_1, z_2) = \frac{(p \cdot q)^2}{(2\pi)^4} \int \varphi(p, k_1, k_2) dy_1 dy_2 d^2 r_1 d^2 r_2 \quad (7-7)$$



The integration is carried out in any colinear frame where

$$r_1^0 = r_2^0 = r_1^3 = r_2^3 = 0.$$

Letting  $l^2, p \cdot l \rightarrow \infty$  with  $l^2/p \cdot l$  finite, the support of the wavefunction is restricted to  $0 < (z_1, z_2) < 1$  and we assume that  $f(z_1, z_2)$  becomes independent of  $l^2$  and  $p \cdot l$ . This limiting form of the two-dimensional wavefunction is presumably the 3-quark part of the infinite-momentum-frame wavefunction of the parton model. The other pieces of the parton model wavefunction, the amplitudes to find three valence quarks plus specified quark, antiquark, and gluon combinations can be similarly related to "reducible" Bethe-Salpeter wavefunctions such as  $\langle 0 | T q(x_1) q(x_2) q(x_3) q(x_4) \bar{q}(0) | p \rangle$  which, in turn, can be computed from the "irreducible" wavefunction (Expression 7-3) by definite diagrammatic rules [4].

### 7.3 Evaluating Diagrams

In evaluating the diagrams of Figure 7.1, quark electric charge and the gluon coupling constant will be set equal to unity and the correct charges inserted later when the SU(6) wavefunction is considered. Color wavefunctions and matrices will be ignored because all diagrams carry the same color factor. One might expect that the set of order- $g^4$  diagrams would include trilinear Yang-Mills gluon couplings, but these vanish if the fermions are in a color singlet state. This can be proven by keeping track of color indices as below:

$$\text{Color Singlet} \left\{ \begin{array}{l} \text{---} d \\ \text{---} e \\ \text{---} f \end{array} \right. = \epsilon_{abc} T_{ad}^\alpha T_{be}^\beta T_{cf}^\gamma f_{\alpha\beta\gamma}$$

Greek indices run over 1-8 and Latin indices over 1-3. The point at which the photon attaches has no significance. The right-hand part of this diagram will be multiplied by an antisymmetric color singlet wavefunction,  $\epsilon_{def}$ . Using the antisymmetry of  $\epsilon_{abc}$  and  $f_{\alpha\beta\gamma}$  and the symmetry of  $T_{ab}$ , one can show that the above diagram is completely symmetric in the indices  $def$ . It follows that a distinction between abelian and non-abelian vector glue cannot be made at our level of approximation, with only color singlet nucleons available.

All diagrams contain at least one quark with a single gluon attached. Working in the nucleon-photon Breit frame in which the outgoing nucleon has its three-momentum reversed and energy unchanged, one can evaluate the amplitude for the emission of a single gluon.

$$\frac{q \downarrow \left. \vphantom{q} \right\}^{\alpha}}{S \quad S'} = -i \bar{u}'_{S'} \gamma^{\alpha} u_S \quad (7-8)$$

Using the spinor identities of Chapter II

$$\frac{q \downarrow \left. \vphantom{q} \right\}^{\alpha}}{S \quad S'} = -\frac{iE}{6} \bar{e}_{S'(-S')} \gamma^{\alpha} e_{S(S)}$$

But  $E = Q/2$ , and chirality is unchanged by the vector gluon, giving

$$\frac{q \downarrow \left. \vphantom{q} \right\}^{\alpha}}{S \quad S'} = -\frac{iSQ}{12} \delta_{S(-S')} \left( x^{\alpha} + iS y^{\alpha} \right) \quad (7-9)$$

where  $t^{\alpha} = (1,0,0,0)$ ,  $x^{\alpha} = (0,1,0,0)$ ,  $q^{\alpha} = -Qz^{\alpha}$ , and  $S = \pm 1$ . Expression (7-9) tells us that, to leading order, the gluon must be circularly-polarized and must flip the quark spin.

Diagrams of Class a can now be worked out by evaluating the top fermion line. For example,

$$\begin{array}{c}
 \left. \begin{array}{l}
 1 \xrightarrow{k_c} \xrightarrow{k_d} \\
 \downarrow k_b \\
 2 \\
 \downarrow k_a \\
 3
 \end{array} \right\} = \left(\frac{Q}{4}\right)^3 \frac{(-i)^7 (i)^2 S_2 S_3 \delta_{S_2}(-S_2') \delta_{S_3}(-S_3') N}{27 k_a^2 k_b^2 k_c^2 k_d^2} \quad (7-10)
 \end{array}$$

where, in the Feynman gauge with gluon propagator  $-ig_{\mu\nu}/k^2$ ,

$$N = \bar{e}_{S_1'}(-S_1) \gamma^\mu k_d (\not{x} + iS_2 \not{y}) k_c (\not{x} + iS_3 \not{y}) e_{S_1} S_1 \quad (7-11)$$

Working in the Breit Frame,  $k_d$  and  $k_c$  involve only the Dirac matrices  $\gamma^0$  and  $\gamma^3$ , because we are neglecting transverse momentum.

$$k_c^\alpha = \left( z_1 + z_3 - z_3' \right) \frac{Q}{2}, 0, 0, \left( z_1 + z_3 + z_3' \right) \frac{Q}{2} \quad (7-12)$$

$$k_d^\alpha = z_1' \frac{Q}{2}, 0, 0, (2 - z_1') \frac{Q}{2} \quad (7-13)$$

To evaluate  $N$ , we can operate on the right-hand spinor with  $\not{x} + iS_3 \not{y}$  according to the rules of Chapter II, which give

$$(\not{x} + iS_3 \not{y}) e_{S_1} S_1 = -S_1 (1 - S_1 S_3) e_{(-S_1)}(-S_1)$$

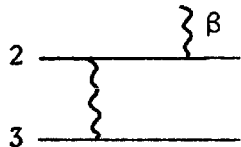
We see that  $S_1$  and  $S_3$  must be opposed, and next act on  $e_{(-S_1)}(-S_1)$  with  $k_c$ .

$$k_c e_{(-S_1)}(-S_1) = Q z_3' e_{(-S_1)}(S_1)$$

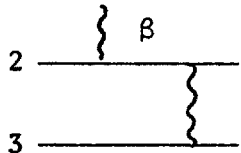
Continuing in this fashion, the right-hand spinor is moved to the left, changing its chirality and/or spin and picking up a factor at each vertex and propagator. Finally,

$$N = Q^2 z_3' (1 - S_1 S_3) (1 + S_1 S_2) S_1 (x^\mu + i S_1 y^\mu) \delta_S (-S_1') \quad (7-14)$$

Diagrams of Class c can be worked out in the same way, while diagrams of Class b differ slightly in having one longitudinal gluon. Up to an overall factor, one finds



$$= A \frac{t^\beta - z^\beta}{1 - z_1'} \quad (7-15)$$



$$= A \frac{t^\beta + z^\beta}{1 - z_1'} \quad (7-16)$$

in any Fermi gauge, that is, any gauge with gluon propagator

$$D_{\mu\nu} = -i \frac{g_{\mu\nu} - (1-\alpha) k_\mu k_\nu / k^2}{k^2} \quad (7-17)$$

In the Feynman gauge ( $\alpha=1$ ), one finds the peculiar result that half of the Class b diagrams are non-leading, as indicated in Figure 7.1. This is not true for  $\alpha \neq 1$  and occurs because the gluon polarization vector enters the upper line as  $\not{k} \pm \not{z}$  in the Feynman gauge. In the leading approximation, this is a multiple of the incoming or outgoing nucleon momentum and annihilates the incoming or outgoing spinor.

#### 7.4 SU(6) Results

Figure 7.1 summarizes our results for the Born diagrams in the Feynman gauge. These amplitudes are to be convoluted with nucleon (or other L=0 baryon) "normal" wavefunctions. It is interesting to assume SU(6) symmetry for the normal wavefunction, as this allows us to obtain relations between transition form factors within an SU(6) multiplet. We will compare the p-p and p- $\Delta$  transitions using the "normal" wavefunctions

$$\begin{aligned}
 |\text{Proton}, S_z = \frac{1}{2}\rangle &= \frac{1}{3\sqrt{2}} \left[ 2|u\uparrow u\uparrow d\downarrow\rangle + 2|u\uparrow d\downarrow u\uparrow\rangle + 2|d\downarrow u\uparrow u\uparrow\rangle \right. \\
 &- |u\uparrow u\downarrow d\uparrow\rangle - |u\downarrow u\uparrow d\uparrow\rangle - |u\uparrow d\uparrow u\downarrow\rangle - |u\downarrow d\uparrow u\downarrow\rangle \\
 &\left. - |d\uparrow u\downarrow u\downarrow\rangle - |d\uparrow u\downarrow u\downarrow\rangle \right] \tag{7-18}
 \end{aligned}$$

$$\begin{aligned}
 |\Delta^+, S_z = \frac{1}{2}\rangle &= \frac{1}{3} \left[ |u\downarrow u\downarrow d\uparrow\rangle + |u\downarrow d\uparrow u\downarrow\rangle + |d\uparrow u\downarrow u\downarrow\rangle \right. \\
 &+ |u\downarrow u\uparrow d\downarrow\rangle + |u\uparrow u\downarrow d\downarrow\rangle + |u\downarrow d\downarrow u\uparrow\rangle + |u\uparrow d\downarrow u\downarrow\rangle \\
 &\left. + |d\downarrow u\downarrow u\uparrow\rangle + |d\downarrow u\uparrow u\downarrow\rangle \right] \tag{7-19}
 \end{aligned}$$

In the leading approximation, all three quarks have their spin flipped at the output. This means that only one of the three helicity amplitudes connecting  $|\text{proton}, S_z = \frac{1}{2}\rangle$  to  $\Delta$  is leading.

The photon acts on the state  $|u\uparrow u\uparrow d\downarrow\rangle$  to produce

$$\begin{aligned}
J^\mu |u\uparrow u\uparrow d\uparrow\rangle = & -i \left\{ q_u \left[ a_1(123) + a_2(123) + a_1(213) + a_2(213) \right. \right. \\
& + 2b(123) + 2b(213) + 2b(132) + 2b(231) \left. \right] + q_d \left[ c(312) \right. \\
& \left. \left. + c(321) \right] \right\} |u\uparrow u\uparrow d\uparrow\rangle \quad (7-20)
\end{aligned}$$

The amplitudes  $a_1$ ,  $a_2$ ,  $b$ , and  $c$  are defined in Figure 7.1. Quark spins are specified in the nucleon rest frame on the left side of this equation and in the rest frame of the outgoing hadron on the right side. Similarly, one finds

$$\begin{aligned}
J^\mu |d\uparrow u\uparrow u\uparrow\rangle = & -i \left\{ q_d \left[ a_1(123) + a_2(123) + 2b(123) \right. \right. \\
& + 2b(132) \left. \right] + q_u \left[ a_1(213) + a_2(213) + 2b(213) + 2b(231) \right. \\
& \left. \left. + c(312) + c(321) \right] \right\} |d\uparrow u\uparrow u\uparrow\rangle \quad (7-21)
\end{aligned}$$

Using the SU(6) wavefunction and permuting indices in (7-20) and (7-21)

$$\langle \text{Proton}^\uparrow | J^\mu | \text{Proton} \rangle = \frac{-i}{9} \left[ \bar{\alpha} (5q_u + q_d) + \bar{\beta} (q_u + 2q_d) \right] \quad (7-22)$$

$$\langle \Delta^+ | J^\mu | \text{Proton} \rangle = \frac{-i\sqrt{2}}{9} (q_u - q_d) (\bar{\alpha} - \bar{\beta}) \quad (7-23)$$

where  $\bar{\alpha}$  and  $\bar{\beta}$  are the averages over the nucleon wavefunctions of the amplitudes  $\alpha$  and  $\beta$  that the struck quark has spin parallel or anti-parallel to that of the nucleon.

$$\alpha = a_1(123) + a_2(123) + 4b(123) + 5 \text{ permutations} \quad (7-24)$$

$$\beta = 2c(123) + 5 \text{ permutations} \quad (7-25)$$

$$\begin{Bmatrix} \bar{\alpha} \\ \bar{\beta} \end{Bmatrix} = \int_0^1 dz_1 dz_2 dz'_1 dz'_2 f(z_1, z_2) f^*(z'_1, z'_2) \begin{Bmatrix} \alpha \\ \beta \end{Bmatrix} \quad (7-26)$$

Not having a definite  $z$ -distribution, we will take  $\bar{\alpha}$  and  $\bar{\beta}$  as free parameters. Experiment indicates that  $\langle \Delta^+ | J^\mu | \text{Proton} \rangle$  falls off faster with  $q^2$  than  $\langle \text{Proton}' | J^\mu | \text{Proton} \rangle$  [5], which leads us to set

$$\bar{\alpha} = \bar{\beta} \quad (7-27)$$

This has an interesting consequence for the neutron form factors. First note that the amplitudes of Figure 7.1 are proportional to  $\bar{u}'_N \gamma_\mu u_N$  which means that we are calculating  $F_1(q^2)$ . Interchanging up- and down-quark indices in (7-22), the neutron form factor is predicted to vanish. Of course, the prediction is really that the neutron  $F_2$  falls off at least as fast as  $Q^{-6}$ . This result is consistent with the existing data [6], which have large errors and only extend to  $Q^2 = 2.5 \text{ (GeV)}^2$ .

For  $\bar{\alpha} = \bar{\beta}$ , no preference is given to quarks with spin parallel or antiparallel to the nucleon. Struck and unstruck quarks are treated in any case democratically; all must flip their spin in going through the Born diagram. In these circumstances it is easy to see why  $\bar{\alpha} = \bar{\beta}$  suppresses the  $p \rightarrow \Delta^+$  (and  $n \rightarrow \Delta^0$ ) transition: The quarks at the output are in the same SU(6) state as the input quarks, giving no overlap with the  $\Delta$ . Further, as each diagram is weighted by the electric charge of the struck quark, the overall amplitude will be proportional to the sum of quark charges if no selection of the spin of the struck quark is made.

This suppresses the neutron  $F_1$ , as indicated above.

For scalar glue, the results are quite different. As noted earlier, Class b diagrams are non-leading. There are two leading  $p\Delta$  form factors because the quark spin selection rules are less stringent with scalar glue. Photons with spin opposed to the nucleon spin and striking quarks with spin parallel to the nucleon spin contribute to the form factor

$$\frac{\langle \Delta^+, S_z = \frac{1}{2} | J^- | \text{Proton}, S_z = \frac{1}{2} \rangle}{\langle \text{Proton}, S_z = \frac{1}{2} | J^- | \text{Proton}, S_z = \frac{1}{2} \rangle} = \frac{\sqrt{2} (q_u - q_d)}{q_d - 4q_u} \quad (7-28)$$

Photons of the opposite helicity striking antiparallel quarks contribute to the form factor

$$\frac{\langle \Delta^+, S_z = \frac{3}{2} | J^+ | \text{Proton}, S_z = \frac{1}{2} \rangle}{\langle \text{Proton}, S_z = -\frac{1}{2} | J^- | \text{Proton}, S_z = \frac{1}{2} \rangle} = \frac{2}{3} \frac{q_u - q_d}{4q_u - q_d} \quad (7-29)$$

With scalar glue, then, the  $p \rightarrow \Delta$  transition must be leading, in contradiction to experiment.

Feynman [7] has proposed a simple breaking rule in which the struck quark is required to have the same isospin as the parent nucleon as  $x \rightarrow 1$ . After the photon strikes, the hadronic final state must still be an SU(2) doublet having no overlap with the  $\Delta$ . This rule, though lacking a dynamical explanation, also seems to be in agreement with the observed neutron/proton inclusive cross-section ratio in deep inelastic scattering. This topic is discussed in the next chapter in connection with the quark spin selection rule.



## 7.6 Asymptotic Freedom

The simple scaling prediction for the pion form factor was found to be modified by one inverse power of  $\ln q^2$ . This power could be traced to the effective coupling constant of the single gluon, which prompts the conjecture that the proton form factor should contain two inverse powers of  $\ln q^2$ . This presumes that, as for the pion, the operator anomalous dimensions contribute negative fractional powers except for one dominant operator having no anomalous dimension. The possible appearance of logarithms in experimental data is discussed at the end of Chapter VIII.

Chapter VII References and Footnotes

1. S. J. Brodsky and G. R. Farrar, Phys. Rev. Letters 31, 1153 (1973), and Phys. Rev. D 11, 1309 (1975); V. Matveev et al., Lett. Nuovo Cimento 7, 719 (1973).
2. P. N. Kirk et al., Phys. Rev. D 8, 63 (1973); K. M. Hanson et al., Phys. Rev. D 8, 753 (1973); W. Bartel et al., Nuc. Phys. B 58, 429 (1973); W. B. Atwood, SLAC Rept. No. 185 (1975).
3. R. P. Feynman et al., Phys. Rev. D 3, 2706 (1971).
4. K. Huang and H. A. Weldon, Phys. Rev. D 11, 257 (1975).
5. See Atwood, Ref. 2 above; S. Stein et al., SLAC-PUB-1528 (1975).
6. See Hanson et al., and Bartel et al., Ref. 2 above.
7. R. P. Feynman, Photo-Hadron Interactions, W. A. Benjamin, Reading, Mass., 1972. See also R. D. Field and R. P. Feynman, California Institute of Technology preprint CALT-68-565, 1977.

## Chapter VIII

## NUCLEON STRUCTURE FUNCTIONS

In this chapter, the Born diagrams contributing to the nucleon structure functions will be evaluated under the assumptions used for the form factor calculation. The predicted threshold behavior  $W_T \propto (\omega-1)^3$  and  $W_T(\text{neutron})/W_T(\text{proton}) = 3/7$  is found to be in rough agreement with experiment. It appears that the discrepancy in the threshold power of  $\omega-1$  may be due to our neglect of higher-order (in  $g^2$ ) diagrams, whose effect should be to lower the gluon coupling constant at large momentum transfers, while the discrepancy in the neutron/proton ratio could be either a fault of our model or a result of ignorance of the deuterium wavefunction.

Our model gives  $W_L/W_T = \mu^2/Q^2$  near threshold with  $\mu^2$  an  $x$ -independent constant whose magnitude depends upon details of the nucleon wavefunction. This result is consistent with the present, inadequate, data.

8.1 Born Diagrams

Compared to the pion case, there are many more diagrams to be considered. No helicity-chirality conflict occurs in  $W_L$  or  $W_T$ , which give the "expected"  $(\omega-1)^3$  dependence.

In the Feynman gauge, the following diagrams make leading contributions to

Nucleon + Transverse Photon  $\rightarrow$  3 Quarks.

$$A_\mu = \begin{array}{c} \Rightarrow \\ \Rightarrow \\ \leftarrow \end{array} \begin{array}{c} \text{---} \\ \text{---} \\ \text{---} \end{array} \begin{array}{c} \text{---} \\ \text{---} \\ \text{---} \end{array} + \begin{array}{c} \Rightarrow \\ \Rightarrow \\ \leftarrow \end{array} \begin{array}{c} \text{---} \\ \text{---} \\ \text{---} \end{array} \begin{array}{c} \text{---} \\ \text{---} \\ \text{---} \end{array} + \begin{array}{c} \Rightarrow \\ \Rightarrow \\ \leftarrow \end{array} \begin{array}{c} \text{---} \\ \text{---} \\ \text{---} \end{array} \begin{array}{c} \text{---} \\ \text{---} \\ \text{---} \end{array} \quad (8-1)$$

$$B_{\mu} = \begin{array}{c} \Rightarrow \\ \Leftarrow \\ \Rightarrow \end{array} \begin{array}{c} \text{---} \\ \text{---} \\ \text{---} \end{array} \begin{array}{c} \text{---} \\ \text{---} \\ \text{---} \end{array} + \begin{array}{c} \Rightarrow \\ \Leftarrow \\ \Rightarrow \end{array} \begin{array}{c} \text{---} \\ \text{---} \\ \text{---} \end{array} \begin{array}{c} \text{---} \\ \text{---} \\ \text{---} \end{array} + \begin{array}{c} \Rightarrow \\ \Leftarrow \\ \Rightarrow \end{array} \begin{array}{c} \text{---} \\ \text{---} \\ \text{---} \end{array} \begin{array}{c} \text{---} \\ \text{---} \\ \text{---} \end{array} \quad (8-2)$$

The amplitudes  $A_{\mu}$  and  $B_{\mu}$  are to be convoluted with the nucleon wavefunction, after which the forward Compton amplitude can be found by squaring and integrating over the phase space of the three outgoing quarks.

There are 16 diagrams to be considered, which will be denoted

$$\mu_0^3 W_{\mu\nu}^{ij} \quad i, j = 1, 2, 3, 4$$

where  $\mu_0$  is a mass parameter coming from the wavefunction. The superscript convention will be defined by giving a few examples.

$$\mu_0^3 W_{\mu\nu}^{11} = \begin{array}{c} \Rightarrow \\ \Rightarrow \\ \Leftarrow \end{array} \begin{array}{c} \text{---} \\ \text{---} \\ \text{---} \end{array} \begin{array}{c} \text{---} \\ \text{---} \\ \text{---} \end{array} \begin{array}{c} \Rightarrow \\ \Rightarrow \\ \Leftarrow \end{array} \quad (8-3a)$$

$$\mu_0^3 W_{\mu\nu}^{22} = \begin{array}{c} \Rightarrow \\ \Leftarrow \\ \Rightarrow \end{array} \begin{array}{c} \text{---} \\ \text{---} \\ \text{---} \end{array} \begin{array}{c} \text{---} \\ \text{---} \\ \text{---} \end{array} \begin{array}{c} \Rightarrow \\ \Leftarrow \\ \Rightarrow \end{array} \quad (8-3b)$$

$$\mu_0^3 W_{\mu\nu}^{33} = \begin{array}{c} \Rightarrow \\ \text{---} \\ \text{---} \end{array} \begin{array}{c} \text{---} \\ \text{---} \\ \text{---} \end{array} \begin{array}{c} \text{---} \\ \text{---} \\ \text{---} \end{array} \begin{array}{c} \Rightarrow \\ \text{---} \\ \text{---} \end{array} \quad (8-3c)$$

$$\mu_0^3 W_{\mu\nu}^{44} = \begin{array}{c} \Rightarrow \\ \text{---} \\ \text{---} \end{array} \begin{array}{c} \text{---} \\ \text{---} \\ \text{---} \end{array} \begin{array}{c} \text{---} \\ \text{---} \\ \text{---} \end{array} \begin{array}{c} \Rightarrow \\ \text{---} \\ \text{---} \end{array} \quad (8-3d)$$

$$\mu_0^3 W_{\mu\nu}^{12} = \begin{array}{c} \Rightarrow \\ \Rightarrow \\ \Leftarrow \end{array} \begin{array}{c} \text{---} \\ \text{---} \\ \text{---} \end{array} \begin{array}{c} \text{---} \\ \text{---} \\ \text{---} \end{array} \begin{array}{c} \Rightarrow \\ \Leftarrow \\ \Rightarrow \end{array} \quad (8-3e)$$

$$\mu_0^3 W_{\mu\nu}^{34} = \begin{array}{c} \Rightarrow \\ \Rightarrow \\ \Leftarrow \end{array} \begin{array}{c} \text{---} \\ \text{---} \\ \text{---} \end{array} \begin{array}{c} \text{---} \\ \text{---} \\ \text{---} \end{array} \begin{array}{c} \Rightarrow \\ \Leftarrow \\ \Rightarrow \end{array} \quad (8-3f)$$

$$\mu_0^3 W_{\mu\nu}^{13} = \begin{array}{c} \Rightarrow \\ \Rightarrow \\ \Leftarrow \end{array} \begin{array}{c} \text{---} \\ \text{---} \\ \text{---} \end{array} \begin{array}{c} \text{---} \\ \text{---} \\ \text{---} \end{array} \begin{array}{c} \Rightarrow \\ \Rightarrow \\ \Leftarrow \end{array} \quad (8-3g)$$

Only two of the sixteen diagrams must be worked out in detail, say  $(ij)=(11)$  and  $(33)$ . The other diagrams either involve a relabeling of the lower two quarks, or are interference terms proportional to a mean of diagrams  $(ij) = (11)$  and  $(33)$ .

The list of diagrams would be considerably longer if we did not work in the Feynman gauge where the amplitudes of Figure 8.1 are non-leading and if we included Class c diagrams (Figure 8.2). As shown in Appendix B, Class c diagrams make a non-leading contribution to the transverse structure functions (even though they do make a leading contribution to the form factors) because the photon momentum is forced to go through a quark propagator, giving an extra factor in the structure function.

Diagrams  $(ij) = (21)$  and  $(12)$  are actually non-leading, because they are interference terms between amplitudes that connect to final states with differing quark spins.

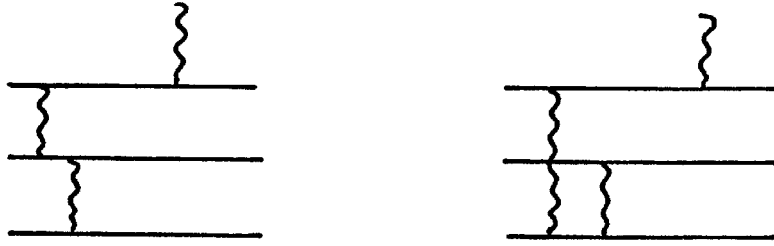


Figure 8.1

Diagrams making a non-leading contribution to the nucleon transverse structure function in the Feynman gauge



Figure 8.2

Diagrams that do not contribute to the transverse structure function in the scaling limit



if all four components of quark transverse momentum are limited to finite values as  $q^2 \rightarrow \infty$ , giving, symbolically,

$$\int d^8k \delta^3(k^2) = \frac{m^4}{W^2} \quad (8-5)$$

As for the pion, off-shell quarks and gluons have

$$(\text{momentum})^2 = 0 \left( \frac{m^2}{\omega-1} \right) \quad (8-6)$$

For every gluon vertex, there is a factor  $m(\omega-1)^{-1/2}$ , which combines with the propagator denominators to give a factor  $(\omega-1)^{1/2}$  for every off-shell quark. Transverse photon vertices receive a factor  $Q$ , while longitudinal photon vertices receive a factor  $m$ . Putting this together with the phase space factor gives

$$W_T \propto (\omega-1)^3 \quad (8-7)$$

$$W_L \propto \frac{(\omega-1)^3}{Q^2} \quad (8-8)$$

The detailed analysis of Appendix B reaches the same conclusion and also gives the following rule: With vector glue, the spin of the struck quark must be parallel to that of the nucleon for  $\omega \approx 1$ . This result is easily obtained from the spinology rules, and is a direct consequence of the suppression of Class c diagrams (see the spinology discussion at the beginning of Chapter VII and the analysis of non-leading diagrams in Appendix B).



### 8.3 Consequences of the Spin Selection Rule

If one is willing to assume SU(6) symmetry for the "normal" wavefunction, the spin selection rule can be translated into a statement about isospin. According to the SU(6) wavefunction (Expression 7-18), a quark carrying the same spin as the parent proton is 5 times more likely to be an up quark than a down quark. The situation is reversed for the neutron, so the ratio of neutron to proton structure functions near threshold is predicted to be

$$\frac{W_T^n}{W_T^p} = \frac{5\left(\frac{1}{3}\right)^2 + \left(\frac{2}{3}\right)^2}{5\left(\frac{2}{3}\right)^2 + \left(\frac{1}{3}\right)^2} = \frac{3}{7} \quad (8-9)$$

For comparison, Feynman's isospin selection rule gives

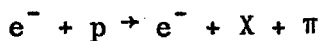
$$\frac{W_T^n}{W_T^p} = \frac{\left(\frac{1}{3}\right)^2}{\left(\frac{2}{3}\right)^2} = \frac{1}{4} \quad (8-10)$$

while a naive prediction is that, because a proton contains two up quarks and one down quark,

$$\frac{W_T^n}{W_T^p} = \frac{2\left(\frac{1}{3}\right)^2 + \left(\frac{2}{3}\right)^2}{2\left(\frac{2}{3}\right)^2 + \left(\frac{1}{3}\right)^2} = \frac{2}{3} \quad (8-11)$$

These predictions will be compared with experiment in Section 8.5.

Another consequence of the spin selection rule, pointed out by Landshoff [1], is that fast pions produced in



near threshold should be preferentially  $\pi^+$ . If u-quarks turn into  $\pi^+$  with unit probability and d-quarks turn into  $\pi^-$  with unit probability, the expected ratio is

$$\frac{\pi^+}{\pi^-} = \frac{5\left(\frac{2}{3}\right)^2}{\left(\frac{1}{3}\right)^2} = 20 \quad (8-12)$$

to be compared with the isospin selection prediction

$$\frac{\pi^+}{\pi^-} = \infty \quad (8-12)$$

and the most naive prediction

$$\frac{\pi^+}{\pi^-} = \frac{2\left(\frac{2}{3}\right)^2}{\left(\frac{1}{3}\right)^2} = 8 \quad (8-14)$$

A "fast" pion is one in the quark fragmentation region with momentum nearly equal to the kinematically allowed maximum. Present data [2] contain too few events in this unpopular corner of phase space to permit a test of these predictions.

A cleaner test of the spin selection rule can be found in the neutrino interactions

$$\nu_\mu + p \rightarrow \mu^- + X$$

$$\bar{\nu}_\mu + p \rightarrow \mu^+ + X$$

The antineutrino interacts with u-quarks while the neutrino interacts with d-quarks leading to the prediction

$$\frac{d\sigma^{\bar{\nu}p}}{dx} \bigg/ \frac{d\sigma^{\nu p}}{dx} = \frac{5}{3} \quad (8-15)$$

near  $\omega = 1$ . This ratio takes on the values  $\infty$  and  $\frac{2}{3}$ , respectively, for the isospin selection rule and the naive quark counting rule.

#### 8.4 Quark Spin Selection for Longitudinal Structure Functions

The longitudinal structure functions in our model have the same threshold behavior as found for the transverse structure functions and vanish in the scaling limit according to

$$\frac{W_L}{W_T} = \frac{(\text{mass parameter})^2}{p \cdot q} + O(g^2(1-x)) \quad (8-16)$$

Changing the photon polarization from transverse to longitudinal introduces an helicity-chirality conflict that can be resolved by a chirality reversal in one of the propagators of the upper fermion line or by using the "wrong chirality" piece of the spinor of the struck quark. This gives the relation

$$\Rightarrow \begin{array}{c} \text{L} \} \\ \text{T} \} \text{T} \\ \text{T} \} \text{T} \\ \text{T} \} \end{array} \Rightarrow = \frac{\mu_1^2}{2pq} \Rightarrow \begin{array}{c} \text{T} \} \\ \text{T} \} \text{T} \\ \text{T} \} \text{T} \\ \text{T} \} \end{array} \Rightarrow \quad (8-17)$$

where the mass parameter  $\mu_1^2$  depends upon the quark mass. With the transverse gluons, as indicated above, quark spin selection is made in the same way for both transverse and longitudinal photons. Things are actually more complicated than this, owing to the fact that, near threshold, the upper quark is far from its mass shell before the photon strikes.

This makes it possible to exchange a longitudinal gluon and transfer the helicity-chirality conflict to one of the lower quarks. Such a term in diagram (11) is

$$\left( \begin{array}{c} \leftarrow \\ \Rightarrow \\ \Rightarrow \end{array} \right) \left( \begin{array}{c} L \\ | \\ L \\ | \\ T \\ | \\ T \end{array} \right) \left( \begin{array}{c} \leftarrow \\ \Rightarrow \\ \Rightarrow \end{array} \right) = \frac{\mu_2^2}{2p \cdot q} \left( \begin{array}{c} \Rightarrow \\ \leftarrow \\ \Rightarrow \end{array} \right) \left( \begin{array}{c} T \\ | \\ T \\ | \\ T \\ | \\ T \end{array} \right) \left( \begin{array}{c} \Rightarrow \\ \leftarrow \\ \Rightarrow \end{array} \right) \quad (8-18)$$

The longitudinal photon vertices introduce a factor  $\frac{p \cdot k_1}{p \cdot q}$  and the lower longitudinal gluon vertices introduce a factor  $\frac{m^2}{p \cdot k_1}$  relative to the transverse photon diagram.

One concludes that, in this model, the quark spin selection rule is violated by longitudinal photons. Near threshold, we see a departure from parton model ideas, in that knowledge of the wavefunction as measured by transverse photons is insufficient to determine  $W_L$ . This behavior, and the  $\omega$ -dependent  $W_L/W_T$  ratio found for the pion, result from the insistence of our model that quarks with  $\omega \approx 1$  have (momentum)<sup>2</sup> of order  $-4m^2/(\omega-1)$ .

We have not performed an exhaustive evaluation of all diagrams contributing to  $W_L$  as we did for  $W_T$ . Calculating  $W_L$  is quite laborious because

$$p^\mu p^\nu M_{\mu\nu}^{ij} \propto (p \cdot k_1)^{-4} p \cdot q m^2 h^{ij}(y_2) \quad (8-19)$$

with quark mass  $m$  coming from numerous propagators and spinors.

### 8.5 Comparison with Experiment

To test the prediction  $W_T \propto (\omega-1)^3$ , we will consider the wide-angle electroproduction data [3] summarized in Figure 8.3. The appearance of

scaling is enhanced, rightly or wrongly, by use of Atwood's empirically-determined scaling variable

$$x_s = \frac{-1}{\frac{2p \cdot q}{q^2} + \frac{M_s^2}{q^2}} \quad (8-20)$$

with  $M_s^2 = 1.42(\text{GeV})^2$ . The data are fit quite well by  $(1-x_s)^4$  and not nearly as well by  $(1-x_s)^3$ . It is interesting that simple power behavior holds over a very wide range of  $x_s$ .

Accepting  $x_s$  as the correct variable expressing prococious scaling, these data show a possible violation of the Drell-Yan-West relation, as the asymptotic proton magnetic form factor follows  $\frac{1}{(q^2)^2}$  reasonably well [3]. For the proton, a rough argument can be made that the form factor, proportional to  $g^4$  in our model, should actually show a logarithmic dependence on  $q^2$ .

$$G_M \propto \frac{1}{(q^2)^2 \left[ 1 + b g^2 \ln \left| \frac{q^2}{\mu^2} \right| \right]^2} \quad (8-21)$$

The logarithmic factor is borrowed, without benefit of a renormalization group derivation, from the effective coupling constant

$$g^2(q^2) = \frac{g^2}{1 + b g^2 \ln \left| \frac{q^2}{M^2} \right|} \quad (8-22)$$

where  $g$  is the coupling constant at the renormalization point  $M$ , and  $b$  depends upon the number of flavors,  $N_F$ .

$$16\pi^2 b = 11 - \frac{2}{3} N_F \quad (8-23)$$

In the structure function calculation, the gluons carry (momentum)<sup>2</sup> of order  $-4m^2/(1-x)$ , so one might similarly expect

$$W_T \propto \frac{(1-x)^3}{\left[1 + b g^2 \ln \frac{4m^2}{M^2(1-x)}\right]^4} \quad (8-24)$$

If this view is at least qualitatively correct, form factors and structure functions should fall off faster than the simple powers of  $q^2$  and  $1-x$  predicted by our model, with the largest effect appearing in the structure function, which is proportional to  $g^8$ . Expression (8-24) can mimic  $(1-x)^4$  over an appreciable range of  $x$ .

The choice

$$N_F = 6 \text{ flavors}$$

$$\frac{g^2}{4\pi} = \frac{1}{3}$$

$$M = 2 \text{ GeV}$$

gives a reasonable fit to the data over a rather wide range of quark masses. As shown in Figure 8.3, the preferred quark mass is in the neighborhood of 300 MeV. It can be readily verified that (effective coupling constant)<sup>2</sup>/4 $\pi$  is less than unity over the range of the data in Figure 8.3.

One must ask whether the expected logarithmic dependence of the form factor should be visible in present data. The data on  $G_M$  for the

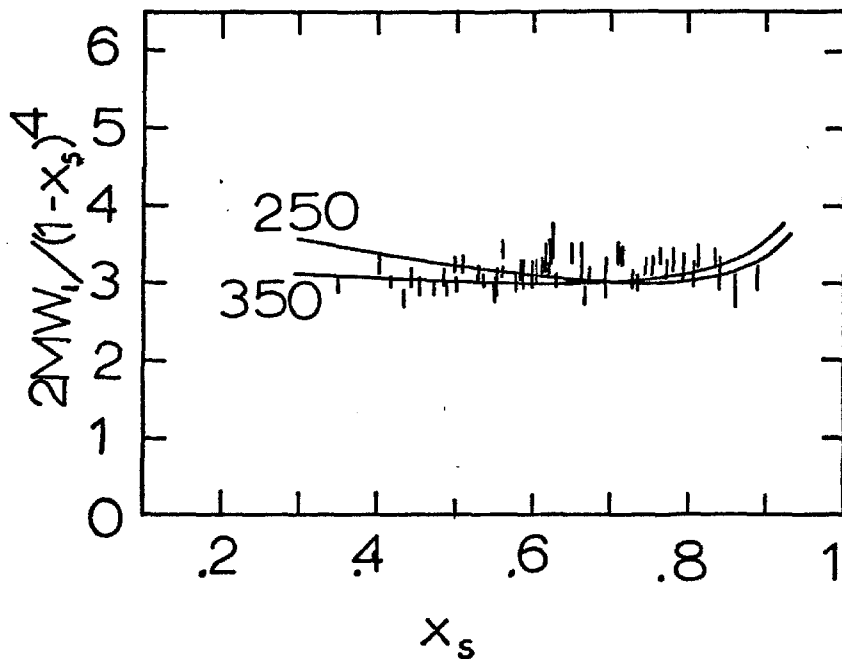


Figure 8.3

Data for proton transverse structure function as presented by Atwood compared to Expression (8-24) with  $m = 250$  and  $350$  MeV

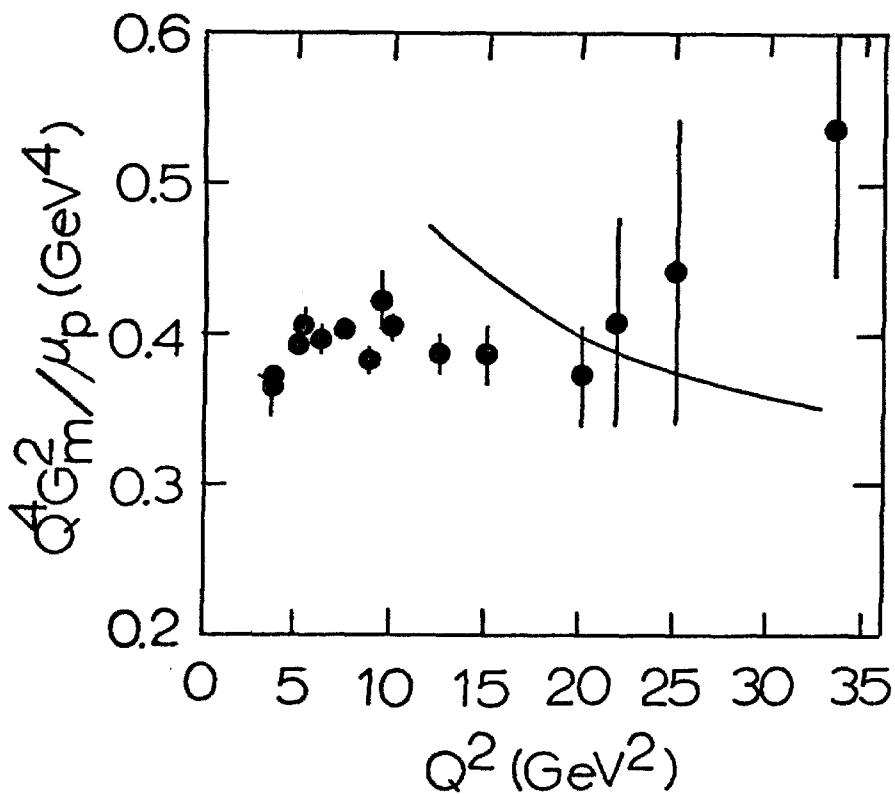


Figure 8.4

Experimental data for proton magnetic form factor presented by Atwood compared to expression (8-21)

proton [3] show approximate  $1/Q^4$  behavior over the range  $10 < Q^2 < 33 \text{ GeV}^2$ . The logarithmic factor of (8-21) drops by 30% as  $Q^2$  increases from 10 to  $33 \text{ GeV}^2$ . This additional predicted fall-off of the form factor is of the order of the experimental error, as Figure 8.4 shows. The  $33 (\text{GeV})^2$  data point may have a large systematic error, as the empty and full target signals were nearly equal. It is an interesting possibility that asymptotic freedom may be more easily discernible in the x-dependence of structure functions near threshold than in scaling violations, where it is often sought.

Atwood summarizes data on the neutron/proton cross-section ratio in inclusive electroproduction [3]. The data tend toward a ratio near the isospin selection value,  $1/4$ , as  $x$  approaches unity. According to our spin selection rule, the threshold ratio should be  $3/7$ . Considering the smearing corrections made for neutron motion in the deuterium nucleus, the data may be consistent with the value  $3/7$ . For example, at  $-\frac{q^2}{2p \cdot q} \approx 0.85$ , nucleon motion smears the true  $x$ -value, measured with respect to the neutron rather than the deuterium nucleus, over the range  $0.7 - 1.0$ . The structure functions change rapidly over this interval, and the correction factor applied to the neutron cross section is on the order of  $0.8$  with a systematic uncertainty of order  $10\%$  [4]. The correction factor becomes rapidly smaller and the uncertainty larger as  $x$  is increased, so the possibility that the neutron/proton ratio is approaching  $3/7$  cannot be ruled out. The value  $3/7$  is only supposed to hold for the ratios of transverse structure functions whereas the data are presented as total cross-section ratios. At large angles ( $50^\circ$  and  $60^\circ$ ), about  $2\%$  of the events are due to longitudinal photons, assuming  $W_L/W_T \approx .2$ , so the



ratio 3/7 should hold accurately. Data at the smaller angles could have up to 15% contamination due to longitudinal photons if  $W_L/W_T \approx .2$ . Data on  $W_L/W_T$  are very poor and we are unable to estimate the degree to which longitudinal photons break the spin selection rule. In principle, longitudinal structure functions of the neutron and proton can provide a test of the spin and isospin selection rules. A better test may be possible in the near future using neutrino data from hydrogen bubble chambers.

Chapter VIII References and Footnotes

1. P. V. Landshoff, private communication to G. R. Farrar.
2. G. Wolf, 1975 International Symposium on Lepton and Photon Interactions at High Energies, Stanford University, DESY 75/40 (1975); J. T. Dakin et al., SLAC-PUB-1421 (1974); C. A. Heusch, EPS International Conference on High-Energy Physics, Palermo, June 1975.
3. W. B. Atwood, SLAC Rept. No. 185 (1975).
4. A Bodek, MIT Lab. for Nuc. Science Tech. Rept. No. COO-3069-116 (1972).

## Appendix A

DETAILED EVALUATION OF BORN  
DIAGRAM FOR PION STRUCTURE FUNCTIONS

Electron-positron annihilation into a pion-plus-anything in this model is described by the diagram of Figure A.1 where the lepton pair is not shown and the dotted vertical line denotes taking the real, delta function part of the quark propagators, corresponding to the parton model assumption of nearly free quarks in the final state. The definition of  $W_{\mu\nu}$  is

$$W_{\mu\nu} = \int d^4x e^{iq \cdot x} \langle \pi, p | J_\mu(x) J_\nu(0) | \pi, p \rangle \quad (\text{A-1})$$

and the most general gauge-and Lorentz-invariant decomposition is

$$\begin{aligned} W_{\mu\nu} = & \left( \bar{g}_{\mu\nu} - \frac{q_\mu q_\nu}{q^2} \right) W_1(q^2, p \cdot q) \\ & + \frac{1}{m_\pi^2} \left( P_\mu - \frac{p \cdot q q_\mu}{q^2} \right) \left( P_\nu - \frac{p \cdot q q_\nu}{q^2} \right) W_2 \end{aligned} \quad (\text{A-2})$$

Figure A.1 contains an unknown mass parameter,  $\mu_0$ , owing to the fact that two free quarks are not really the same thing as one pion. In the correct treatment, these powers of mass are supplied by the pion wavefunction.  $W_1$  and  $W_2$  are the usual dimensionless structure functions, but it will be more convenient to compute the following invariants:

$$W_\alpha^\alpha = -3W_1 + \left( 1 - \frac{(p \cdot q)^2}{m_\pi^2 q^2} \right) W_2 \quad (\text{A-3})$$

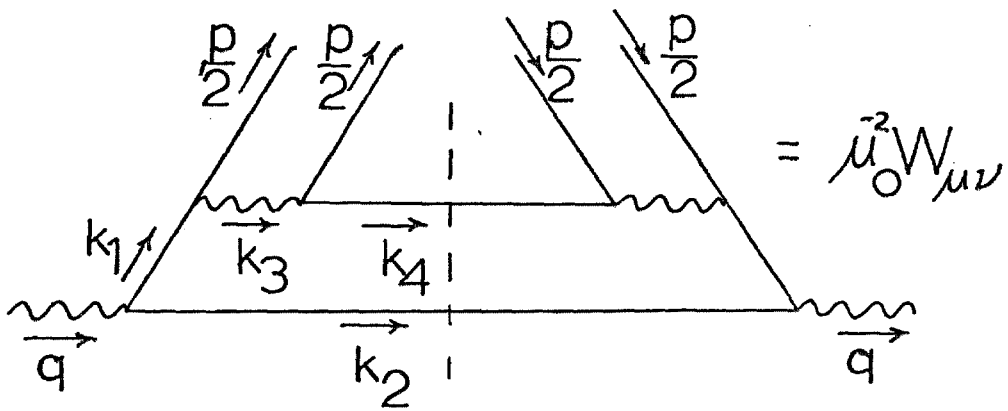


Figure A.1

Born diagram for pion structure functions

$$p^\mu p^\nu W_{\mu\nu} = -m_\pi^3 \left[ 1 - \frac{(p \cdot q)^2}{m_\pi^2 q^2} \right] \left[ W_1 - \left( 1 - \frac{(p \cdot q)^2}{m_\pi^2 q^2} \right) W_2 \right] \quad (\text{A-4})$$

Experimentally, the longitudinal and transverse structure functions are convenient quantities.

$$W_T = W_1 \quad (\text{A-5})$$

$$W_L = W_1 - \left( 1 - \frac{(p \cdot q)^2}{m_\pi^2 q^2} \right) W_2 \quad (\text{A-6})$$

We see that  $p^\mu p^\nu W_{\mu\nu}$  is proportional to  $W_L$ . Furthermore, if  $W_L \ll W_T$ ,  $W_\alpha^\alpha$  is proportional to  $W_T$ .

The struck quark has mass  $m_1$  and the unstruck quark has mass  $m_2$ .

We will actually assume

$$m_1 = m_2 = m$$

but keep the labels for convenience in later calculations. The mass assumption forces the free quarks that mimic the pion to have precisely  $\frac{1}{2}$  the pion mass and  $\frac{1}{2}$  the pion four-momentum,  $p$ . This somewhat awkward assumption will not be necessary when a more realistic pion wavefunction is used, but it is helpful here in permitting use of the completeness relation

$$\sum_s v_s \begin{pmatrix} p \\ 2 \end{pmatrix} \bar{u}_{-s} \begin{pmatrix} p \\ 2 \end{pmatrix} = \left( \frac{\not{p}}{2} + m \right) \gamma_5 \quad (\text{A-7})$$

In spite of appearances, this is a spin-zero combination of  $u$ 's and  $v$ 's. A spin-zero combination of  $u$ 's alone would have the difference of

the direct products. Equation (A-7) will make it possible to use traces in computing pion diagrams, and the symbol  $m$  will be kept distinct from  $m_1$  and  $m_2$  in recognition of its later appearance as a general wavefunction parameter. Omitting overall powers of  $\sqrt{-1}$  and the gluon and photon coupling constants,

$$W_{\mu\nu} = \mu_0^2 \int \frac{d^4 k_1}{(2\pi)^2} \frac{\delta(k_2^2 - m_1^2) \delta(k_4^2 - m_2^2)}{\left(k_1^2 - m_1^2\right)^2 \left(k_3^2\right)^2} T_{\mu\nu} \quad (\text{A-8})$$

With gluon propagator  $-ig_{\mu\nu}/(k_2)^2$ ,

$$\begin{aligned} T_{\mu\nu} &= \text{Tr}(\not{p} - 4m) \left(\not{k}_4 + m_2\right) (\not{p} - 4m) \left(\not{k}_1 + m_1\right) \cdot \\ &\cdot \gamma_\mu \left(\not{k}_2 + m_1\right) \gamma_\nu \left(\not{k}_1 + m_1\right) \end{aligned} \quad (\text{A-9})$$

The free quark picture used here will only be taken seriously in the scaling region

$$q^2, p \cdot q \rightarrow \infty, \quad \omega \text{ finite.}$$

The scaling variable  $\omega$  is defined for time-like photons as

$$\omega = \frac{q^2}{2p \cdot q} \quad (\text{A-10})$$

and ranges between 1 and  $\infty$ . The "threshold" region near  $\omega = 1$  will be of primary interest to us, but  $\omega = 1$  cannot be approached too closely without entering the resonance region. We will always assume  $W^2 \gg m_\pi^2$ , where

$$W^2 = (q-p)^2 \simeq 2p \cdot q(\omega-1) \quad (\text{A-11})$$

A change of integration variables will be made from  $k_{1\mu}$  to the Sudakov variables,  $u, y, r_x, r_y$  defined by

$$\begin{aligned} k_1 &= up + yq + r \\ p \cdot r &= q \cdot r = 0 \end{aligned} \tag{A-12}$$

These new variables are convenient because, as will appear,  $-u$  is very nearly equal to  $\omega$ . Furthermore,  $r$  is the quark transverse momentum in the photon rest frame, where we take

$$\begin{aligned} p &= p_0, 0, 0, p_3 \\ q &= Q, 0, 0, 0 \\ r &= 0, r_1, r_2, 0 \end{aligned}$$

The variable  $y$  will turn out to give a measure of how far from mass shell virtual quarks and gluons are. Doing the integration over  $\phi = \tan^{-1} \frac{r_2}{r_1}$ ,

$$\int d^4 k_1 = \pi p \cdot q \int dr^2 du dy \tag{A-13}$$

Because

$$k_2^2 = u^2 \frac{m^2}{\pi} + 2u(y+1)p \cdot q + (y+1)^2 q^2 + r^2 \tag{A-14}$$

we have

$$\int \delta(k_2^2 - m_1^2) dr^2 = 1 \tag{A-15}$$

The two mass-shell conditions  $k_2^2 = m_1^2$ ,  $k_4^2 = m_2^2$ , give

$$u = -\omega + y(1-2\omega) + O\left(\frac{m^2}{q^2}\right) \tag{A-16}$$

$$r^2 = m_2^2 - (\omega-1)^2 m_\pi^2 + 2p \cdot q (\omega-1) y (1+y) \quad (\text{A-17})$$

The transverse momentum four-vector  $r$  is space-like so (A-17) expresses kinematic limits on  $y$ . For  $\omega-1 \ll 1$ , the limits set by  $r^2 < 0$  are

$$-1 < y < -\frac{m_2^2}{2p \cdot q (\omega-1)} \quad (\text{A-18})$$

The maximum transverse momentum occurs for  $y \approx \frac{1}{2}$  and has the magnitude  $-r^2 = \frac{1}{4} W^2$ . In actuality, the transverse momentum is limited to values of order  $m^2$  by the quark and gluon propagators. The squared momenta of the virtual quarks and gluons are, respectively.

$$k_1^2 = m_2^2 - (1+2u)m_\pi^2 - 2yp \cdot q \quad (\text{A-19})$$

$$k_3^2 = m_2^2 - \left( \frac{3}{4} + 2u \right) m_\pi^2 - yp \cdot q \quad (\text{A-20})$$

These denominator factors accentuate the small  $-y$  region, so that

$$y = 0 \left( \frac{-m_2^2}{2p \cdot q (\omega-1)} \right) \quad (\text{A-21})$$

$$-r^2 = 0 \left( m_2^2 \right) \quad (\text{A-22})$$

$$u = -\omega + 0 \left( \frac{m_2^2}{q} \right) \quad (\text{A-23})$$

Most important is the fact that the virtual quarks and gluons have

$$k_1^2, k_3^2 = 0 \left( \frac{m_2^2}{\omega-1} \right) \quad (\text{A-24})$$



If  $m_2^2$  is not too small, all virtual particles are far off-shell, giving hope that our perturbation approach makes sense for  $\omega \rightarrow 1$  in an asymptotically-free theory.

With this look at the magnitude of things, it follows that, for  $q^2$  large and  $\omega \rightarrow 1$ ,

$$\int \delta(k_4^2 - m_2^2) du = \frac{1}{2p \cdot q} \quad (\text{A-25})$$

$$W_{\mu\nu} = - \frac{\mu_0^2}{32\pi (p \cdot q)^4} \int_{\frac{-m_2^2}{2}}^{-1} T_{\mu\nu} \frac{dy}{y^4} \quad (\text{A-26})$$

Turning to the trace,  $T_{\mu\nu}$ ,

$$T_{\mu}^{\mu} = 8p \cdot q k_1^2 \left(4m + m_1\right)^2 - m_2^2 + (\omega - 1)k_1^2 \quad (\text{A-27})$$

$$p^{\mu} p^{\nu} T_{\mu\nu} = 4p \cdot q \left(k_1^2\right)^3 (1 + \gamma) \quad (\text{A-28})$$

The leading approximation to  $T_{\alpha}^{\alpha}$  depends on the wavefunction mass parameter  $m$ . The unstruck quark mass,  $m_2$ , also enters through the kinematic limit (A-18).

Doing the  $y$ -integration, the structure functions are

$$W_{\alpha}^{\alpha} = - \frac{\mu_0^2 (-1)}{\pi m_2^4} m_2^2 + \left(4m + m_1\right)^2 \quad (\text{A-29})$$

$$p^{\mu} p^{\nu} W_{\mu\nu} = \frac{\mu_0^2}{\pi} \left[ -1 + \ln \frac{W^2}{m_2^2} \right] \quad (\text{A-30})$$

In terms of these quantities, the transverse and longitudinal structure functions are

$$W_T = -\frac{1}{2} \left( W_\alpha^\alpha + W_L \right) \quad (\text{A-31})$$

$$W_L = \frac{p^\mu p^\nu W_{\mu\nu}}{(p \cdot q)^2 / q^2 - m_\pi^2} \quad (\text{A-32})$$

A glance at expression (A-31) makes it apparent that we have cheated a bit in discussing the region

$$\omega - 1 < \frac{\mu^2}{W} \quad (\text{A-33})$$

in Chapter II. The issue is whether

$$W_T \propto (\omega - 1)^2$$

in this region or whether  $W_T$  also contains an  $\omega$ -independent, non-scaling piece comparable to  $W_L$ . In the first case,

$$\frac{W_L}{W_T} \rightarrow \infty, \quad \begin{array}{l} \omega \rightarrow 1 \\ q^2 \text{ fixed, large} \end{array}$$

while, in the second case,  $W_L/W_T$  approaches a finite, non-zero value in this limit. There is no problem here with the order of limits  $\omega \rightarrow 1$ ,  $q^2 \rightarrow \infty$ , because (A-33) can be readily satisfied for finite  $q^2$  with  $W^2$  well above the resonance region.

Expressions (A-30, 31, 32) show that there is an  $\omega$ -independent, non-scaling contribution to  $W_T$  coming from  $p^\mu p^\nu W_{\mu\nu}$ . Furthermore, the

non-scaling contribution to  $W_\alpha^\alpha$  from diagram A.1 is suppressed near threshold, offering no hope of a cancellation from this source. We find, however, that the other diagrams of fourth order give cancelling terms such that

$$W_T \propto (\omega-1)^2 + O \frac{(\omega-1)m^2}{q^2}$$

Furthermore, these additional diagrams give no new contributions to  $\bar{W}_L$ , and  $W_L/W_T \rightarrow \infty$  as  $\omega \rightarrow 1$ . The additional diagrams of order  $g^4$  are shown in Figure A.2. We have omitted diagrams of the forms shown in Figure A.3 as these make no provision for the struck quark to absorb the momentum of its partner and so do not contribute for  $\omega \rightarrow 1$ . Explicit calculation of the diagram of Figure A.2a shows that it can be forgotten as it contributes pieces

$$W_T \propto (\omega-1)m^2/q^2$$

$$W_L \propto (\omega-1) \left( \frac{m^2}{q} \right)^2$$

For A.2b and c we find that the contribution to  $W_L$  falls off as  $\left(1/q^2\right)^2$  and can be forgotten, while the contribution to  $W_T$  just cancels the  $1/q^2$  piece coming from A.1, as asserted above.

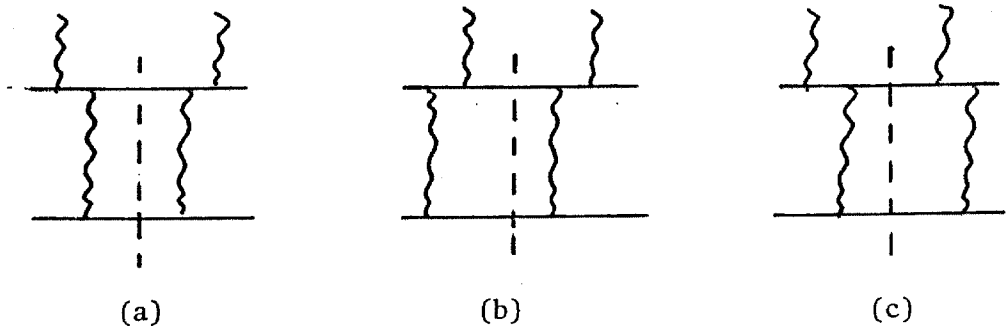


Figure A.2

Additional order  $g^4$  diagrams for pion structure functions

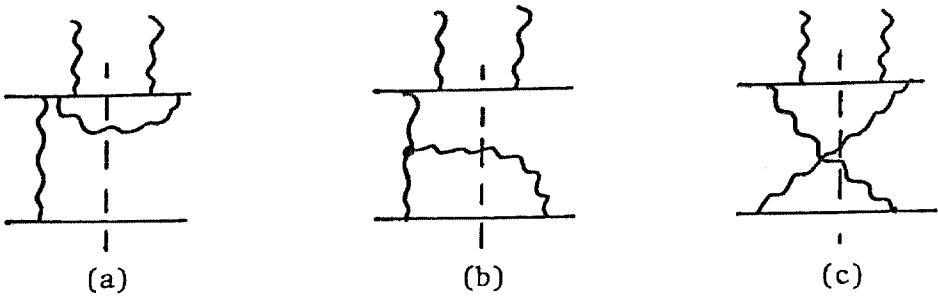


Figure A.3

Some diagrams that do not contribute to the pion structure function in the limit  $\omega \rightarrow 1$

## Appendix B

DETAILED EVALUATION OF BORN DIAGRAMS  
FOR NUCLEON STRUCTURE FUNCTIONS

In performing the phase space integral of Expression (8-4), two sets of Sudakov variables will be used.

$$k_1 = x_1 p + y_1 q + r_1 \quad , \quad r_1 \cdot p = r_1 \cdot q = 0 \quad (\text{B-1})$$

$$k_2 = x_2 p + y_2 k_1 + r_2 \quad , \quad r_2 \cdot p = r_2 \cdot k_1 = 0 \quad (\text{B-2})$$

The integration over  $k_1$  will be done after the integration over  $k_2$ . It is convenient to express  $k_2$  in terms of  $p$  and  $k_1$ , rather than  $p$  and  $q$  (compare (B-1) and (B-2) ) because the propagators and traces are most simply expressed in terms of the invariants  $k_1^2$  and  $p \cdot k$ , rather than in terms of  $q^2$  and  $p \cdot q$ . Erasing part of the diagram as in Figure B.1, one can think of the first integration as a calculation of the structure function for a nucleon to emit a quark of momentum  $k_1$ . The transverse momentum of the lower two quarks is  $r_2$  and, as in the pion calculation, the azimuthal integration over  $\tan^{-1} r_{2x}/r_{2y}$  can be done "for free." Expressing this result in terms of the invariants  $k_1^2$  and  $k_1 \cdot p$ , the  $d^4 k_1$  integrand is independent of  $\tan^{-1} r_{1x}/r_{1y}$ . The integrations over  $r_1^2$  and  $r_2^2$  can also be done trivially thanks to the mass-shell delta functions.

$$\int dr_2^2 \delta(k_2^2 - m^2) = \int dr_1^2 \delta\left[\left(k_1 + q\right)^2 - m^2\right] = 1 \quad (\text{B-3})$$

Using

$$\int dx_2 \delta(k_3^2 - m^2) = \frac{1}{2|p \cdot k_1|} \quad (\text{B-4})$$

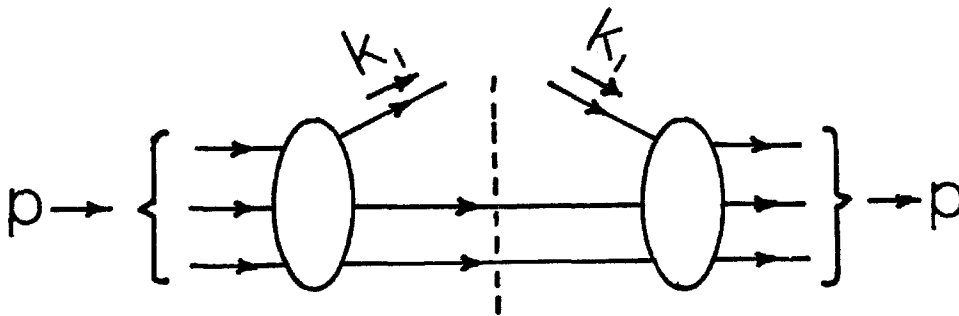


Figure B.1

The first phase space integration viewed as a calculation of the structure function for nucleon  $\rightarrow$  quark + anything

the non-trivial integration is

$$\int_{\mu_0}^{-4} W_{\mu\nu}^{ij} = \frac{p \cdot q}{64\pi^3} \int dy_2 \, dx_1 \, dy_1 \, M_{\mu\nu}^{ij} \quad (\text{B-5})$$

The main task is to determine the limits imposed by kinematics on the integration variables  $y_2$ ,  $x_1$  and  $y_1$ . It is also important to determine which regions of integration are accentuated by dynamics, that is, which regions have large values for the gluon and quark propagators. It will prove advantageous to change variables from  $x_1$  and  $y_1$  to  $w^2$  and  $w_m^2$ , where  $w^2$  is the invariant mass of the unstruck quarks in the final state and  $w_m^2$  is the maximum value of  $w^2$  at fixed  $y_1$ . These variables range over values of order  $m^2$ , which makes it possible to extract the power behavior in  $q^2$  and  $1-x$  without actually doing the final integration.

The mass shell conditions for the two unstruck quarks can be used to obtain the relation

$$x_2 = \xi(1 + 2y_2) + 1 + y_2 \quad (\text{B-6})$$

where

$$\xi = \frac{-k_1^2 + m_N^2}{2p \cdot k_1 - 2m_N^2} \quad (\text{B-7})$$

As in the pion calculation, the kinematic limits on  $y_2$  are imposed by the positive definiteness of

$$-r_2^2 = y_2(y_2+1)(1+\xi) \left[ 2p \cdot k_1 + 2(2\xi+1)m_N^2 \right] + (1+\xi)^2 m_N^2 - m^2 \quad (\text{B-8})$$

It will be assumed now, and shown later, that  $k_1^2$  and  $p \cdot k_1$  are large compared to all squared masses, giving

$$\xi = \frac{-k_1^2}{2p \cdot k_1} + O\left(\frac{m^2}{p \cdot k_1}\right) \quad (\text{B-9})$$

$$-r_2^2 = -y_2(y_2+1)w^2 + (1+\xi)^2 m_N^2 - m^2 \quad (\text{B-10})$$

where

$$w^2 = (p \cdot k_1)^2 \quad (\text{B-11})$$

is the invariant (mass)<sup>2</sup> of the unstruck quarks. Positivity of  $w^2$  and  $-r_2^2$  then gives the constraint

$$-\frac{1}{2} - \sqrt{\frac{1}{4} - \frac{m^2}{w^2}} < y_2 < -\frac{1}{2} + \sqrt{\frac{1}{4} - \frac{m^2}{w^2}} \quad (\text{B-12})$$

In writing (B-12), the condition

$$w^2 = O(m^2) \quad (\text{B-13})$$

has been assumed. The condition for the validity of (B-13) is discussed later in this Appendix.

The kinematic limits on  $x_1$  and  $y_1$  follow from

$$-r_1^2 > 0 \quad (\text{B-14})$$

and

$$w^2 > 4m^2 \quad (\text{B-15})$$



In the dynamically-favored region

$$y_1 = 0 \left( \frac{m^2}{W^2} \right) \quad (\text{B-16})$$

the limits (B-14) and (B-15) can be expressed, respectively, as

$$x_1 > \frac{m^2 - m_N^2}{2p \cdot q} + x(1 + y_1) \quad (\text{B-17})$$

$$x_1 < y_1(2x - 1) + x - \frac{3m^2 + m_N^2}{2p \cdot q} \quad (\text{B-18})$$

where  $x$  is the usual scaling variable

$$x = \frac{-q^2}{2p \cdot q} = \frac{1}{\omega} \quad (\text{B-19})$$

Inequalities (B-17) and (B-18) confine  $x_1$  and  $y_1$  to a narrow wedge-shaped region in the  $x_1, y_1$  plane as shown in Figure B.2.

As in the pion calculation, the amplitude  $M_{\mu\nu}^{ij}$  will contain inverse powers of  $y_1$ , favoring the region given by (B-16). In this region,

$$x_1 = x - 0 \left[ \frac{4m^2}{2p \cdot q(1-x)} \right] \quad (\text{B-20})$$

Replacing  $x_1$  by the integration variable

$$w^2 = m_N^2 + m^2 - 2x_1 m_N^2 - 2(x_1 - x)p \cdot q - 2p \cdot q y_1(1 - 2x), \quad (\text{B-21})$$

the limits on the  $w^2$  integration are, at constant,  $y_1$ ,

$$4m^2 \leq w^2 \leq w_m^2 \quad (\text{B-22})$$

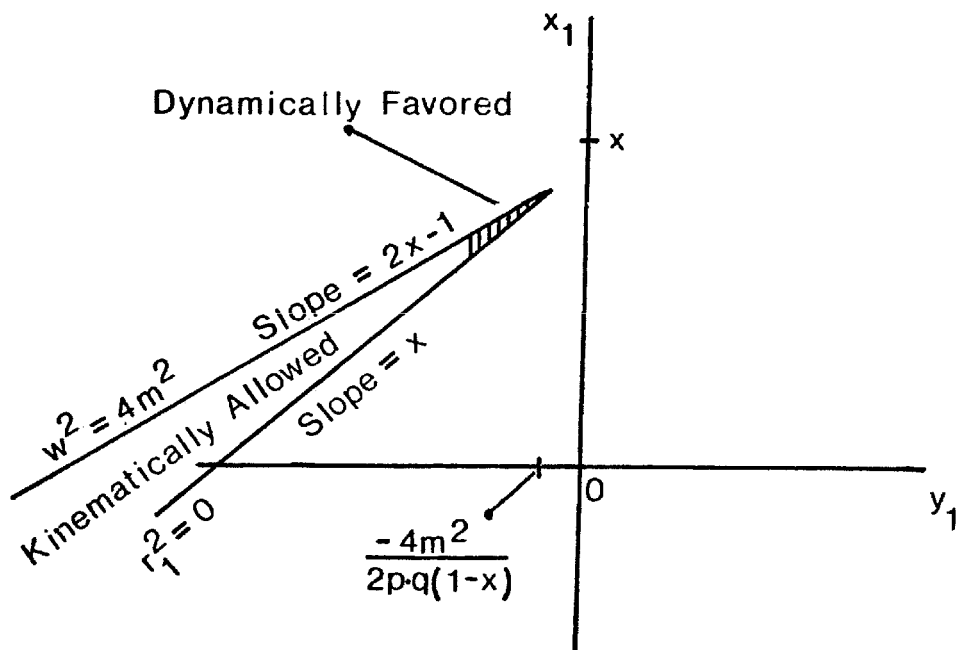


Figure B.2

Allowed and favored regions for the final phase space integration in the nucleon structure function calculation

where

$$w_m^2 = -y_1 \ 2p \cdot q(1-x) \quad (\text{B-23})$$

serves as an integration variable replacing  $y_1$ .

Expression (8-4) can now be written as

$$\bar{\mu}_0^{-4} W_{\mu\nu}^{ij} = \frac{1}{256\pi^3 p \cdot q(1-x)} \int_{4m^2}^{\infty} \int_{4m^2}^{w_m^2} \int_{-\frac{1}{2} - \sqrt{\frac{1}{4} - \frac{m^2}{w^2}}}^{-\frac{1}{2} + \sqrt{\frac{1}{4} - \frac{m^2}{w^2}}} M_{\mu\nu}^{ij} dy_2^2 dw^2 dw_m^2 \quad (\text{B-24})$$

We will be interested in evaluating  $W_{\alpha}^{\alpha}$  and  $p^{\mu} p^{\nu} W_{\mu\nu}$ . The diagrams to be considered have  $M_{\alpha}^{ij}$  of the form

$$M_{\alpha}^{ij\alpha} = (p \cdot q)^m (p \cdot k_1)^{-n} (w^2)^{\mathcal{L}} g^{ij}(y_2) \quad (\text{B-25})$$

with a similar form for  $p^{\mu} p^{\nu} M_{\mu\nu}^{ij}$ . In principle,  $\mathcal{L}$ ,  $m$  and  $n$  vary from diagram to diagram and should carry subscripts  $i$  and  $j$ . Noting that

$$2p \cdot k_1 \approx k_1^2 \approx -\frac{w_m^2}{1-x} \quad (\text{B-26})$$

one obtains

$$\bar{\mu}_0^{-4} W_{\mu\nu}^{ij} = \frac{(p \cdot q)^{m-1} [2(1-x)]^{n-1}}{128\pi^3} \int_{4m^2}^{\infty} \frac{1}{(w_m^2)^n} \int_{4m^2}^{w_m^2} (w^2)^{\mathcal{L}} \cdot I^{ij}(w^2) dw^2 dw_m^2 \quad (\text{B-27})$$

where

$$I^{ij}(w^2) = \int_{-\frac{1}{2} - \sqrt{\frac{1}{4} - \frac{m^2}{w^2}}}^{-\frac{1}{2} + \sqrt{\frac{1}{4} - \frac{m^2}{w^2}}} g^{ij}(y_2) dy_2 \quad (\text{B-28})$$

The integrands in (B-25) do not involve  $x$  or  $p \cdot q$ , so one can see that  $M_\alpha^{ij\alpha} \propto p \cdot q$  if the diagrams "scales" and  $M_\alpha^{ij\alpha} \propto (p \cdot k_1)^{-4}$  if the diagram has  $(1-x)^3$  threshold behavior.

We will close this section with some expressions useful in reducing  $M_\alpha^{ij\alpha}$  to the form (B-25).

$$2k_1 \cdot q = -q^2 - k_1^2 + m^2 \quad (\text{B-29})$$

$$p \cdot k_2 = y_2 p \cdot k_1 + O(m^2) \quad (\text{B-30})$$

$$p \cdot k_3 = -(1+y_2)p \cdot k_1 + O(m^2) \quad (\text{B-31})$$

$$k_1 \cdot k_2 = y_2 p \cdot k_1 + O(m^2) \quad (\text{B-32})$$

$$k_2 \cdot k_3 = O(m^2) \quad (\text{B-33})$$

Tracing through the approximations made in this section, a sufficient condition for their validity is that  $w^2$  be restricted to values of order  $m^2$ . The function  $I^{ij}(w^2)$  tends to a constant for  $w^2 \gg m^2$ , so the final integration is restricted to small  $w_m$  if

$$n - 1 > 2 \quad (\text{B-34})$$

Most of the diagrams considered in the next section have  $l = 0$ ,  $n = 4$  and satisfy the above condition. (Actually, some  $I^{ij}(w^2)$  tend to infinity logarithmically as  $w^2 \rightarrow \infty$ , as can be seen from (B-28) and the results to follow. This does not alter condition (B-34) however.)

The conventions and approximations used in evaluating the  $M_{\mu\nu}^{ij}$  will be introduced with reference to the sub-diagram below, a frequently-occurring component of the diagrams we wish to consider.

$$S_i \begin{array}{c} \alpha \} \\ \rightarrow z_i p \end{array} \xrightarrow{k_i} \begin{array}{c} | \\ | \\ | \end{array} \begin{array}{c} \} \beta \\ \rightarrow z_i p \end{array} S_1 = n_{(i)}^{\alpha\beta} 2\pi\delta(k_i^2 - m^2) \quad (\text{B-35})$$

$$n_{(i)}^{\alpha\beta} = \text{Tr} \gamma^\beta k_i \gamma^\alpha \frac{1 + \gamma_5 S_i}{2} \frac{\not{p}}{3} \quad (\text{B-36})$$

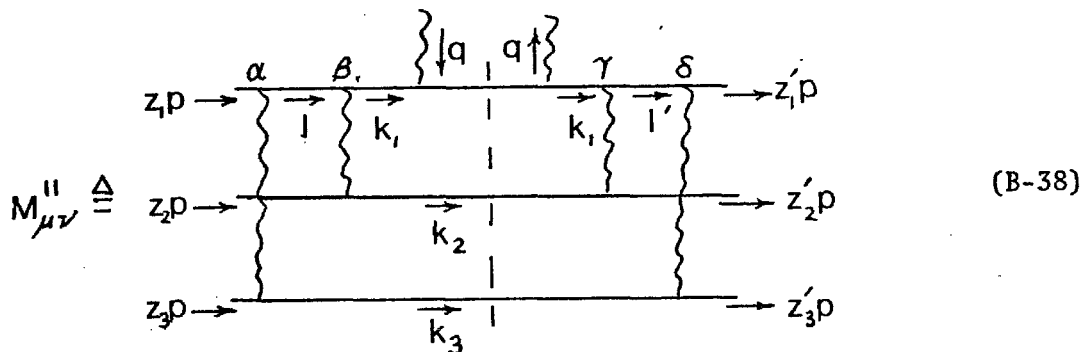
As before, the spinor normalization  $\bar{u} u = \frac{2}{3} m_N$  is used. The input and output spins are assumed to be the same, as the spin flip amplitude is non-leading. Quark mass is neglected and the spin projection operator is approximated by the chirality projection operator. Even though the incoming and outgoing quark lines carry different momenta, the spinors are taken, as before, to have the same rest frame as the nucleon. For the forward Compton amplitude, the incoming and outgoing nucleons have identical momentum and spin.

Factors  $\pm \sqrt{-1}$  normally appearing in vertices and propagators are omitted along with factors  $g$  and  $\frac{2}{3} e$ ,  $-\frac{1}{3} e$  at the gluon and photon vertices.

Carrying out the trace,

$$n^{(i)\alpha\beta} = \frac{2}{3} \left( p^\alpha k_i^\beta + p^\beta k_i^\alpha - p \cdot k_i g^{\alpha\beta} + i S_i \epsilon^{\alpha\beta\gamma\delta} p_\gamma k_{i\delta} \right) \quad (B-37)$$

This appears twice in the first diagram of Equation (8-3). Using  $\underline{\Delta}$  to denote equality to within phase space integrals defined in equation (8-4), diagram (11) is:



In finding the transverse structure function, (B-38) is contracted on  $\mu$  and  $\nu$ .

$$D^{11} M_{\mu}^{11\mu} = -\frac{1}{3} T_{\alpha\beta\gamma\delta} \gamma_\alpha \gamma_\beta \gamma_\gamma \gamma_\delta \left( \frac{k_1 + q}{1} \right) k_{1\gamma} \gamma_\beta \gamma_\alpha \left( 1 + S_1 \gamma_5 \right) n^{(3)\alpha\delta} n^{(2)\beta\gamma} \quad (B-39)$$

where  $D^{11}$  is the denominator due to propagators. Throwing out terms proportional to  $m_N^2$ ,

$$n^{(3)\alpha\delta} \gamma_\alpha \not{p} \gamma_\beta = \frac{4}{3} p \cdot k_3 \not{p} + i S_3 \epsilon^{\alpha\beta\gamma\delta} \gamma_\alpha \not{p} \gamma_\beta p_\gamma k_{3\delta} .$$

This can be simplified by using the identity

$$\epsilon^{\alpha\beta\gamma\delta} \gamma_\alpha \not{p} \gamma_\beta = 2i \gamma_5 \left( a \gamma_\gamma \delta - a \delta \gamma_\gamma \right) \quad (B-40)$$

which gives

$$n^{(3)\alpha\delta} \gamma_\alpha \not{p} \gamma_5 = \frac{4}{3} p \cdot k_3 \left( 1 + S_3 \gamma_5 \right) \not{p} \quad (B-41)$$

The spin selection rule  $S_1 = -S_3$  is obeyed. To leading order,



$$p^{\alpha\beta} = \frac{1}{3} \text{Tr} \not{p} \gamma_\delta (\not{p} - z'_1 \not{p} - k_3) \gamma^\beta k_2 \gamma^\alpha (\not{p} - z_1 \not{p} - k_3) \gamma_\gamma \frac{1+S_2 \gamma_5}{2} n^{(3)\gamma\delta} \quad (\text{B-47})$$

Taking the trace and making the usual approximations,

$$p^{\alpha\beta} = \frac{32}{9} (p \cdot k_3)^2 [k_2^\alpha k_3^\beta + k_2^\beta k_3^\alpha - i S_3 \epsilon^{\delta\beta\eta\alpha} k_{3\delta} k_{2\eta}] \quad (\text{B-48})$$

with the selection rule

$$S_2 = - S_3 \quad (\text{B-49})$$

Inserting (B-48) into (B-46)

$$D^{\mu 33} M_\mu^{33} = \frac{512}{27} 2p \cdot q (p \cdot k_1)^4 (1+y_2)^3 y_2 \quad (\text{B-50})$$

Either spin choice  $S_1 = S_3$  or  $S_1 = - S_3$  gives the same result, in agreement with the selection rule derived heuristically. After calculating the propagator denominator factor, the final result shows scaling and  $(1-x)^3$  threshold behavior:

$$M_\mu^{33} = \frac{4p \cdot q y_2}{27 z_3 z'_3 (1-z_1)^2 (1-z'_1)^2 (1+y_2) (p \cdot k_1)^4} \quad (\text{B-51})$$

Diagram (22) is essentially the same as (11) and (44) is essentially the same as (33). Permuting the lower two quark lines is equivalent to  $z_2 \leftrightarrow z_3$ ,  $z'_2 \leftrightarrow z'_3$ ,  $y_2 \leftrightarrow 1 + y_2$ .

$$M_\mu^{22} = \frac{4p \cdot q}{27 z_2 z'_2 z_3 z'_3 (1-z_3) (1-z'_3) y_2 (1+y_2) (p \cdot k_1)^4} \quad (\text{B-52})$$

$$M_\mu^{44} = \frac{4p \cdot q (1+y_2)}{27 z_2 z'_2 (1-z_1)^2 (1-z'_1)^2 y_2 (p \cdot k_1)^4} \quad (\text{B-53})$$



Unsymmetrical interference diagrams are a good deal more difficult to evaluate directly, but they are equal to an obvious mean of the appropriate symmetric graphs. For example, we have evaluated

$$M_{\mu}^{34\mu} \stackrel{\Delta}{=} \begin{array}{c} \text{---} \mu \text{---} \\ | \\ \text{---} \mu \text{---} \\ | \\ \text{---} \mu \text{---} \\ | \\ \text{---} \mu \text{---} \end{array} \quad (\text{B-59})$$

directly using traces, but omitting the chirality projectors  $\frac{1}{2} (1+S\gamma_5)$  to simplify the calculation. The result is

$$M_{\mu}^{34\mu} = - \frac{4p \cdot q}{27(1-z_1)^2 (1-z_1')^2 z_3 z_2' (p \cdot k_1)^4} \quad (\text{B-55})$$

The same result could be gotten simply by taking the geometric mean of the numerator factors for  $M_{\mu}^{33\mu}$  and  $M_{\mu}^{44\mu}$  and inserting the appropriate denominator factors. The direct calculation without chirality projection operators gives a result four times larger owing to counting of the four leading spin configurations

$$\begin{array}{cccc} \rightarrow & \rightarrow & \leftarrow & \leftarrow \\ \leftarrow & \rightarrow & \leftarrow & \rightarrow \\ \rightarrow & \leftarrow & \rightarrow & \leftarrow \end{array}$$

This factor of four has been removed in (B-55).

We have not succeeded in doing the remaining phase space integrations defined in equation (B-27) and (B-28). In principle, these can be done independently of the wavefunctions and then, given a wavefunction, the magnitude of the structure function can be determined using the convolution discussed in Chapter VII. For the present, the main conclusions to be drawn are that  $W_T$  should scale with  $(1-x)^3$  threshold

dependence and that the struck quark should always have spin parallel to the nucleon.

Several diagrams of order  $g^8$  do not make leading contributions to  $W_T$ . These will be disposed of without appealing to the spinology rules.

The diagram

$$D_{\mu\nu}^{55} \triangleq \begin{array}{c} \alpha \quad \quad \quad \mu \quad \quad \quad \nu \quad \quad \quad \beta \\ \text{---} \text{---} \text{---} \text{---} \text{---} \text{---} \\ \text{---} \text{---} \text{---} \text{---} \text{---} \text{---} \\ \text{---} \text{---} \text{---} \text{---} \text{---} \text{---} \end{array} \quad (B-56)$$

will be shown to be non-leading in the Feynman gauge. Following steps analogous to those used in evaluating  $M_{\mu}^{33\mu}$

$$D_{\mu}^{55} M_{\mu}^{55} = -\frac{2}{3} \text{Tr} \not{p} \gamma_{\beta} k_1 \not{q} k_1 \gamma_{\alpha} \left( \frac{1+S_1 \gamma_5}{2} \right) q^{\alpha\beta} \quad (B-57)$$

$$q^{\alpha\beta} = \frac{1}{3} \text{Tr} \not{p} \gamma^{\beta} (k_2 - z_3 \not{p} + k_3) \gamma_{\delta} k_2 \gamma_{\gamma} (k_2 - z_3 \not{p} + k_3) \gamma^{\alpha} \frac{1+S_2 \gamma_5}{2} n^{(3)\gamma\delta} \quad (B-58)$$

$$n^{(3)\gamma\delta} \gamma_{\delta} k_2 \gamma_{\gamma} = \frac{4}{3} p \cdot k_2 (1+S_3 \gamma_5) k_3 \quad (B-59)$$

When (B-59) is inserted in (B-58), and  $k_3^2 = m^2$  terms are thrown out as non-leading,

$$q^{\alpha\beta} = \frac{4}{9} p \cdot k_2 \text{Tr} \not{p} \gamma^{\beta} k_2 k_3 k_2 \gamma^{\alpha} (1+S_2 \gamma_5) \quad (B-60)$$

with the selection rule  $S_2 = -S_3$ . In (B-60), terms containing  $p^{\alpha}$  and  $p^{\beta}$  have also been removed, as they give  $m_N^2$  terms when inserted in expression (B-57). Finally,

$$k_2 k_3 k_2 = O(m^2) k_2 + O(m^2) k_3 \quad (B-61)$$

according to the expressions (B-29) through (B-33). With a power of  $m^2$  appearing, one can see that  $W_{\mu}^{55\mu}$  must fall off at least as fast as  $(1-x)^4$  in the Feynman gauge, although it will make a leading contributions in other gauges as does the corresponding form factor diagram.

The spinology rules say that

$$M_{\mu\nu}^{12} \triangleq \begin{array}{c} \Rightarrow \\ \Rightarrow \\ \Leftarrow \end{array} \begin{array}{c} \text{---} \\ \text{---} \\ \text{---} \end{array} \begin{array}{c} \text{---} \\ \text{---} \\ \text{---} \end{array} \begin{array}{c} \Rightarrow \\ \Leftarrow \\ \Rightarrow \end{array} \quad (B-62)$$

should be non-leading owing to conflicting demands on the spins of the two lower quarks. The asymmetry of this diagram makes it difficult to evaluate, but disposing of the spin projectors shortens the labor involved, while hiding the details of spin selection. We have carried this calculation to the point of finding that  $W_{\mu\nu}^{12}$  falls faster than  $(1-x)^3$  and scales.

Much more important than either of the above diagrams is the

"Class c" diagram

$$M_{\mu\nu}^{66} \triangleq \begin{array}{c} \Leftarrow \\ \Rightarrow \\ \Rightarrow \end{array} \begin{array}{c} \text{---} \\ \text{---} \\ \text{---} \end{array} \begin{array}{c} \text{---} \\ \text{---} \\ \text{---} \end{array} \begin{array}{c} \Leftarrow \\ \Rightarrow \\ \Rightarrow \end{array} \quad (B-63)$$

This diagram destroys the purity of the spin selection rule for the struck quark, unless it fails to scale or has falloff faster than  $(1-x)^3$ . If no cancellations occur when traces are taken, it is apparent that

$$M_{\mu}^{66\mu} \propto \frac{(p \cdot q)^0}{(p \cdot k_1)^3} \quad (B-64)$$

In comparison to the leading diagrams calculated so far, a power of  $p \cdot k_1$  in the denominator has been replaced by a power of  $p \cdot q$ , because  $q$  flows

through two additional fermion propagators. In the notation of expression (B-25),  $\ell = 0$ ,  $n = 3$ , and condition (B-34) is satisfied, giving  $W_{\mu}^{66\mu} \propto (1-x)^2/p \cdot q$ . If cancellations occur in the traces, powers of  $p \cdot q$  or  $p \cdot k_1$  in the numerator will be replaced by powers of  $m^2$  or  $w^2$ , but condition (B-34) will still be satisfied. It can be concluded that the contribution of diagram (66) does not scale.